Supporting Information

Mechanophore-Bearing Polymers with Diverse Conformations: Precision Synthesis and Mechanochemical Structure-Reactivity Relationships

Seiyoung Yoon, Javad Tamnanloo, Ling-Jo Wu, Kexing Xiao, Sophia Aracri, Mark D. Foster, Tianbo Liu, Mesfin Tsige, Junpeng Wang

School of Polymer Science and Polymer Engineering, University of Akron, Akron, Ohio 44325, United States.

Contents

Materials

(Z,Z)-1,5-cyclooctadiene, maleic anhydride, tetrabutylammonium fluoride, and silver nitrate were purchased from Acros. Acetic anhydride, acetic acid, ethyl vinyl ether, methyl benzoate, PSS-(3-Mercapto)propyl-heptaisobutyl substituted, 3-butenoic acid, 1,8-diazabicyclo[5.4.0]undec-7-ene, ω-pentadecalactone, p-toluenesulfonic acid monohydrate, Grubbs 1st generation catalyst, Quadrapure TU, 4 Å molecular sieves, aluminum oxide, tetrahydrofuran, diethyl ether, toluene, dichloromethane, and chloroform were purchased from Sigma Aldrich. Triphenylphosphine, 2-Methyl-4'-(methylthio)-2-morpholinopropiophenone and L-lactide were purchased from TCI. Acetone, methanol, ethyl acetate, hexane, hydrochloric acid, sodium hydroxide, benzylamine and 4-dimethylamino pyridine were purchased from Thermo Fisher Scientific. 8-hydroxyoctanoic acid, 15-hydroxylpentadecanoic acid, 2-((tert-butyldimethylsilyl)oxy)ethanol, 1-(3-dimethylaminopropyl)-3-ethylcarbodiimide hydrochloride were synthesized from Ambeed. Aminoacetic acid was purchased from Mallinckrodt Inc. Aminopropylisobutyl POSS was purchased from Hybrid Plastics. Chloroform-d was purchased from Cambridge Isotope Laboratories. Silicycle F60 (230-400 mesh) silica gel was used for column chromatography.

Triphenylphosphine was recrystallized in ethyl acetate two times and stored in N_2 atmosphere. L-lactide was recrystallized in ethyl acetate three times and stored in N_2 atmosphere at -20 °C. THF was purified by passing through a solvent purification column filled with molecular sieves and aluminum oxide and stored with 4 Å molecular sieves in a N_2-filled glovebox. Toluene was filtered through Aura MT Syringe Filters with PTFE 13 mm filter with 0.22 μm pore size seven times before usage. Silver nitrate impregnated silica gel was prepared by mixing 10% silver nitrate solution in water and silica gel with 1/9 weight ratio of silver nitrate and silica gel and removing water by azeotropic distillation in toluene before use. All other chemicals were used without further purification.

Instruments

Size-Exclusion Chromatography

Size-exclusion chromatography was carried out with Tosoh EcoSEC HLC-8320GPC with two TSKgel GMHHR-M(S) analytical columns (7.8 mm ID × 30 cm, 13 μm) and one TSKgel guard column HHR(S) (7.5 mm ID × 7.5 cm, 13 μm), connected in series with a built-in refractive index (RI) detector and a miniDAWN TREOS multi-angle light scattering (MALS) detector (Wyatt Technology). Relative molecular weights were obtained from linear polystyrene calibration and absolute molecular weights were measured using online RI and MALS detectors. The refractive index increment (dn/dc) values were determined by the on-line method assuming 100% mass elution.

Nuclear Magnetic Resonance Spectroscopy

^{1}H NMR, ^{13}C NMR, COSY NMR, and HSQC NMR spectra were obtained using a

Varian 500 MHz spectrometer at the University of Akron Magnetic Resonance Center with chloroform-d as the solvent. Chemical shifts were referenced to residual chloroform signal (δ = 7.26 [^{1}H] and 77.16 [^{13}C]). T1 measurements were performed to obtain the longest ^{1}H relaxation delay needed for quantitative analysis.

High-Resolution Mass Spectrometry

High-resolution mass spectrometry (HRMS) was obtained using Bruker Q/TOF Mass Spectrometer. Samples were dissolved in either acetonitrile or methanol in 10-100 ng/mL and filtered through Syringe Filters with PTFE filter with 0.22 μm pore size and injected for ESI analysis.

Ultrasonication

Pulsed ultrasonication experiments were conducted using a Vibracell model VCX500 (Sonics & Materials) with a standard solid probe (tip diameter = 13 mm, titanium alloy Ti6Al-4V). Ultrasonication was carried out under a pulse sequence of 1 second sonication and 1 second of rest at 24 kHz with amplitude of 25% (9.3 W/cm^{2}). The reaction vessel for the experiment was made by the University of Akron Glassblowing Shop.

Light Scattering

Static and dynamic light scattering experiments were conducted using a commercial Brookhaven light scattering spectrometer equipped with a diode-pumped solid-state laser operating at 532 nm and a BI-9000AT multichannel digital correlator. All DLS and SLS measurements were conducted at 20 °C unless stated otherwise.

Atomic Force Microscopy

Atomic Force Microscopy (AFM) was taken using Veeco Dimension Icon AFM with Scan Assyst. The AFM images were taken with non-contact tapping mode using RTESPA-300 tip from Bruker with spring constant of 40 N/m, frequency of 300 kHz, and radius of 8 nm.

Synthesis

Synthesis of Small Molecules and Monomers

Synthesis of acid **2**

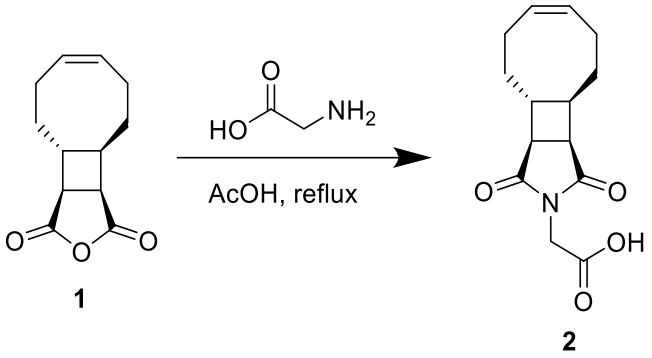

1 **2**

1 was synthesized according to literature.[1] In a 50 mL round-bottom flask with 1 (1287.5 mg, 6.25 mmol, 1.00 eq.) and aminoacetic acid (492.0 mg, 6.56 mmol, 1.05 eq.) were added glacial acetic acid (14 mL) and stirred under reflux for 15 h. Acetic acid was removed via vacuum distillation. The crude product was purified via column chromatography (AcOH:MeOH:DCM = 1:5:94). The obtained yellow solid was further purified via recrystallization in water to afford **2** as a colorless solid (1.30 g, yield: 79%).^{1}H NMR (500 MHz, $CDCl_3$) δ 8.10 (s, 1H), 5.66 – 5.52 (m, 2H), 4.32 (s, 2H), 3.27 (dd, *J* = 10.5, 6.5 Hz, 1H), 2.93 (dd, *J* = 6.3, 6.3 Hz, 1H), 2.77 – 2.67 (m, 1H), 2.49 – 2.40 (m, 1H), 2.30 – 2.20 (m, 1H), 2.20 – 2.13 (m, 1H), 2.12 – 2.02 (m, 2H), 2.02 – 1.94 (m, 1H), 1.85 – 1.74 (m, 1H), 1.59 – 1.49 (m, 1H), 1.43 – 1.33 (m, 1H). ^{13}C NMR (126 MHz, $CDCl_3$) δ 178.52, 177.24, 171.61, 130.08, 129.75, 44.71, 41.83, 40.19, 39.85, 38.96, 32.90, 28.75, 24.09, 23.78. HRMS-ESI (m/z): calculated for $C_{14}H_{17}NNaO_4^+$ $[M+Na]^+$, 286.1050; found, 286.1039.

Synthesis of *Z*SS

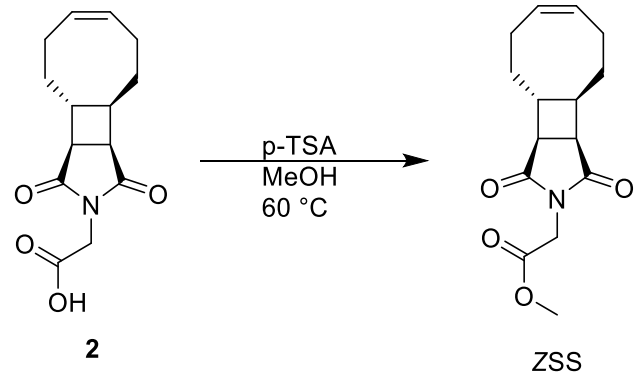

2 *Z*SS

To a 50 mL round-bottom flask was added **2** (1431.1 mg, 5.44 mmol, 1.00 eq.) and MeOH (18 mL). While stirring, p-TSA (103.5 mg, 0.54 mmol, 0.10 eq.) was added. The mixture was heated at 60 °C for 15 h. MeOH was removed under reduced pressure. The crude product was dissolved in 100 mL DCM and washed with water and brine. The organic layer was dried with Na_2SO_4 and filtered. DCM was removed

via rotary evaporation to afford ZSS as a white solid (1.50 g, yield: 99%). ^{1}H NMR (500 MHz, $CDCl_3$) δ 5.65 – 5.53 (m, 2H), 4.25 (s, 2H), 3.75 (s, 3H), 3.24 (dd, *J* = 10.5, 6.5 Hz, 1H), 2.90 (dd, *J* = 6.3, 6.3 Hz, 1H), 2.75 – 2.66 (m, 1H), 2.49 – 2.41 (m, 1H), 2.27 – 2.15 (m, 2H), 2.11 – 2.01 (m, 2H), 2.00 – 1.94 (m, 1H), 1.82 – 1.75 (m, 1H), 1.56 – 1.48 (m, 1H), 1.45 – 1.36 (m, 1H). ^{13}C NMR (126 MHz, $CDCl_3$) δ 178.58, 177.30, 167.50, 130.25, 129.90, 52.71, 44.82, 41.98, 40.29, 39.94, 39.27, 33.06, 28.91, 24.25, 23.97. HRMS-ESI (m/z): calculated for $C_{15}H_{20}NO_4^+$ $[M+H]^+$, 278.1387; found, 278.1386; $C_{15}H_{19}NNaO_4^+$ $[M+Na]^+$, 300.1206; found, 300.1208.

Synthesis of *Z*MS

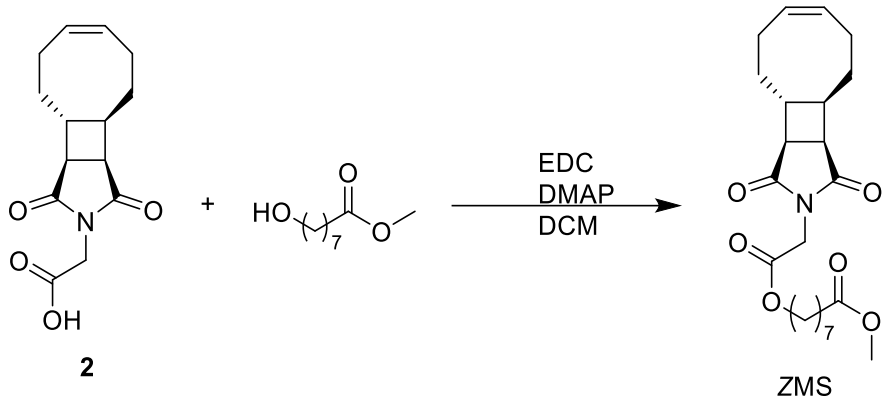

Methyl 8-hydroxyoctanoate was synthesized according to literature.[2] Methyl 8-hydroxyoctanoate (772.3 mg, 4.44 mmol, 1.10 eq.) and **2** (1061.1 mg, 4.00 mmol, 1.00 eq.) were dissolved in DCM (5 mL). At 0 °C, 1-(3-dimethylaminopropyl)-3-ethylcarbodiimide hydrochloride (EDC) (1536.0 mg, 8.00 mmol, 2.00 eq.) and 4-dimethylamino pyridine (DMAP) (48.9 mg, 0.40 mmol, 0.10 eq.) were added to the mixture while stirring. The mixture was warmed up to 20 °C and stirred for 24 h. The solution was diluted with 100 mL DCM and washed with water and brine. The organic layer was dried with Na_2SO_4 and filtered. DCM was removed in rotary evaporator to afford pale yellow oil as crude product. The crude was purified via column chromatography (MeOH:DCM = 5:95) to afford ZMS as a colorless liquid (1340.0 mg, yield: 80%).^{1}H NMR (500 MHz, cdcl$_3$) δ 5.68 – 5.55 (m, 2H), 4.25 (s, 2H), 4.15 (t, *J* = 6.8 Hz, 2H), 3.67 (s, 3H), 3.25 (dd, *J* = 10.4, 6.5 Hz, 1H), 2.91 (dd, *J* = 6.3, 6.3 Hz, 1H), 2.78 – 2.68 (m, 1H), 2.51 – 2.42 (m, 1H), 2.31 (t, *J* = 7.5 Hz, 2H), 2.28 – 2.18 (m, 2H), 2.13 – 2.03 (m, 2H), 2.03 – 1.96 (m, 1H), 1.85 – 1.77 (m, 1H), 1.69 – 1.58 (m, 4H), 1.58 – 1.50 (m, 2H), 1.48 – 1.38 (m, 1H), 1.38 – 1.29 (m, 6H). ^{13}C NMR (126 MHz, $CDCl_3$) δ 178.43, 177.13, 174.09, 166.92, 130.12, 129.78, 65.84, 51.39, 44.72, 41.85, 40.13, 39.81, 39.29, 33.98, 32.97, 28.92, 28.77, 28.41, 25.55, 24.78, 24.14, 23.84. HRMS-ESI (m/z): calculated for $C_{23}H_{34}NO_6^+$ $[M+H]^+$, 420.2381; found, 420.2380; $C_{23}H_{33}NNaO_6^+$ $[M+Na]^+$, 442.2200; found, 442.2199.

Synthesis of *Z*LS

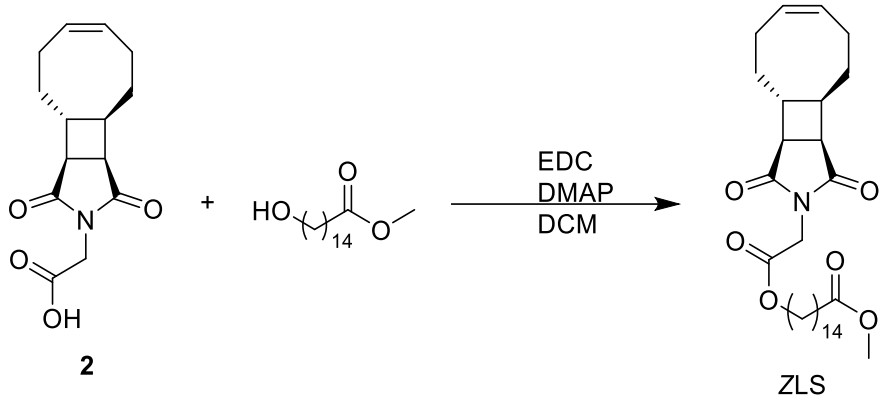

Methyl 15-hydroxypentadecanoate was synthesized according to literature.[3] Methyl 15-hydroxypentadecanoate (813.0 mg, 3.0 mmol, 1.10 eq.) and **2** (715.0 mg, 2.7 mmol, 1.00 eq.) were dissolved in DCM (4 mL). At 0 °C, EDC (1044.0 mg, 5.4 mmol, 2.00 eq.) and 4-dimethylamino pyridine (DMAP) (33.0 mg, 0.27 mmol, 0.10 eq.) were added to the mixture while stirring. The mixture was warmed up to 20 °C and stirred for 24 h. The solution was diluted with 100 mL Et_2O and washed with water and brine. The organic layer was dried with Na_2SO_4 and filtered. Et_2O was removed in rotary evaporator to afford crude product. The crude was purified via column chromatography (MeOH:DCM = 2:98) to afford ZLS as a white solid (990.5 mg, yield: 71%). ^{1}H NMR (300 MHz, $CDCl_3$) δ 5.68 – 5.51 (m, 2H), 4.24 (s, 2H), 4.14 (t, *J* = 6.8 Hz, 2H), 3.65 (s, 3H), 3.24 (dd, *J* = 10.4, 6.5 Hz, 1H), 2.90 (dd, *J* = 6.3, 6.3 Hz, 1H), 2.79 – 2.63 (m, 1H), 2.53 – 2.39 (m, 1H), 2.29 (t, *J* = 6.4 Hz, 2H), 2.25 – 2.14 (m, 2H), 2.14 – 1.91 (m, 3H), 1.86 – 1.71 (m, 1H), 1.69 – 1.50 (m, 5H), 1.49 – 1.39 (m, 1H), 1.38 – 1.16 (m, 20H). ^{13}C NMR (126 MHz, $CDCl_3$) δ 178.43, 177.14, 174.22, 166.95, 130.14, 129.80, 65.99, 51.37, 44.72, 41.88, 40.14, 39.83, 39.32, 34.09, 33.00, 29.59, 29.56, 29.54, 29.47, 29.43, 29.24, 29.20, 29.15, 28.81, 28.52, 25.76, 24.96, 24.19, 23.88. HRMS-ESI (m/z): calculated for $C_{30}H_{47}NNaO_6^+$ $[M+Na]^+$, 540.3296; found, 540.3290.

Synthesis of *Z*Bn

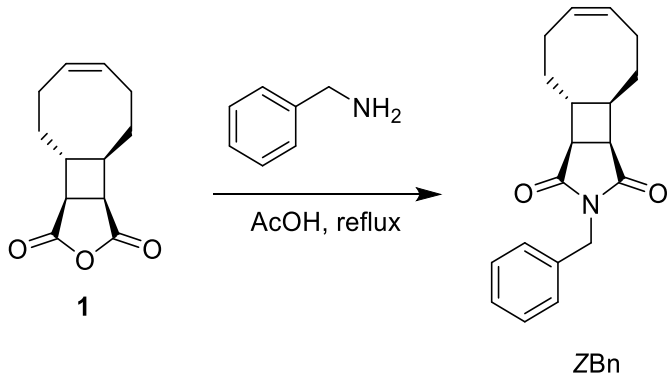

In a 5 mL round-bottom flask with **1** (275.9 mg, 1.34 mmol, 1.00 eq.) was added benzylamine (145.8 µL, 1.34 mmol, 1.00 eq.) and glacial acetic acid (1.5 mL). The mixture was stirred under reflux for 15 h. Acetic acid was removed under vacuum

distillation. Crude was purified via column chromatography in chloroform to afford ZBn as a white solid (230.0 mg, yield: 58%). ^{1}H NMR (500 MHz, $CDCl_3$) δ 7.40 – 7.35 (m, 2H), 7.34 – 7.26 (m, 3H), 5.64 – 5.49 (m, 2H), 4.66 (s, 2H), 3.17 (dd, *J* = 10.4, 6.6 Hz, 1H), 2.84 (dd, *J* = 6.3, 6.3 Hz, 1H), 2.70 – 2.61 (m, 1H), 2.27 – 2.16 (m, 2H), 2.13 – 1.91 (m, 4H), 1.83 – 1.75 (m, 1H), 1.56 – 1.47 (m, 1H), 1.22 – 1.12 (m, 1H). ^{13}C NMR (126 MHz, $CDCl_3$) δ 179.17, 177.70, 136.32, 130.15, 129.90, 128.73, 127.95, 44.96, 42.39, 41.87, 40.20, 39.89, 32.97, 29.13, 24.21, 23.97. HRMS-ESI (m/z): calculated for $C_{19}H_{22}NO_2^+$ $[M+H]^+$, 296.1645; found, 296.1647; $C_{19}H_{21}NNaO_2^+$ $[M+Na]^+$, 318.1465; found, 318.1467.

Synthesis of 8-hydroxy isobutylPOSS-propyloctanamide **3**

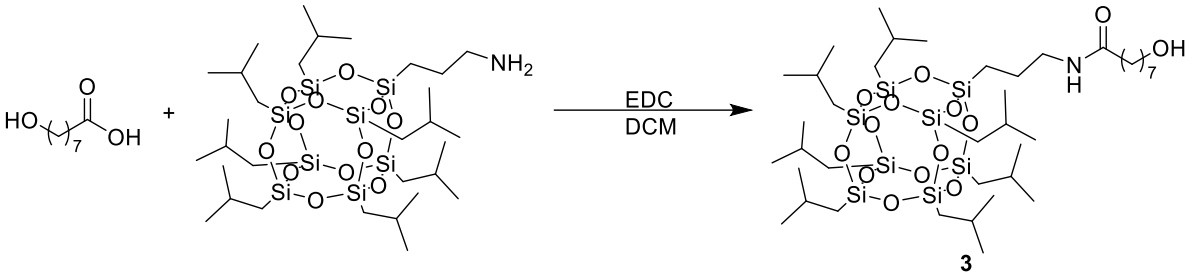

3

Aminopropylisobutyl POSS (5977.0 mg, 6.83 mmol, 1.00 eq.) and 8-hydroxyoctanoic acid (1093.0 mg, 6.83 mmol, 1.00 eq.) were dissolved in 70 mL DCM. EDC (2623.0 mg, 13.66 mmol, 2.00 eq.) was added while stirring. The mixture was stirred for 18 h. The mixture was diluted with chloroform and washed with NH_4Cl solution and water. The aqueous layer was combined and extracted with chloroform. The organic layer was combined and washed with brine. The organic layer was dried with Na_2SO_4 and filtered. The crude was obtained after removal of volatiles through rotary evaporation. The product was purified via column chromatography (MeOH:DCM = 5:95) to afford **3** as a white powder (2.82 g, yield: 41%). ^{1}H NMR (500 MHz, $CDCl_3$) δ 5.42 (t, *J* = 5.9 Hz, 1H), 3.63 (t, *J* = 6.6 Hz, 2H), 3.24 (td, *J* = 7.0, 5.7 Hz, 2H), 2.15 (t, *J* = 7.8 Hz, 2H), 1.91 – 1.77 (m, 7H), 1.67 – 1.51 (m, 6H), 1.40 – 1.30 (m, 6H), 0.95 (d, *J* = 6.5 Hz, 42H), 0.60 (dd, *J* = 7.0, 2.2 Hz, 16H). ^{13}C NMR (126 MHz, $CDCl_3$) δ 173.01, 62.97, 41.82, 36.97, 32.82, 29.38, 29.21, 25.81, 25.80, 25.69, 24.02, 23.97, 23.20, 22.63, 22.60, 9.60. HRMS-ESI (m/z): calculated for $C_{39}H_{86}NO_{14}Si_8^+$ $[M+H]^+$, 1016.4197; found, 1016.4198; $C_{39}H_{85}NNaO_{14}Si_8^+$ $[M+Na]^+$, 1038.4016; found, 1038.4017.

Synthesis of 15-hydroxy isobutylPOSS-propylpentadecanamide **4**

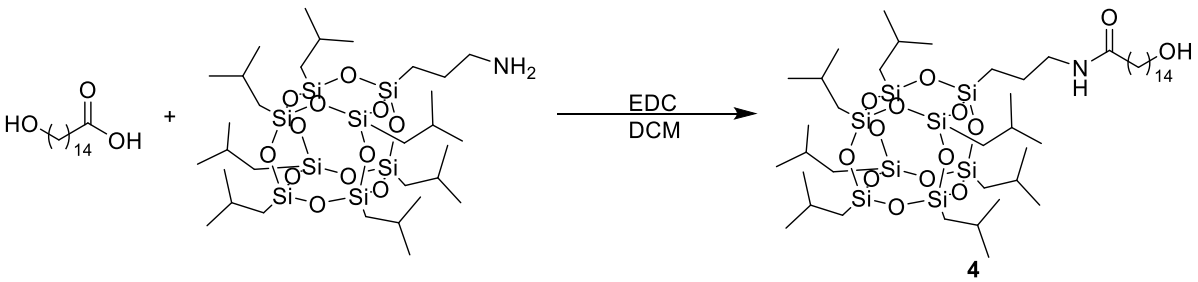

4

Aminopropylisobutyl POSS (4.1 g, 4.65 mmol, 1.20 eq.) and 15-hydroxypentadecanoic acid (1.0 g, 3.88 mmol, 1.00 eq.) were dissolved in 70 mL DCM. EDC (1.5 g, 7.75 mmol, 2.00 eq.) was added while stirring. The mixture was stirred for 12 h. The mixture was diluted with DCM and washed with water and brine. The organic layer was dried with Na_2SO_4 and filtered. The crude was obtained after removal of volatiles through rotary evaporation. The product was purified via column chromatography (MeOH:DCM = 5:95) to afford **4** as a white powder (2.10 g, yield: 48%).). ^{1}H NMR (500 MHz, $CDCl_3$) δ 5.40 (s, 1H), 3.64 (t, *J* = 6.6 Hz, 2H), 3.24 (td, *J* = 6.7, 6.7 Hz, 2H), 2.15 (t, *J* = 7.4 Hz, 2H), 1.94 – 1.78 (m, 7H), 1.66 – 1.53 (m, 6H), 1.36 – 1.25 (m, 20H), 0.96 (d, *J* = 6.6 Hz, 42H), 0.60 (dd, *J* = 7.0, 2.3 Hz, 16H). ^{13}C NMR (126 MHz, $CDCl_3$) δ 173.10, 63.13, 41.80, 37.08, 32.96, 29.71, 29.67, 29.59, 29.55, 29.49, 25.99, 25.94, 25.89, 25.81, 25.80, 24.02, 23.97, 23.21, 22.64, 22.61, 9.60. HRMS-ESI (m/z): calculated for $C_{46}H_{100}NO_{14}Si_8^+$ $[M+H]^+$, 1114.5292; found, 1114.5298; $C_{46}H_{99}NNaO_{14}Si_8^+$ $[M+Na]^+$, 1136.5112; found, 1136.5116.

Synthesis of *Z*SSPOSS

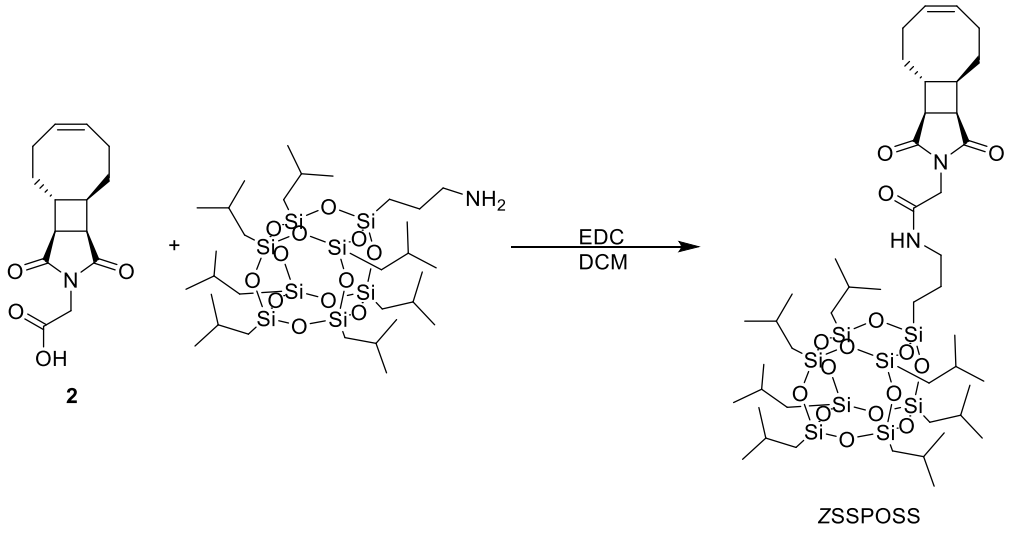

In a vial were added **2** (350.0 mg, 1.33 mmol, 1.00 eq.), aminopropylisobutyl POSS (1222.7 mg, 1.40 mmol, 1.05 eq.) and DCM (7 mL). EDC (511.0 mg, 2.66 mmol, 2.00 eq.) was added to the mixture while stirring at 0 °C. The mixture was warmed up to 20 °C and stirred for 16 h. The mixture was diluted with 100 mL Et_2O and washed with water and brine. The organic layer was dried with Na_2SO_4 and filtered. Et_2O was removed in rotary evaporator to give crude product as white solid. The crude was purified via column chromatography (Et_2O:Hex = 7:3) to afford ZSSPOSS as a white powder (983.0 mg, yield: 66%). ^{1}H NMR (500 MHz, $CDCl_3$) δ 5.66 – 5.54 (m, 3H), 4.13 (s, 2H), 3.31 – 3.21 (m, 3H), 2.90 (dd, *J* = 6.3, 6.3 Hz, 1H), 2.79 – 2.62 (m, 1H), 2.54 – 2.39 (m, 1H), 2.30 – 2.16 (m, 2H), 2.14 – 2.08 (m, 1H), 2.08 – 2.03 (m, 1H), 2.03 – 1.95 (m, 1H), 1.92 – 1.76 (m, 8H), 1.65 – 1.57 (m, 2H), 1.55 – 1.44 (m, 2H), 0.96 (dd, *J* = 6.6, 2.5 Hz, 42H), 0.61 (dd, *J* = 7.0, 5.5 Hz, 16H). ^{13}C NMR (126 MHz, $CDCl_3$) δ 178.92, 177.66, 165.39, 130.32, 129.99, 45.02, 42.34, 42.02, 41.13, 40.26, 39.99, 33.26, 28.92, 25.85, 25.83, 24.40, 24.05, 23.99, 23.08, 22.66,

22.62, 9.61. HRMS-ESI (m/z): calculated for $C_{45}H_{87}N_2O_{15}Si_8^+$ [M+H]$^+$, 1119.4255; found, 1119.4252; $C_{45}H_{86}N_2NaO_{15}Si_8^+$ [M+Na]$^+$, 1141.4075; found, 1141.4071.

Synthesis of *Z*MSPOSS

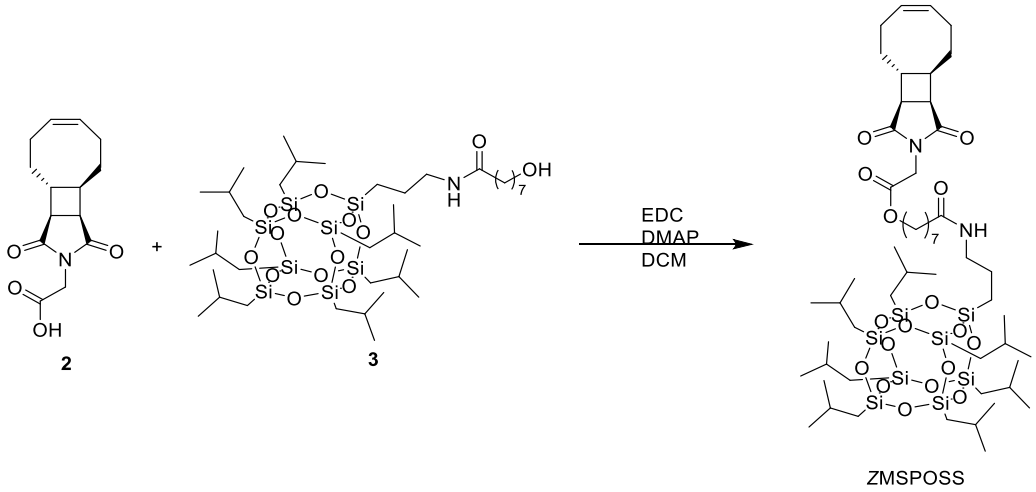

In a vial were added **2** (350.0 mg, 1.33 mmol, 1.00 eq.) and **3** (1421.0 mg, 1.40 mmol, 1.05 eq.) was added. The mixture was dissolved in DCM (7 mL). EDC (511.0 mg 2.66 mmol, 2.00 eq.) and DMAP (16.2 mg, 0.13 mmol, 0.10 eq.) were added at 0 °C while stirring. The mixture was warmed up to 20 °C and stirred for 24 h. The mixture was diluted in DCM and washed with water and brine. The organic layer was dried with Na_2SO_4 and filtered. DCM was removed in rotary evaporator to give crude product as white solid. The crude was purified via column chromatography (Et_2O:Hex = 7:3) to afford ZMSPOSS as a white powder (1250.0 mg, yield: 74%). ^{1}H NMR (500 MHz, $CDCl_3$) δ 5.66 – 5.55 (m, 2H), 5.45 (d, *J* = 6.0 Hz, 1H), 4.25 (s, 2H), 4.18 – 4.12 (m, 2H), 3.28 – 3.20 (m, 3H), 2.91 (dd, *J* = 6.3, 6.3 Hz, 1H), 2.76 – 2.68 (m, 1H), 2.51 – 2.43 (m, 1H), 2.29 – 2.17 (m, 2H), 2.17 – 2.13 (m, 2H), 2.12 – 2.03 (m, 2H), 2.03 – 1.95 (m, 1H), 1.89 – 1.79 (m, 8H), 1.68 – 1.50 (m, 7H), 1.48 – 1.39 (m, 1H), 1.37 – 1.31 (m, 6H), 0.96 (d, *J* = 6.6 Hz, 42H), 0.60 (dd, *J* = 7.0, 2.1 Hz, 16H). ^{13}C NMR (126 MHz, $CDCl_3$) δ 178.43, 177.13, 172.70, 166.89, 130.11, 129.78, 65.84, 44.72, 41.86, 41.68, 40.14, 39.81, 39.30, 36.76, 32.98, 29.13, 28.84, 28.78, 28.43, 25.65, 24.14, 23.86, 23.82, 23.07, 22.48, 22.45, 9.46. HRMS-ESI (m/z): calculated for $C_{53}H_{101}N_2O_{17}Si_8^+$ [M+H]$^+$, 1261.5249; found, 1261.5253; $C_{45}H_{86}N_2NaO_{15}Si_8^+$ [M+Na]$^+$, 1283.5068; found, 1283.5072.

Synthesis of *Z*LSPOSS

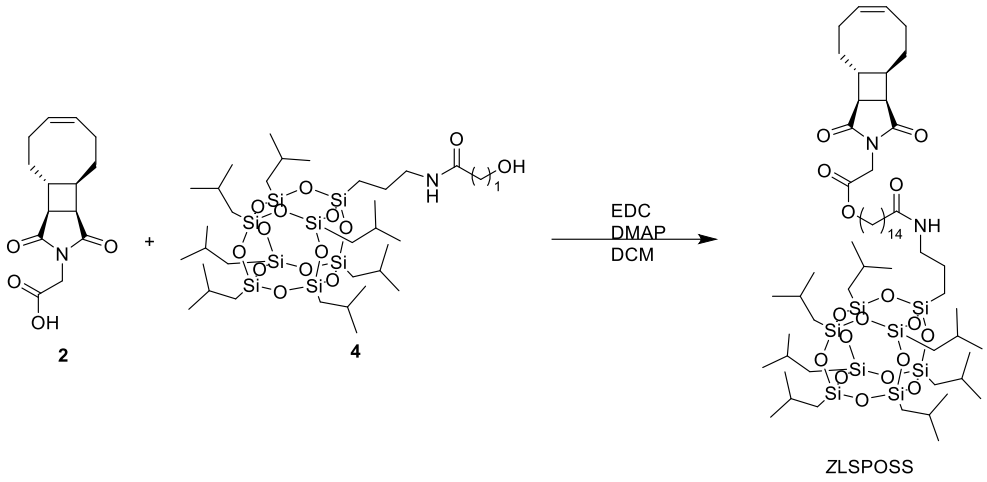

In a vial were added **2** (423.9 mg, 1.60 mmol, 1.00 eq.) and **4** (1797.0 mg, 1.60 mmol, 1.00 eq.) was added. The mixture was dissolved in DCM (10 mL). EDC (618.9 mg 3.20 mmol, 2.00 eq.) and DMAP (19.7 mg, 0.16 mmol, 0.10 eq.) were added at 0 °C while stirring. The mixture was warmed up to 20 °C and stirred for 24 h. The mixture was diluted in Et_2O and washed with water and brine. The organic layer was dried with Na_2SO_4 and filtered. Et_2O was removed in rotary evaporator to give crude product as white solid. The crude was purified via column chromatography (Et_2O:Hex = 7:3) to afford ZLSPOSS as a white powder (1799.5 mg, yield: 83%). ^{1}H NMR (500 MHz, $CDCl_3$) δ 5.66 – 5.55 (m, 2H), 5.41 (t, *J* = 5.9 Hz, 1H), 4.25 (s, 2H), 4.15 (t, *J* = 6.8 Hz, 2H), 3.27 – 3.22 (m, 3H), 2.91 (dd, *J* = 6.3, 6.3 Hz, 1H), 2.76 – 2.68 (m, 1H), 2.50 – 2.43 (m, 1H), 2.29 – 2.17 (m, 2H), 2.15 (t, *J* = 7.7 Hz, 2H), 2.12 – 2.03 (m, 2H), 2.03 – 1.96 (m, 1H), 1.91 – 1.77 (m, 8H), 1.68 – 1.51 (m, 8H), 1.47 – 1.39 (m, 1H), 1.34 – 1.25 (m, 20H), 0.96 (d, *J* = 6.6 Hz, 42H), 0.60 (dd, *J* = 7.0, 2.3 Hz, 16H). ^{13}C NMR (126 MHz, $CDCl_3$) δ 178.56, 177.27, 173.00, 167.06, 130.26, 129.92, 66.13, 44.86, 41.99, 41.77, 40.28, 39.95, 39.45, 37.07, 33.12, 29.73, 29.66, 29.61, 29.60, 29.50, 29.31, 28.92, 28.63, 25.97, 25.87, 25.80, 25.78, 24.29, 24.00, 23.96, 23.21, 22.62, 22.59, 9.58. HRMS-ESI (m/z): calculated for $C_{60}H_{115}N_2O_{17}Si_8^+$ $[M+H]^+$, 1359.6344; found, 1359.6348; $C_{45}H_{86}N_2NaO_{15}Si_8^+$ $[M+Na]^+$, 1381.6164; found, 1381.6165.

Synthesis of tert-butyldimethylsilyl ether **5**

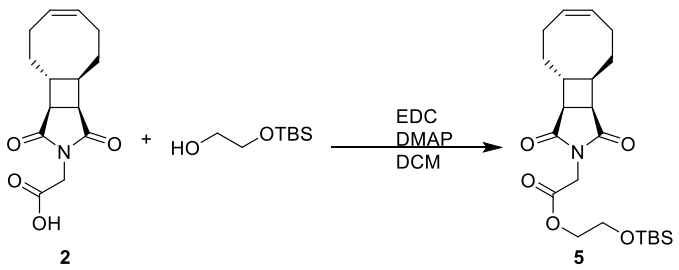

In a vial with **2** (3443.0 mg, 13.08 mmol, 1.0 eq.) and 2-((tert-butyldimethylsilyl)oxy)ethanol (3138.6 µL, 15.70 mmol, 1.2 eq.) was added DCM (10 mL). EDC (5016.0 mg, 26.17 mmol, 2.0 eq.) and DMAP (160.0 mg 1.31 mmol, 0.10

eq.) were added at 0 °C while stirring. The mixture was warmed up to 20 °C and stirred for 24 h. The mixture was diluted with DCM and washed with water three times. The organic layer was dried with Na_2SO_4 and filtered. DCM was removed in rotary evaporator. The crude was purified via column chromatography (Et_2O:Hex = 2:3) to afford **5** as a pale yellow liquid. Purified **5** was kept in freezer. ^{1}H NMR (500 MHz, $CDCl_3$) δ 5.68 – 5.54 (m, 2H), 4.28 (s, 2H), 4.26 – 4.20 (m, 2H), 3.82 (t, *J* = 5.1 Hz, 2H), 3.25 (dd, *J* = 10.5, 6.5 Hz, 1H), 2.91 (dd, *J* = 6.3, 6.3 Hz, 1H), 2.77 – 2.67 (m, 1H), 2.51 – 2.43 (m, 1H), 2.29 – 2.17 (m, 2H), 2.13 – 2.03 (m, 2H), 2.03 – 1.96 (m, 1H), 1.84 – 1.76 (m, 1H), 1.60 – 1.49 (m, 1H), 1.49 – 1.38 (m, 1H), 0.90 (s, 9H), 0.08 (s, 6H). ^{13}C NMR (126 MHz, $CDCl_3$) δ 178.53, 177.25, 167.05, 130.26, 129.90, 67.00, 61.09, 44.86, 41.98, 40.27, 39.94, 39.33, 33.12, 30.99, 28.88, 25.95, 24.29, 23.96, 18.41, -5.21. HRMS-ESI (m/z): calculated for $C_{22}H_{35}NNaO_5Si^+$ $[M+Na]^+$, 444.2177; found, 444.2178.

Synthesis of SS

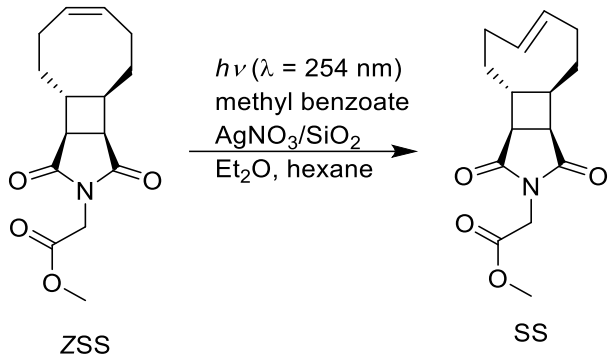

*Z*SS SS

A flow photochemistry setup demonstrated in our previous works[4] was used for the syntheses of all tCBtCO monomers. *Z*SS (1850.0 mg, 6.68 mmol, 1.00 eq.) and methyl benzoate (1682.0 µL, 13.36 mmol, 2.00 eq.) were dissolved in 67 mL of solvent mixture (Et_2O:Hex = 8:2) and transferred into a quartz tube. The solution was irradiated under UV light (λ = 254 nm) while stirring and continuously circulated through a column filled with $AgNO_3$-impregnated silica gel ($AgNO_3$: 2271.0 mg, 13.36 mmol, 2.00 eq.), followed by regular silica gel, for 16 h. After irradiation, the remaining solution was removed from the circulation column. The crude product was extracted via column chromatography using a three-layer separation column consisting of regular silica gel at the bottom (10 mL), fresh $AgNO_3$-impregnated silica gel in the middle (40 mL), and the used silica gel mixture from the circulation column (50 mL) at the top. Solvent mixture (Et_2O:Hex = 8:2) (500 mL) was flushed through the separation column to remove remaining ZSS. Acetone (500 mL) was flushed through the separation column to collect the crude product. Acetone was removed in rotary evaporator. Collected solid was redissolved in 250 mL DCM and 250 mL 5% ammonium hydroxide solution and stirred for 30 min. DCM layer was collected and the aqueous layer was extracted with 250 mL DCM three times. The combined organic layers were dried over Na_2SO_4, filtered, and concentrated in a rotary evaporator. The crude was purified via column chromatography (MeOH:DCM = 3:97)

to afford SS as a pale yellow powder (499.5 mg, yield: 27%). SS contains 7.97% of *Z*SS. SS was stored in freezer until use. ^{1}H NMR (500 MHz, $CDCl_3$) δ 5.84 – 5.42 (m, 2H), 4.29 – 4.24 (m, 2H), 3.80 – 3.76 (m, 3H), 3.29 – 3.16 (m, 1H), 2.95 – 2.80 (m, 1H), 2.57 – 2.29 (m, 3H), 2.21 – 1.94 (m, 5H), 1.92 – 1.74 (m, 1H), 1.61 (m, 1H). ^{13}C NMR (126 MHz, $CDCl_3$) δ 178.77, 178.49, 177.41, 177.07, 167.61, 135.70, 135.48, 134.37, 133.66, 52.76, 49.42, 48.13, 44.18, 41.60, 40.19, 39.24, 35.18, 33.54, 33.42. HRMS-ESI (m/z): calculated for $C_{15}H_{20}NO_4^+$ $[M+H]^+$, 278.1387; found, 278.1388; $C_{15}H_{19}NNaO_4^+$ $[M+Na]^+$, 300.1206; found, 300.1208.

Synthesis of MS

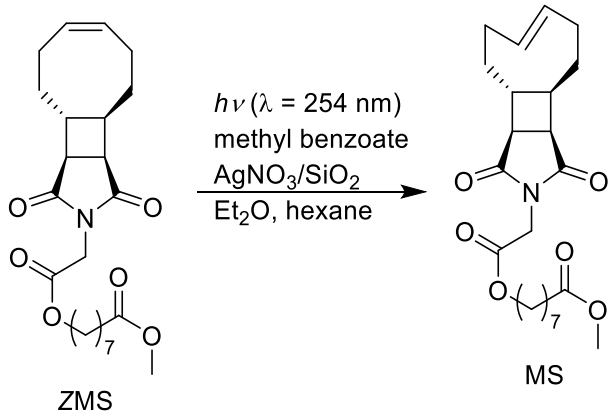

*Z*MS (1200.0 mg, 2.86 mmol, 1.00 eq.) and methyl benzoate (721.3 μL, 5.73 mmol, 2.00 eq.) were dissolved in 100 mL of solvent mixture (Et_2O:Hex = 7:3) and transferred into a quartz tube. The solution was irradiated under UV light (λ = 254 nm) while stirring and continuously circulated through a column filled with $AgNO_3$-impregnated silica gel ($AgNO_3$: 974.0 mg, 5.73 mmol, 2.00 eq.), followed by regular silica gel, for 24 h. After irradiation, the remaining solution was removed from the circulation column. The crude product was extracted via column chromatography using a three-layer separation column consisting of regular silica gel at the bottom (10 mL), fresh $AgNO_3$-impregnated silica gel in the middle (20 mL), and the used silica gel mixture from the circulation column (30 mL) at the top. The column was first flushed with 350 mL of Et_2O:Hex (7:3) to remove unreacted starting material followed by 350 mL of acetone to elute the crude product. The acetone fraction was concentrated using a rotary evaporator. The collected solid was redissolved in 150 mL DCM and 150 mL of 5% ammonium hydroxide solution, then stirred for 30 min. The DCM layer was collected, and the aqueous layer was extracted with 150 mL DCM three times. The combined organic layers were dried over Na_2SO_4, filtered, and concentrated in a rotary evaporator. The crude was purified via column chromatography (MeOH:DCM = 5:95) to afford MS as a pale yellow liquid (446.4 mg, yield: 37%). MS contains 10% of *Z*MS. MS was stored in chloroform at concentration of 96 mM with 3.8 mg BHT. ^{1}H NMR (500 MHz, $CDCl_3$) δ 5.86 – 5.37 (m, 2H), 4.29 – 4.20 (m, 2H), 4.19 – 4.12 (m, 2H), 3.67 (s, 3H), 3.28 – 3.14 (m, 1H), 2.93 – 2.80 (m, 1H), 2.48 – 2.28 (m, 5H), 2.26 – 1.94 (m, 5H), 1.91 – 1.73 (m, 1H), 1.69 – 1.60 (m, 5H), 1.40 – 1.30 (m, 6H). ^{13}C NMR (126 MHz, $CDCl_3$) δ 178.61, 178.33, 177.24,

176.90, 174.10, 167.00, 135.54, 135.29, 134.18, 133.48, 65.87, 51.40, 49.25, 47.95, 44.05, 43.95, 42.94, 41.37, 40.71, 40.04, 39.55, 39.23, 39.12, 35.62, 35.01, 33.98, 33.38, 33.25, 28.93, 28.79, 28.43, 25.71, 25.57, 25.25, 24.79. HRMS-ESI (m/z): calculated for $C_{23}H_{34}NO_6^+$ $[M+H]^+$, 420.2381; found, 420.2379; $C_{23}H_{33}NNaO_6^+$ $[M+Na]^+$, 442.2200; found, 442.2200.

Synthesis of LS

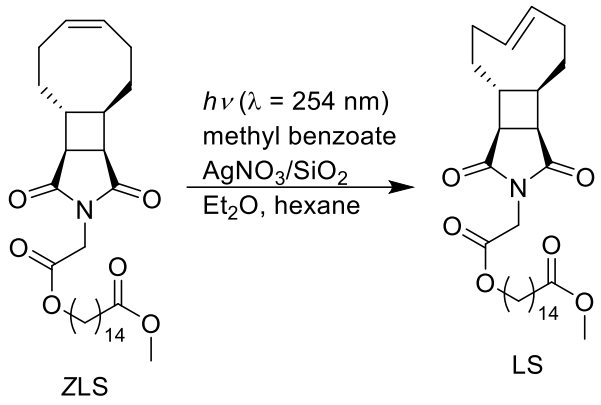

*Z*LS (900.0 mg, 1.74 mmol, 1.00 eq.) and methyl benzoate (438.4 μL, 3.48 mmol, 2.00 eq.) were dissolved in 100 mL of solvent mixture (Et_2O:Hex = 7:3) and transferred into a quartz tube. The solution was irradiated under UV light (λ = 254 nm) while stirring and continuously circulated through a column filled with $AgNO_3$-impregnated silica gel ($AgNO_3$: 592.0 mg, 3.48 mmol, 2.00 eq.), followed by regular silica gel, for 24 h. After irradiation, the remaining solution was removed from the circulation column. The crude product was extracted via column chromatography using a three-layer separation column consisting of regular silica gel at the bottom (5 mL), fresh $AgNO_3$-impregnated silica gel in the middle (12 mL), and the used silica gel mixture from the circulation column (30 mL) at the top. The column was first flushed with 300 mL of Et_2O:Hex (7:3) to remove unreacted starting material followed by 300 mL of acetone to elute the crude product. The acetone fraction was concentrated using a rotary evaporator. The collected solid was redissolved in 150 mL DCM and 150 mL of 5% ammonium hydroxide solution, then stirred for 30 min. The DCM layer was collected, and the aqueous layer was extracted with 150 mL DCM three times. The combined organic layers were dried over Na_2SO_4, filtered, and concentrated in a rotary evaporator. The crude was purified via column chromatography (MeOH:DCM = 2:98) to afford LS as a pale yellow solid (430.0 mg, yield: 48%). LS was stored in a freezer. ^{1}H NMR (500 MHz, $CDCl_3$) δ 5.84 – 5.43 (m, 2H), 4.28 – 4.20 (m, 2H), 4.16 (td, *J* = 6.8, 3.2 Hz, 2H), 3.66 (s, 3H), 3.25 – 3.14 (m, 1H), 2.82 (dd, *J* = 6.3, 6.3 Hz, 1H), 2.56 – 2.32 (m, 3H), 2.30 (t, *J* = 7.4 Hz, 2H), 2.21 – 1.97 (m, 5H), 1.91 – 1.75 (m, 1H), 1.72 – 1.55 (m, 5H), 1.28 (d, *J* = 16.2 Hz, 20H). ^{13}C NMR (126 MHz, $CDCl_3$) δ 178.77, 178.49, 177.40, 177.05, 174.42, 167.17, 135.70, 135.46, 134.36, 133.65, 66.19, 51.52, 49.40, 48.10, 44.22, 44.12, 43.10, 41.54, 40.87, 40.20, 39.71, 39.40, 39.28, 35.79, 35.17, 34.26, 33.54, 33.41, 31.01, 29.73, 29.70, 29.67, 29.61, 29.57, 29.38, 29.34, 29.29, 28.68, 25.91, 25.41, 25.10.

HRMS-ESI (m/z): calculated for $C_{30}H_{48}NO_6^+$ [M+H]$^+$, 518.3476; found, 518.3476; $C_{30}H_{47}NNaO_6^+$ [M+Na]$^+$, 540.3296; found, 540.3294.

Synthesis of Bn

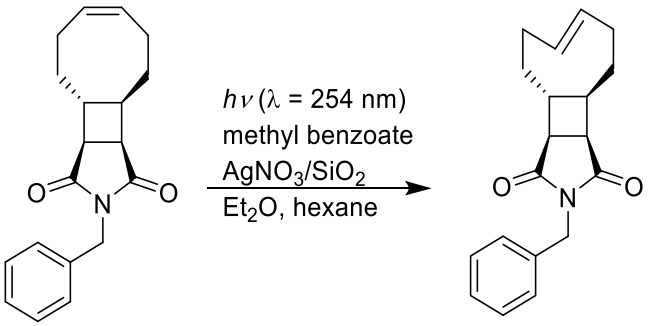

*Z*Bn Bn

*Z*Bn (201.4 mg, 0.68 mmol, 1.00 eq.) and methyl benzoate (171.9 μL, 1.36 mmol, 2.00 eq.) were dissolved in 100 mL of solvent mixture (Et_2O:Hex = 6:4) and transferred into a quartz tube. The solution was irradiated under UV light (λ = 254 nm) while stirring and continuously circulated through a column filled with $AgNO_3$-impregnated silica gel ($AgNO_3$: 232.0 mg, 1.36 mmol, 2.00 eq.), followed by regular silica gel, for 13 h. After irradiation, the remaining solution was removed from the circulation column. The crude product was extracted via column chromatography using a three-layer separation column consisting of regular silica gel at the bottom (5 mL), fresh $AgNO_3$-impregnated silica gel in the middle (5 mL), and the used silica gel mixture from the circulation column (30 mL) at the top. The column was first flushed with 250 mL of Et_2O:Hex (6:4) to remove unreacted starting material followed by 250 mL of acetone to elute the crude product. The acetone fraction was concentrated using a rotary evaporator. The collected solid was redissolved in 100 mL DCM and 100 mL of 5% ammonium hydroxide solution, then stirred for 30 min. The DCM layer was collected, and the aqueous layer was extracted with 100 mL DCM three times. The combined organic layers were dried over Na_2SO_4, filtered, and concentrated in a rotary evaporator. The crude was purified via column chromatography in chloroform to afford Bn as a white solid (103.3 mg, yield: 51%). Bn was stored in a freezer. ^{1}H NMR (500 MHz, $CDCl_3$) δ 7.41 – 7.26 (m, 5H), 5.80 – 5.26 (m, 2H), 4.66 (d, *J* = 2.5 Hz, 2H), 3.23 – 3.06 (m, 1H), 2.76 (dd, *J* = 6.8, 5.4 Hz, 1H), 2.51 – 2.22 (m, 3H), 2.16 – 2.08 (m, 2H), 2.08 – 1.94 (m, 2H), 1.90 – 1.76 (m, 2H), 1.31 – 1.21 (m, 1H). ^{13}C NMR (126 MHz, $CDCl_3$) δ 179.20, 177.67, 136.14, 133.92, 133.62, 128.68, 128.61, 127.86, 48.10, 43.89, 42.25, 41.27, 39.92, 39.02, 35.23, 33.37, 33.20. HRMS-ESI (m/z): calculated for $C_{19}H_{22}NO_2^+$ [M+H]$^+$, 296.1645; found, 296.1645; $C_{19}H_{21}NNaO_2^+$ [M+Na]$^+$, 318.1465; found, 318.1465.

Synthesis of SSPOSS

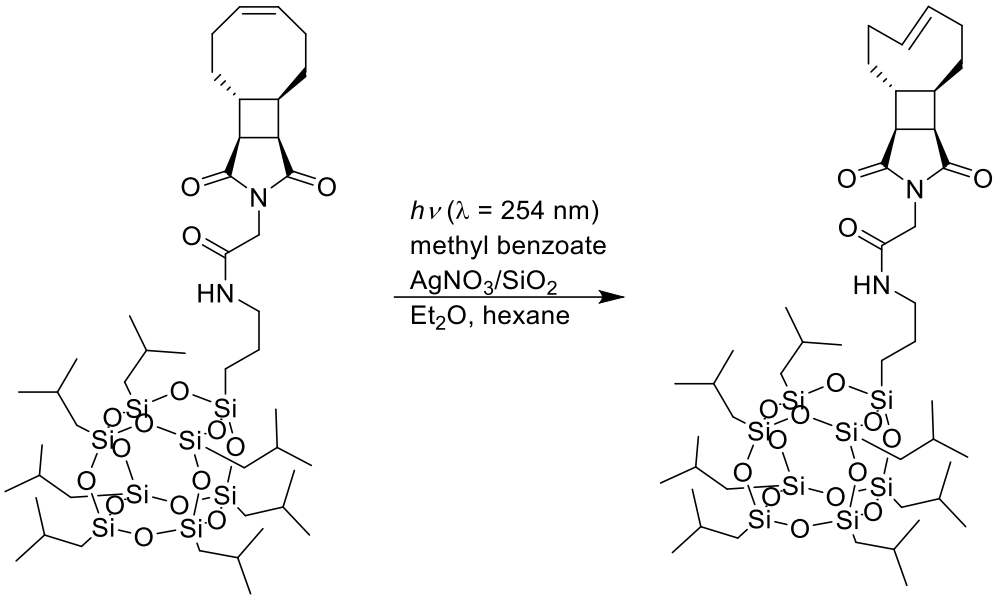

*Z*SSPOSS SSPOSS

*Z*SSPOSS (1143.9 mg, 1.02 mmol, 1.00 eq.) and methyl benzoate (257.2 μL, 2.04 mmol, 2.00 eq.) were dissolved in 100 mL of solvent mixture (Et_2O:Hex = 8:2) and transferred into a quartz tube. The solution was irradiated under UV light (λ = 254 nm) while stirring and continuously circulated through a column filled with $AgNO_3$-impregnated silica gel ($AgNO_3$: 347.3 mg, 2.04 mmol, 2.00 eq.), followed by regular silica gel, for 18 h. After irradiation, the remaining solution was removed from the circulation column. The crude product was extracted via column chromatography using a three-layer separation column consisting of regular silica gel at the bottom (5 mL), fresh $AgNO_3$-impregnated silica gel in the middle (7 mL and the used silica gel mixture from the circulation column (30 mL) at the top. The column was first flushed with 200 mL of Et_2O:Hex (8:2) to remove unreacted starting material followed by 200 mL of acetone to elute the crude product. The acetone fraction was concentrated using a rotary evaporator. The collected solid was redissolved in 100 mL DCM and 100 mL of 5% ammonium hydroxide solution, then stirred for 30 min. The DCM layer was collected, and the aqueous layer was extracted with 150 mL DCM three times. The combined organic layers were dried over Na_2SO_4, filtered, and concentrated in a rotary evaporator. The crude was purified via column chromatography (Et_2O:Hex = 8:2) to afford SSPOSS as a white powder (374.9 mg, yield: 33%). SSPOSS was stored in a freezer. ^{1}H NMR (500 MHz, $CDCl_3$) δ 5.82 – 5.44 (m, 3H), 4.16 – 4.07 (m, 2H), 3.32 – 3.25 (m, 2H), 3.24 – 3.14 (m, 1H), 2.81 (dd, *J* = 6.7, 5.8 Hz, 1H), 2.39 – 2.25 (m, 3H), 2.21 – 1.96 (m, 5H), 1.86 (dtd, *J* = 13.5, 6.8, 2.0 Hz, 8H), 1.70 – 1.58 (m, 3H), 0.96 (dd, *J* = 6.6, 3.5 Hz, 42H), 0.61 (dd, *J* = 7.0, 6.0 Hz, 16H). ^{13}C NMR (126 MHz, $CDCl_3$) δ 179.09, 177.76, 165.40, 134.52, 133.53, 48.08, 44.27, 42.35, 41.56, 40.99, 40.27, 39.27, 35.15, 33.51, 33.46, 25.83, 24.02, 23.09, 22.64, 9.61. HRMS-ESI (m/z): calculated for $C_{45}H_{87}N_2O_{15}Si_8^+$ $[M+H]^+$, 1119.4255; found, 1119.4254; $C_{45}H_{86}N_2NaO_{15}Si_8^+$ $[M+Na]^+$, 1141.4074; found,

1141.4071.

Synthesis of MSPOSS

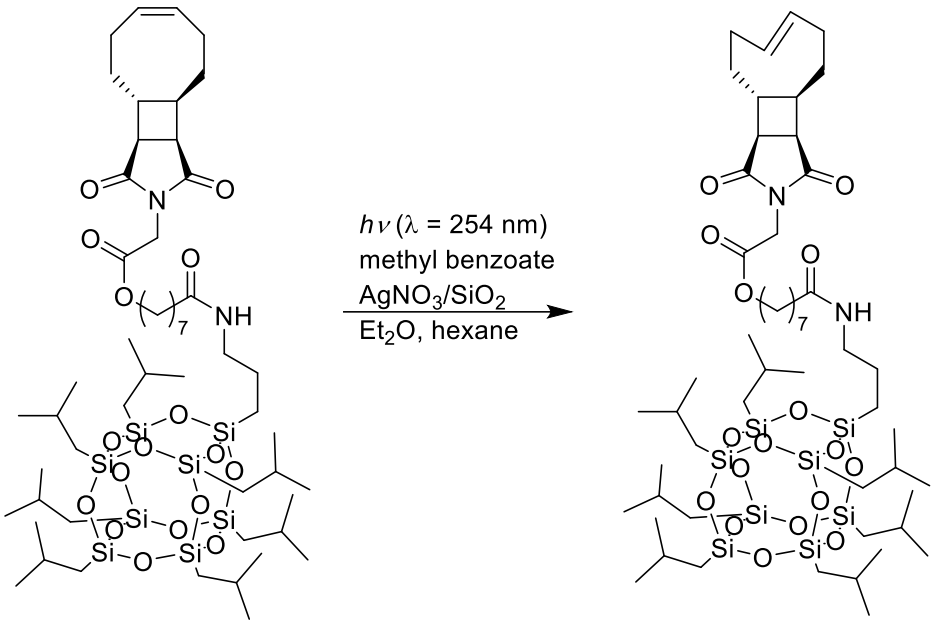

ZMSPOSS MSPOSS

*Z*MSPOSS (1200 mg, 0.95 mmol, 1.00 eq.) and methyl benzoate (240.0 μL, 1.90 mmol, 2.00 eq.) were dissolved in 100 mL of solvent mixture (Et_2O:Hex = 8:2) and transferred into a quartz tube. The solution was irradiated under UV light (λ = 254 nm) while stirring and continuously circulated through a column filled with $AgNO_3$-impregnated silica gel ($AgNO_3$: 323 mg, 1.90 mmol, 2.00 eq.), followed by regular silica gel, for 15 h. After irradiation, the remaining solution was removed from the circulation column. The crude product was extracted via column chromatography using a three-layer separation column consisting of regular silica gel at the bottom (5 mL), fresh $AgNO_3$-impregnated silica gel in the middle (7 mL), and the used silica gel mixture from the circulation column (30 mL) at the top. The column was first flushed with 200 mL of Et_2O:Hex (8:2) to remove unreacted starting material followed by 200 mL of acetone to elute the crude product. The acetone fraction was concentrated using a rotary evaporator. The collected solid was redissolved in 100 mL DCM and 100 mL of 5% ammonium hydroxide solution, then stirred for 30 min. The DCM layer was collected, and the aqueous layer was extracted with 150 mL DCM three times. The combined organic layers were dried over Na_2SO_4, filtered, and concentrated in a rotary evaporator. The crude was purified via column chromatography (Et_2O:Hex = 8:2) to afford MSPOSS as a white powder (499.0 mg, yield: 42%). MSPOSS was stored in a freezer. ^{1}H NMR (500 MHz, $CDCl_3$) δ 5.84 – 5.29 (m, 3H), 4.28 – 4.20 (m, 2H), 4.18 – 4.14 (m, 2H), 3.28 – 3.15 (m, 3H), 2.94 – 2.81 (m, 1H), 2.48 – 2.29 (m, 3H), 2.19 – 1.98 (m, 6H), 1.92 – 1.79 (m, 8H), 1.70 – 1.54 (m, 8H), 1.41 – 1.29 (m, 6H), 0.96 (d, *J* = 6.6 Hz, 42H), 0.61 (dd, *J* = 7.1, 2.2 Hz, 16H). ^{13}C NMR (126 MHz, $CDCl_3$) δ 178.61, 177.23, 172.69, 166.98, 134.17, 133.48, 65.87, 47.95, 44.05, 41.68, 41.37, 40.03, 39.22, 39.12, 36.76, 35.01, 33.38,

33.24, 29.13, 28.85, 28.45, 25.64, 23.86, 23.81, 23.06, 22.48, 22.45, 9.46. HRMS-ESI (m/z): calculated for $C_{53}H_{101}N_2O_{17}Si_8^+$ $[M+H]^+$, 1261.5249; found, 1261.5250; $C_{45}H_{86}N_2NaO_{15}Si_8^+$ $[M+Na]^+$, 1283.5068; found, 1283.5070.

Synthesis of LSPOSS

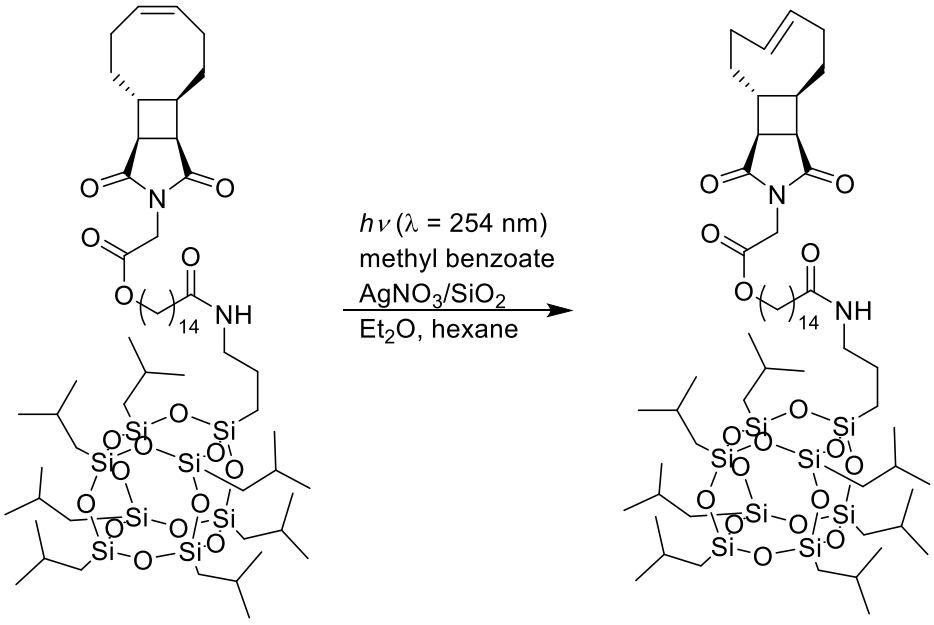

ZLSPOSS LSPOSS

*Z*LSPOSS (1200 mg, 0.95 mmol, 1.00 eq.) and methyl benzoate (240.0 μL, 1.90 mmol, 2.00 eq.) were dissolved in 100 mL of a solvent mixture (Et_2O:Hex = 8:2) and transferred into a quartz tube. The solution was irradiated under UV light (λ = 254 nm) while stirring and continuously circulated through a column filled with $AgNO_3$-impregnated silica gel ($AgNO_3$: 323.0 mg, 1.90 mmol, 2.00 eq.), followed by regular silica gel, for 15 h. After irradiation, the remaining solution was removed from the circulation column. The crude product was extracted via column chromatography using a three-layer separation column consisting of regular silica gel at the bottom (5 mL), fresh $AgNO_3$-impregnated silica gel in the middle (7 mL), and the used silica gel mixture from the circulation column (30 mL) at the top. The column was first flushed with 200 mL of Et_2O:Hex (8:2) to remove unreacted starting material followed by 200 mL of acetone to elute the crude product. The acetone fraction was concentrated using a rotary evaporator. The collected solid was redissolved in 100 mL DCM and 100 mL of 5% ammonium hydroxide solution, then stirred for 30 min. The DCM layer was collected, and the aqueous layer was extracted with 150 mL DCM three times. The combined organic layers were dried over Na_2SO_4, filtered, and concentrated in a rotary evaporator. The crude was purified via column chromatography (Et_2O:Hex = 8:2) to afford LSPOSS as a white powder (499.0 mg, yield: 42%). LSPOSS was stored in a freezer. ^{1}H NMR (500 MHz, $CDCl_3$) δ 5.85 – 5.43 (m, 2H), 5.40 (t, *J* = 5.8 Hz, 1H), 4.29 – 4.19 (m, 2H), 4.18 – 4.13 (m, 2H), 3.29 – 3.12 (m, 3H), 2.85 – 2.79 (m, 1H), 2.46 – 2.29 (m, 3H), 2.20 – 1.99 (m, 7H), 1.90 – 1.80 (m, 8H), 1.68 – 1.56 (m, 7H), 1.38 – 1.25 (m, 20H), 0.96 (d, *J* = 6.6 Hz, 42H),

0.60 (dd, *J* = 7.1, 2.3 Hz, 16H). ^{13}C NMR (126 MHz, $CDCl_3$) δ 178.76, 177.39, 173.02, 167.15, 134.34, 133.63, 66.18, 48.09, 44.20, 41.78, 41.52, 40.19, 39.38, 39.27, 37.08, 35.16, 33.53, 33.40, 29.74, 29.67, 29.62, 29.60, 29.51, 29.33, 28.66, 25.98, 25.90, 25.81, 25.79, 24.01, 23.96, 23.21, 22.63, 22.59, 9.59. HRMS-ESI (m/z): calculated for $C_{60}H_{115}N_2O_{17}Si_8^+$ $[M+H]^+$, 1359.6344; found, 1359.6340; $C_{45}H_{86}N_2NaO_{15}Si_8^+$ $[M+Na]^+$, 1381.6164; found, 1381.6168.

Synthesis of alcohol **6**

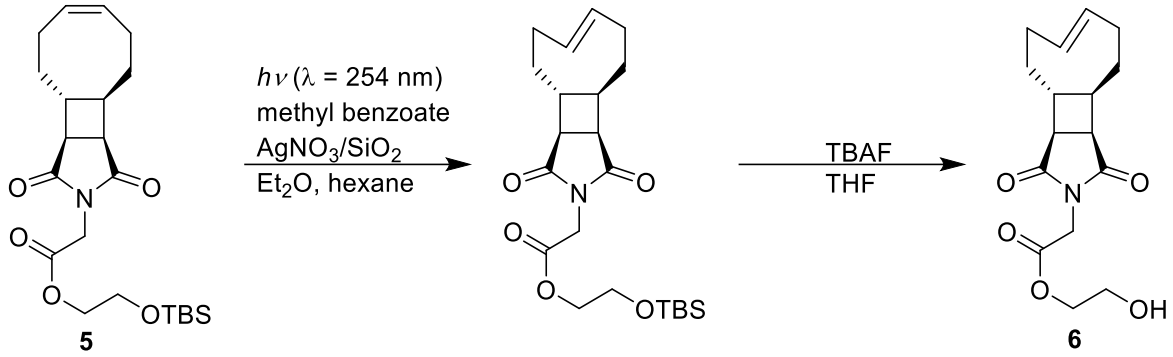

tert-Butyldimethylsilyl ether **5** (4423.3 mg, 10.50 mmol, 1.00 eq.) and methyl benzoate (2647.0 µL, 21.00 mmol, 2.00 eq.) were dissolved in 100 mL of a solvent mixture (Et_2O:Hex = 85:15) and transferred into a quartz tube. The solution was irradiated under UV light (λ = 254 nm) while stirring and continuously circulated through a column filled with $AgNO_3$-impregnated silica gel ($AgNO_3$: 3567.0 mg, 21.00 mmol, 2.00 eq.), followed by regular silica gel, for 15 h. After irradiation, the remaining solution was removed from the circulation column. The crude product was extracted via column chromatography using a three-layer separation column consisting of regular silica gel (30 mL) at the bottom, fresh $AgNO_3$-impregnated silica gel (70 mL) in the middle, and the used silica gel mixture from the circulation column (100 mL) at the top. The column was first flushed with 1000 mL of Et_2O:Hex (85:15) to remove unreacted starting material, followed by 1000 mL of acetone to elute the crude product. The acetone fraction was concentrated using a rotary evaporator. The collected solid was redissolved in 300 mL DCM and 300 mL of 5% ammonium hydroxide solution, then stirred for 30 min. The DCM layer was collected, and the aqueous layer was extracted with 300 mL DCM three times. The combined organic layers were dried over Na_2SO_4, filtered, and concentrated in a rotary evaporator. The crude was purified via column chromatography (Et_2O:Hex = 2:3), yielding a yellow liquid. The obtained yellow liquid was dissolved in THF (5.66 mL) and treated with TBAF (1 M in THF, 5.66 mL, 1.2 eq.), then stirred for 30 min. The mixture was diluted with 200 mL of water and extracted with ethyl acetate (3 × 200 mL). The combined organic layers were dried over Na_2SO_4, filtered, and concentrated using a rotary evaporator. The crude product was further purified by column chromatography (acetone:hexane = 2:3) to afford **6** as a white solid (859 mg, overall yield: 31%). **6** was stored in a freezer. ^{1}H NMR (400 MHz, $CDCl_3$) δ 5.87 – 5.36 (m, 2H), 4.39 – 4.22 (m, 4H), 3.91 – 3.80 (m, 2H), 3.31 – 3.13 (m, 1H), 2.89 – 2.79 (m, 1H), 2.47 –

2.29 (m, 3H), 2.22 – 1.93 (m, 6H), 1.93 – 1.78 (m, 1H), 1.69 – 1.51 (m, 1H). ^{13}C NMR (126 MHz, $CDCl_3$) δ 178.92, 177.51, 167.30, 134.36, 133.68, 67.45, 60.95, 48.14, 44.22, 41.55, 40.19, 39.45, 39.34, 35.21, 33.54, 33.41. HRMS-ESI (m/z): calculated for $C_{16}H_{21}NNaO_5^+$ $[M+Na]^+$, 330.1312; found, 330.1314.

Synthesis of PLLA

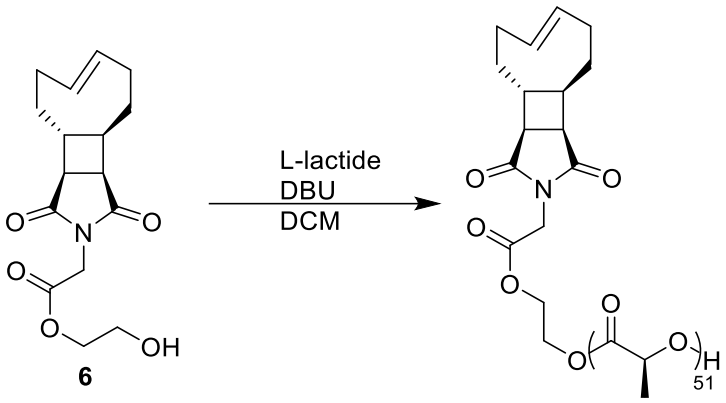

6

PLLA

The synthesis was performed in a nitrogen-filled MBraun Labstar Pro glovebox. In a vial with alcohol **6** (175.4 mg, 0.57 mmol, 1.0 eq.) and L-lactide (2140.0 mg, 14.8 mmol, 26.0 eq.) was added 13.3 mL of DCM. The mixture was stirred at ambient temperature for 1 h for complete dissolution. While rigorous stirring, 1% DBU solution in DCM (870.0 µL, 57.1 µmol, 0.1 eq.) was added. The polymerization was quenched with 6.53 µL acetic acid. The mixture was precipitated into methanol to afford PLLA as a white powder. (conversion: 96%)

Synthesis of 4-(isobutylPOSS-propylthio)butanoic acid **7**

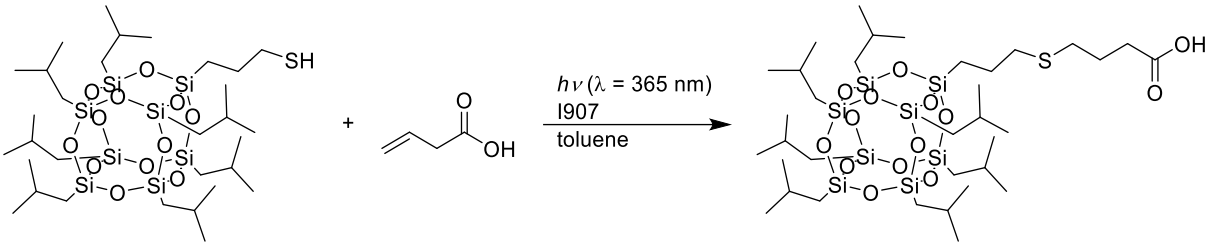

7

A 4 mL vial was charged with PSS-(3-Mercapto)propyl-heptaisobutyl (200.0 mg, 224.3 µmol, 1.0 eq.), 3-butenoic acid (56.8 µL, 672.6 µmol. 3.0 eq.) and I907 in toluene (2 mL, 2.2 nmol, 1.0 x 10^{-5} eq.). The solution was degassed via nitrogen gas sparging for 30 min. The degassed mixture was stirred under irradiation for 3 h. Toluene was removed at reduced pressure and purified via column chromatography (MeOH:DCM = 5:95) to afford **7** as a white solid (135.7 mg, yield: 61.9%). ^{1}H NMR (500 MHz, $CDCl_3$) δ 2.83 – 2.39 (m, 6H), 1.95 – 1.79 (m, 9H), 1.75 – 1.62 (m, 2H), 0.96 (dd, *J* = 6.6, 1.0 Hz, 42H), 0.74 – 0.69 (m, 2H), 0.60 (dd, *J* = 7.0, 2.6 Hz, 14H). ^{13}C NMR (126 MHz, $CDCl_3$) δ 178.99, 34.90, 32.81, 31.16, 25.92, 25.85, 25.83, 25.71, 24.55, 24.11, 24.05, 24.01, 23.23, 22.68, 22.65, 11.80. HRMS-ESI (m/z):

calculated for $C_{35}H_{76}NaO_{14}SSi_8^+$ $[M+Na]^+$, 999.3002; found, 999.2990.

Synthesis of M'SPOSS

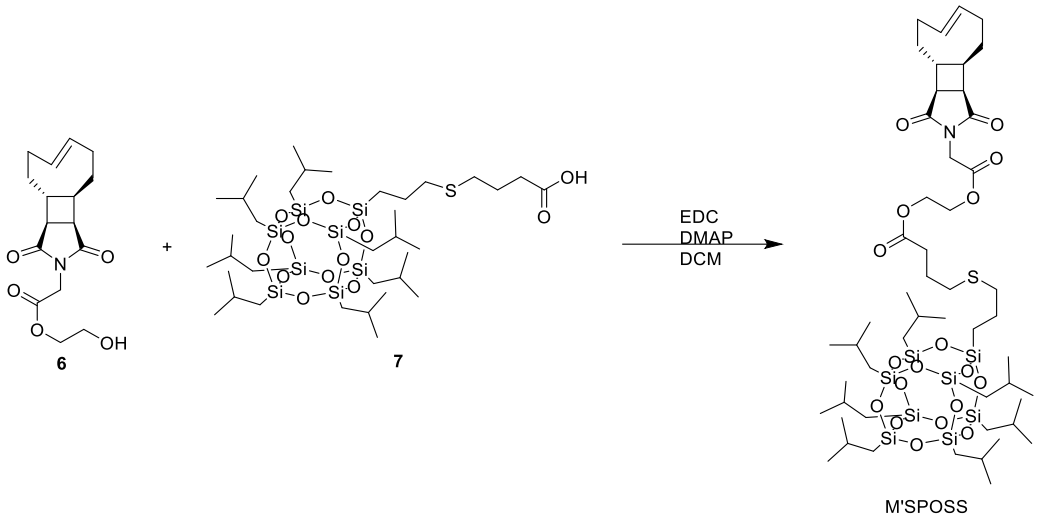

In a vial with **6** (135.7 mg, 0.44 mmol. 1.0 eq.) and **7** (475.0 mg, 0.49 mmol, 1.1 eq.) were added 5 mL DCM for dissolution. EDC (169.7 mg, 0.88 mmol, 2.0 eq.) and DMAP (5.4 mg, 0.044 mmol, 0.1 eq.) were subsequently added to the mixture. The mixture was stirred for 24 h. The solution was diluted in DCM and washed with water and brine. The organic layer was collected, dried with Na2SO4, filtered, and concentrated. The crude was purified via column chromatography (EA:DCM = 2:98) to afford M'SPOSS as a white powder (250 mg, yield: 45%). ^{1}H NMR (500 MHz, $cdcl_3$) δ 5.88 – 5.40 (m, 2H), 4.44 – 4.22 (m, 6H), 3.27 – 3.17 (m, 1H), 2.88 – 2.80 (m, 1H), 2.59 – 2.44 (m, 6H), 2.41 – 2.26 (m, 3H), 2.22 – 2.06 (m, 4H), 2.08 – 1.99 (m, 1H), 1.96 – 1.79 (m, 10H), 1.72 – 1.63 (m, 2H), 1.65 – 1.57 (m, 1H), 0.96 (d, *J* = 6.6 Hz, 42H), 0.74 – 0.68 (m, 2H), 0.68 – 0.52 (m, 14H). ^{13}C NMR (126 MHz, $CDCl_3$) δ 178.71, 177.34, 172.95, 167.03, 134.35, 133.65, 63.60, 61.82, 48.15, 44.22, 41.55, 40.20, 39.31, 39.24, 35.20, 34.90, 33.54, 33.42, 32.90, 31.20, 25.82, 24.68, 24.03, 23.99, 23.17, 22.66, 22.62, 11.79.

Synthesis of Polymers

General Procedure for Living Ring-Opening Metathesis Polymerizations

All living ROMP reactions were conducted in a nitrogen-filled MBraun Labstar Pro glovebox. Typically, tCBtCO monomers (100 mg, 1000 eq.) and triphenyl phosphine (30 eq.) were dissolved in degassed THF. For ultrasonication experiments, 1000 eq. of tCBtCO monomers were used, whereas varying equivalents were used for static and dynamic light scattering analyses. Separately, Grubbs 1st generation catalyst (G1) was dissolved in degassed THF to prepare a 5 mM stock solution. The G1 stock solution (1 eq.) was then added to the tCBtCO solution under vigorous stirring. The final concentration of tCBtCO was maintained above 0.05 M to prevent depolymerization. After 2 h of stirring, the polymerization was quenched with ethyl vinyl ether (EVE).

Synthesis of PSS

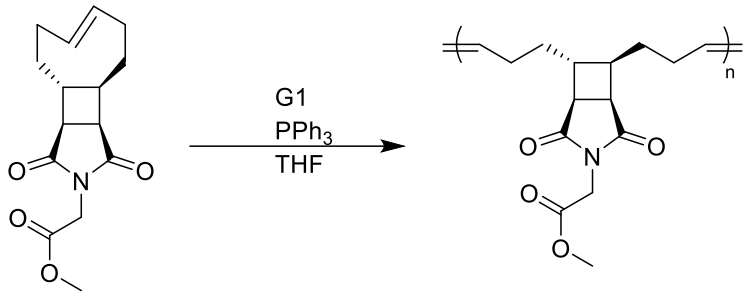

SS PSS

The general polymerization procedure was used. The PSS polymerization solutions were precipitated into methanol three times, yielding PSS as a white solid (conversion: >96%). ^{1}H NMR (500 MHz, $CDCl_3$) δ 5.51 – 5.24 (m br, 2H), 4.26 (s, 2H), 3.75 (s, 3H), 3.41 – 3.29 (m br, 1H), 2.97 – 2.85 (m br, 1H), 2.49 – 2.36 (m br, 1H), 2.22 – 1.94 (m br, 5H), 1.74 – 1.58 (m br, 3H), 1.49 – 1.37 (m br, 1H).

Synthesis of PMS

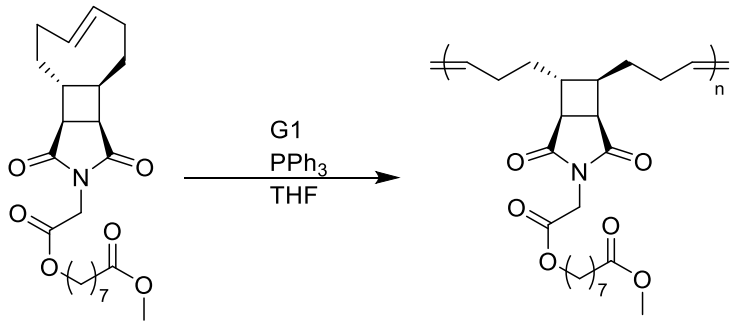

MS PMS

The general polymerization procedure was used. The PMS polymerization solutions were precipitated into methanol three times, yielding PMS as a clear liquid (conversion: >99%). ^{1}H NMR (500 MHz, $CDCl_3$) δ 5.47 – 5.27 (m br, 2H), 4.31 – 4.18 (m, 2H), 4.13 (t, *J* = 6.7 Hz, 2H), 3.66 (s, 3H), 3.40 – 3.28 (m br, 1H), 2.97 – 2.83 (m br, 1H), 2.47 – 2.36 (m br, 1H), 2.30 (t, *J* = 7.5 Hz, 2H), 2.20 – 1.95 (m br, 5H), 1.72 – 1.59 (m br, 7H), 1.48 – 1.39 (m br, 1H), 1.37 – 1.30 (m br, 6H).

Synthesis of PLS

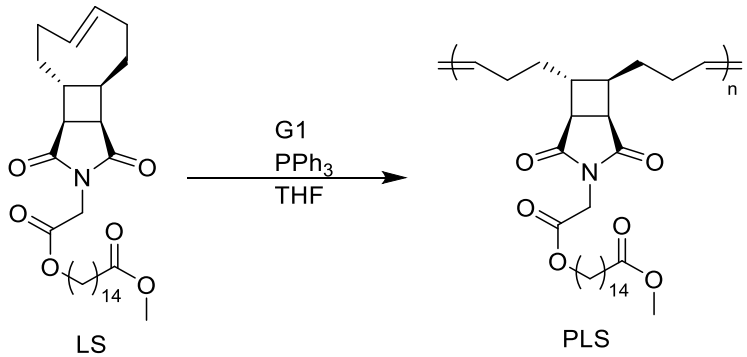

LS PLS

The general polymerization procedure was used. The PLS polymerization solutions were precipitated into methanol three times, yielding PLS as a white solid (conversion: >99%). ^{1}H NMR (500 MHz, $CDCl_3$) δ 5.46 – 5.27 (m br, 2H), 4.29 – 4.19 (m br, 2H), 4.13 (t, *J* = 6.8 Hz, 2H), 3.66 (s, 3H), 3.40 – 3.29 (m br, 1H), 2.97 – 2.85 (m br, 1H), 2.42 (m br, 1H), 2.30 (t, *J* = 7.6 Hz, 2H), 2.20 – 1.96 (m br, 5H), 1.71 – 1.57 (m br, 7H), 1.48 – 1.39 (m br, 1H), 1.36 – 1.25 (m br, 20H).

Synthesis of PSSPOSS

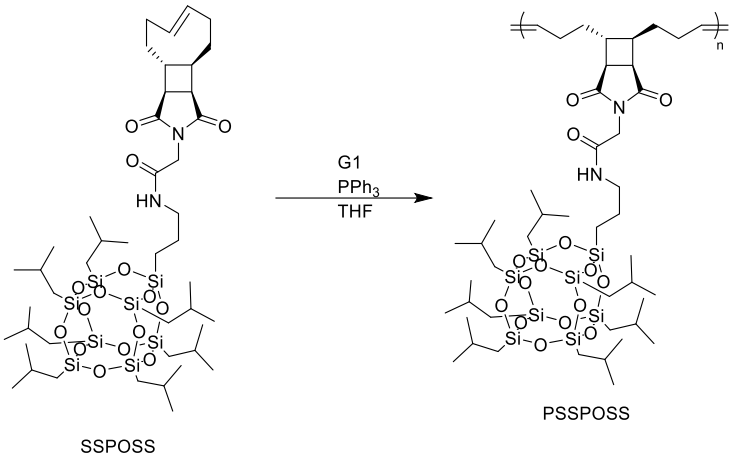

The general polymerization procedure was used. The PSSPOSS polymerization solutions were precipitated into methanol three times, yielding PSSPOSS as a white powder (conversion: >99%). ^{1}H NMR (500 MHz, $cdcl_3$) δ 6.04 – 5.61 (m br, 1H), 5.49 – 5.23 (m br, 2H), 4.30 – 3.96 (m br, 2H), 3.38 – 3.29 (m br, 1H), 3.29 – 3.15 (m br, 2H), 3.04 – 2.80 (m br, 1H), 2.50 – 2.33 (m br, 1H), 2.29 – 1.92 (m br, 5H), 1.89 – 1.81 (m br, 7H), 1.72 – 1.57 (m br, 5H), 1.49 – 1.35 (m br, 1H), 0.96 (d, *J* = 6.6 Hz, 42H), 0.61 (dd, *J* = 7.1, 4.6 Hz, 16H).

Synthesis of PMSPOSS

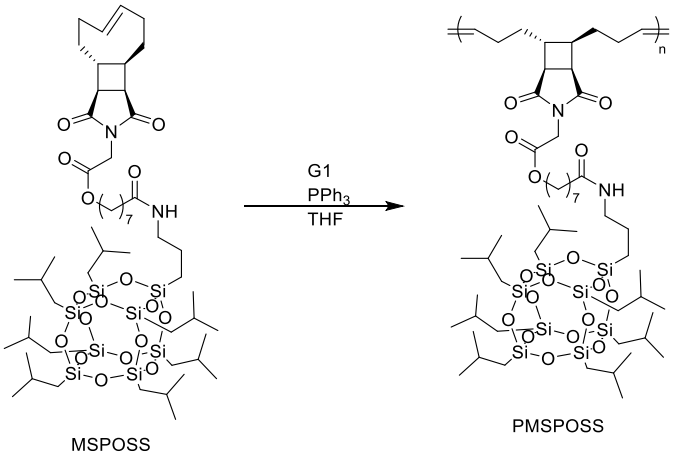

The general polymerization procedure was used. The PMSPOSS polymerization solutions were precipitated into methanol three times, yielding PMSPOSS as a white powder. (conversion: >99%) ^{1}H NMR (500 MHz, $CDCl_3$) δ 5.64 (br, 1H), 5.49 – 5.25

(m br, 2H), 4.24 (t, *J* = 19.9 Hz, 2H), 4.13 (t, *J* = 6.6 Hz, 2H), 3.40 – 3.30 (m br, 1H), 3.24 (dd, *J* = 6.7, 6.6 Hz, 2H), 2.97 – 2.85 (m br, 1H), 2.47 – 2.36 (m br, 1H), 2.25 – 2.11 (m br, 4H), 2.10 – 1.95 (m br, 3H), 1.92 – 1.78 (m br, 8H), 1.65 – 1.56 (m br, 8H), 1.47 – 1.40 (m br, 1H), 1.36 – 1.31 (m br, 6H), 0.96 (d, *J* = 6.6 Hz, 42H), 0.60 (d, *J* = 7.0 Hz, 16H).

Synthesis of PLSPOSS

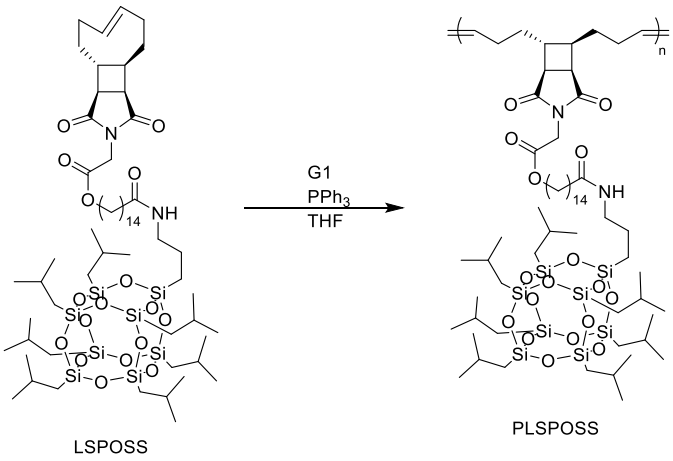

The general polymerization procedure was used. The PLSPOSS polymerization solutions were precipitated into methanol three times, yielding PLSPOSS as a white powder. (conversion: >99%) ^{1}H NMR (500 MHz, $CDCl_3$) δ 5.51 (br, 1H), 5.46 – 5.25 (m br, 2H), 4.26 (t, *J* = 19.5 Hz, 2H), 4.13 (t, *J* = 6.7 Hz, 2H), 3.43 – 3.28 (m br, 1H), 3.24 (dd, *J* = 6.7, 6.7 Hz, 2H), 3.05 – 2.80 (m br, 1H), 2.51 – 2.33 (m br, 1H), 2.31 – 1.92 (m br, 7H), 1.90 – 1.81 (m br, 7H), 1.65 – 1.56 (m br, 9H), 1.47 – 1.39 (m, br 1H), 1.37 – 1.24 (m br, 20H), 0.96 (d, *J* = 6.6 Hz, 42H), 0.60 (dd, *J* = 7.0, 2.1 Hz, 16H).

Synthesis of PPLLA

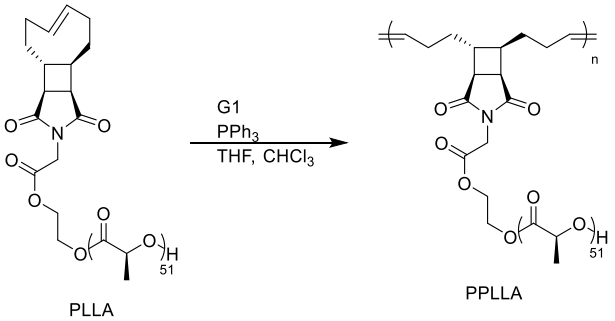

The general polymerization procedure was used except for the solvent. Solvent mixture (THF:$CHCl_3$ = 1:3) was used to facilitate the dissolution of PLLA. The PPLLA polymerization solutions were precipitated into methanol three times, yielding PPLLA as a white powder. (conversion: 97%) ^{1}H NMR (500 MHz, $CDCl_3$) δ 5.57 – 5.27 (m br, 2H), 5.26 – 5.07 (m br, 50H), 4.90 – 3.79 (m br, 7H), 3.58 – 3.24 (m br, 1H), 3.08 – 2.75 (m br, 1H), 2.71 – 2.64 (m br, 1H), 2.54 – 2.33 (m br, 1H), 2.24 – 1.90 (m br,

4H), 1.64 – 1.47 (m br, 153H).

Synthesis of PM'SPOSS

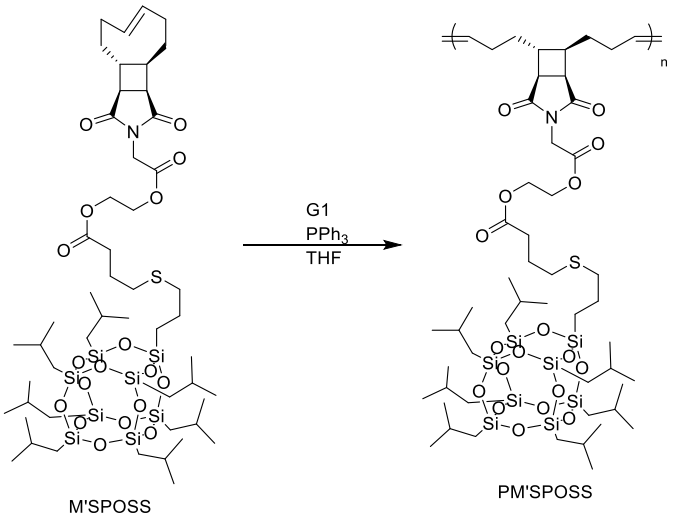

The general polymerization procedure was used. The PM'SPOSS polymerization solution was precipitated into methanol twice to afford PM'SPOSS as a white powder. (conversion: >99%) ^{1}H NMR (500 MHz, $CDCl_3$) δ 5.52 – 5.17 (m br, 2H), 4.45 – 4.14 (m br, 6H), 3.45 – 3.28 (m br, 1H), 3.01 – 2.84 (m br, 1H), 2.63 – 2.31 (m br, 7H), 2.26 – 1.79 (m br, 14H), 1.76 – 1.57 (m br, 5H), 1.49 – 1.36 (m br, 1H), 0.96 (d, *J* = 6.6 Hz, 42H), 0.76 – 0.66 (m br, 2H), 0.60 (d, *J* = 6.8 Hz, 14H).

Synthesis of $PSSPOSS_{500}SS_{500}$

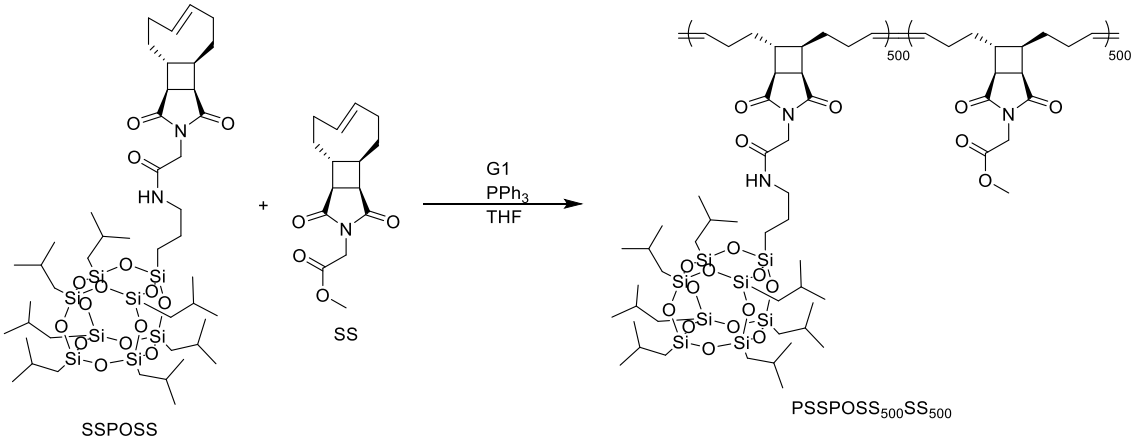

SSPOSS (60.6 mg, 54.1 μmol, 500 eq.) and SS (15.0 mg, 54.1 μmol, 500.0 eq.) were dissolved in THF (178.6 μL). To this mixture, a 1% PPh_3 solution in THF (85.1 μL, 3.2 μmol, 30.0 eq.) was added. While stirring vigorously, a 5 mM G1 solution in THF (21.7 μL, 0.1 μmol, 1.0 eq.) was introduced. The reaction mixture was stirred for 2 h and then quenched with 100 μL of EVE. The resulting product solution was precipitated into methanol three times, affording $PSSPOSS_{500}SS_{500}$ as a white powder (conversion: >99%). ^{1}H NMR analysis confirmed the incorporation ratio (SSPOSS: 50%, SS: 50%).

Synthesis of $PSSPOSS_{300}SS_{700}$

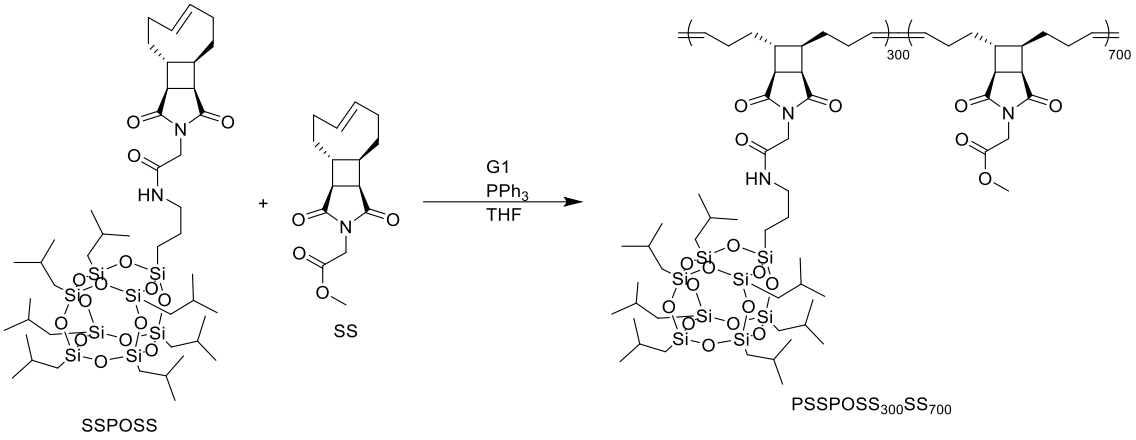

SSPOSS (43.3 mg, 38.7 μmol, 300 eq.) and SS (25.0 mg, 90.3 μmol, 700.0 eq.) were dissolved in THF (234.3 μL). To this mixture, a 1% PPh_3 solution in THF (101.3 μL, 3.9 μmol, 30.0 eq.) was added. While stirring vigorously, a 5 mM G1 solution in THF (25.8 μL, 0.1 μmol, 1.0 eq.) was introduced. The reaction mixture was stirred for 2 h and then quenched with 100 μL of EVE. The resulting product solution was precipitated into methanol three times, affording $PSSPOSS_{300}SS_{700}$ as a white powder (conversion: >99%). ^1H NMR analysis confirmed the incorporation ratio (SSPOSS: 30%, SS: 70%).

Synthesis of $PMSPOSS_{500}SS_{500}$

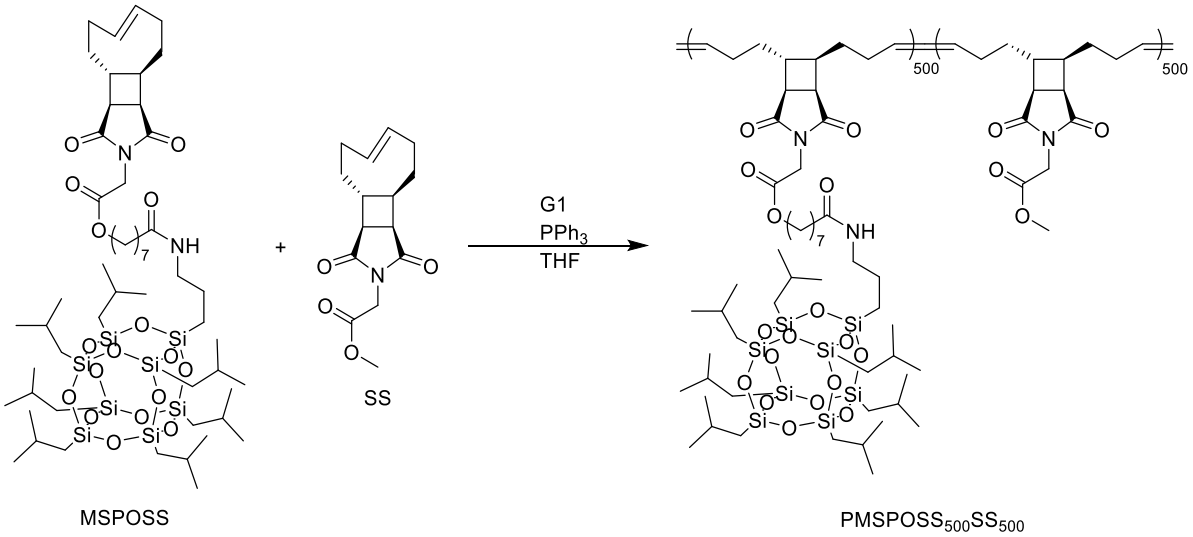

MSPOSS (77.5 mg, 61.4 μmol, 500 eq.) and SS (17.0 mg, 61.4 μmol, 500.0 eq.) were dissolved in THF (187.5 μL). To this mixture, a 1% PPh_3 solution in THF (96.5 μL, 3.7 μmol, 30.0 eq.) was added. While stirring vigorously, a 5 mM G1 solution in THF (24.5 μL, 0.1 μmol, 1.0 eq.) was introduced. The reaction mixture was stirred for 2 h and then quenched with 100 μL of EVE. The resulting product solution was precipitated into methanol three times, affording $PMSPOSS_{500}SS_{500}$ as a white

powder (conversion: >99%). ^{1}H NMR analysis confirmed the incorporation ratio (MSPOSS: 50%, SS: 50%).

Synthesis of $PMSPOSS_{300}SS_{700}$

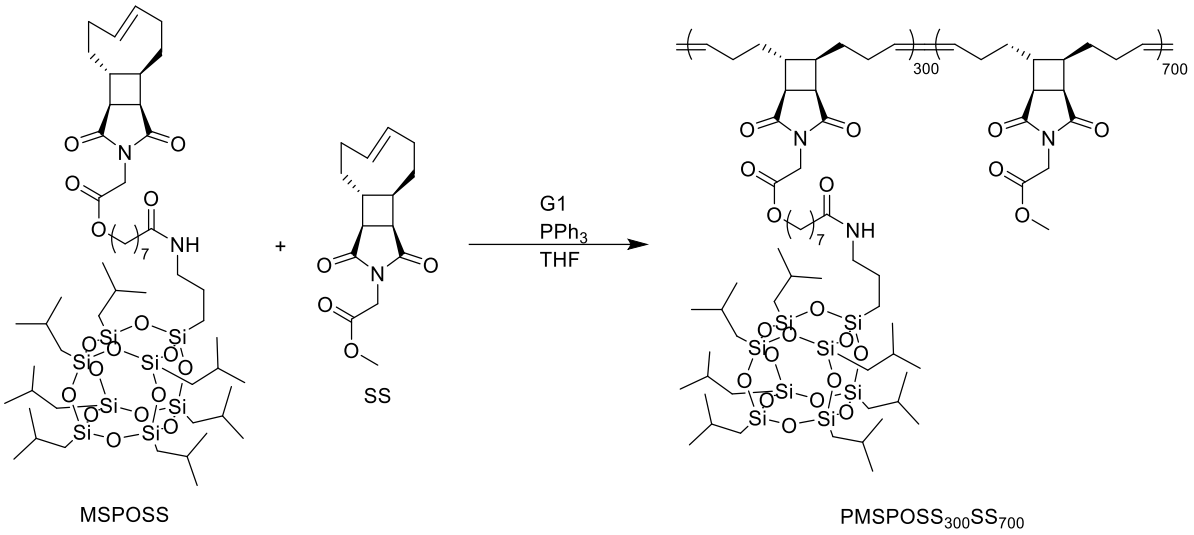

MSPOSS (58.6 mg, 46.4 μmol, 300 eq.) and SS (30.0 mg, 108.3 μmol, 700.0 eq.) were dissolved in THF (274.6 μL). To this mixture, a 1% PPh_3 solution in THF (96.5 μL, 3.7 μmol, 30.0 eq.) was added. While stirring vigorously, a 5 mM G1 solution in THF (30.9 μL, 0.2 μmol, 1.0 eq.) was introduced. The reaction mixture was stirred for 2 h and then quenched with 100 μL of EVE. The resulting product solution was precipitated into methanol three times, affording $PMSPOSS_{300}SS_{700}$ as a white powder (conversion: >99%). ^{1}H NMR analysis confirmed the incorporation ratio (MSPOSS: 30%, SS: 70%).

Synthesis of $PMSPOSS_{300}Bn_{700}$

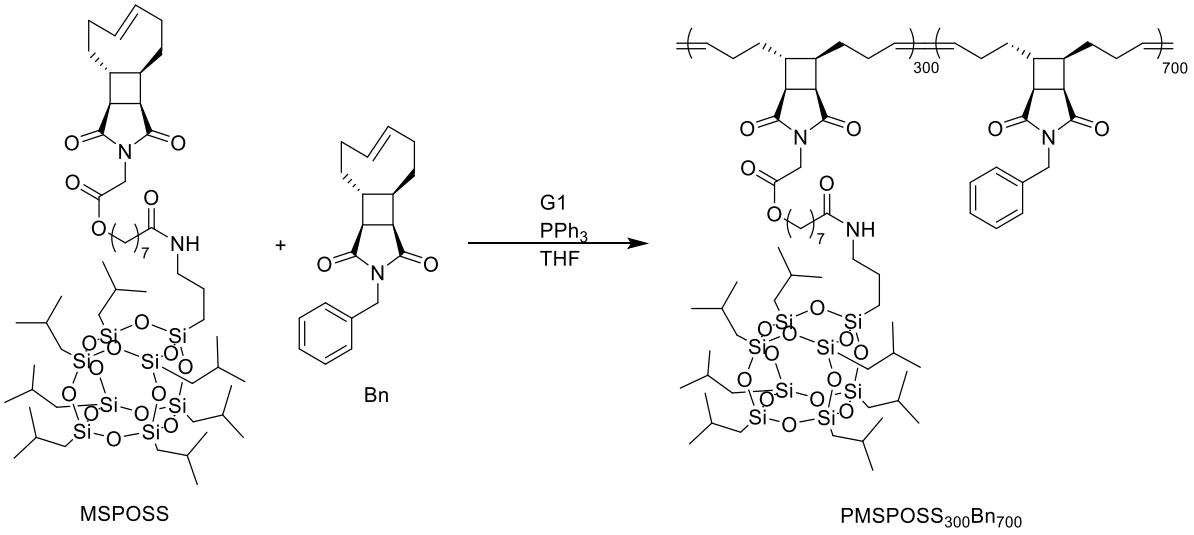

MSPOSS (45.8 mg, 36.3 μmol, 300 eq.) and Bn (25.0 mg, 84.7 μmol, 700.0 eq.) were dissolved in THF (213.3 μL). To this mixture, a 1% PPh_3 solution in THF (95.2 μL, 3.6 μmol, 30.0 eq.) was added. While stirring vigorously, a 5 mM G1 solution in

THF (24.2 μL, 0.1 μmol, 1.0 eq.) was introduced. The reaction mixture was stirred for 2 h and then quenched with 100 μL of EVE. The resulting product solution was precipitated into methanol three times, affording $PMSPOSS_{300}Bn_{700}$ as a white powder (conversion: >99%). ^1H NMR analysis confirmed the incorporation ratio (MSPOSS: 30%, Bn: 70%).

Synthesis of $PLSPOSS_{500}SS_{500}$

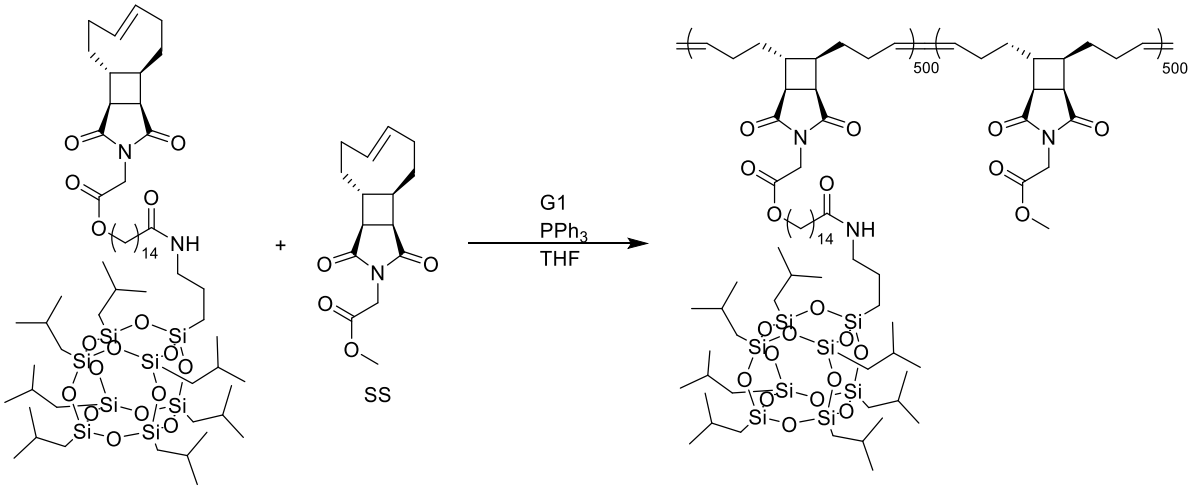

LSPOSS (73.6 mg, 54.1 μmol, 500 eq.) and SS (15.0 mg, 54.1 μmol, 500.0 eq.) were dissolved in THF (165.6 μL). To this mixture, a 1% PPh_3 solution in THF (85.1 μL, 3.2 μmol, 30.0 eq.) was added. While stirring vigorously, a 5 mM G1 solution in THF (21.7 μL, 0.1 μmol, 1.0 eq.) was introduced. The reaction mixture was stirred for 2 h and then quenched with 100 μL of EVE. The resulting product solution was precipitated into methanol three times, affording $PLSPOSS_{500}SS_{500}$ as a white powder (conversion: >99%). ^1H NMR analysis confirmed the incorporation ratio (LSPOSS: 50%, SS: 50%).

Synthesis of $PLSPOSS_{300}SS_{700}$

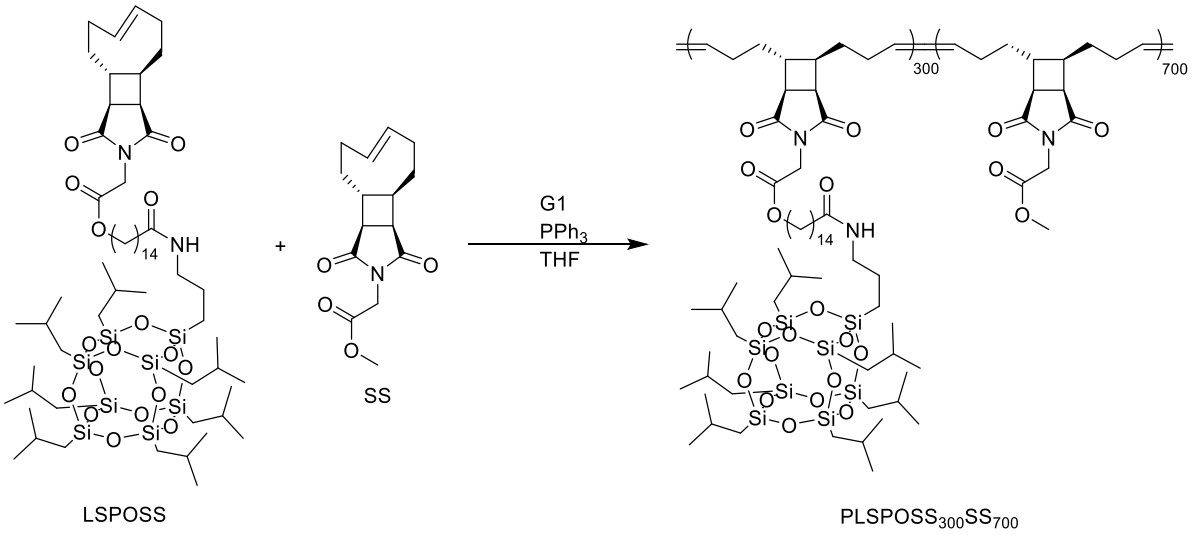

LSPOSS (63.1 mg, 46.4 μmol, 300 eq.) and SS (30.0 mg, 108.3 μmol, 700.0 eq.) were dissolved in THF (270.0 μL). To this mixture, a 1% PPh_3 solution in THF (121.6 μL, 4.6 μmol, 30.0 eq.) was added. While stirring vigorously, a 5 mM G1 solution in THF (30.9 μL, 1.5 μmol, 1.0 eq.) was introduced. The reaction mixture was stirred for 2 h and then quenched with 100 μL of EVE. The resulting product solution was precipitated into methanol three times, affording $PLSPOSS_{300}SS_{700}$ as a white powder (conversion: >99%). ^1H NMR analysis confirmed the incorporation ratio (LSPOSS: 30%, SS: 70%).

Synthesis of $PLSPOSS_{300}Bn_{700}$

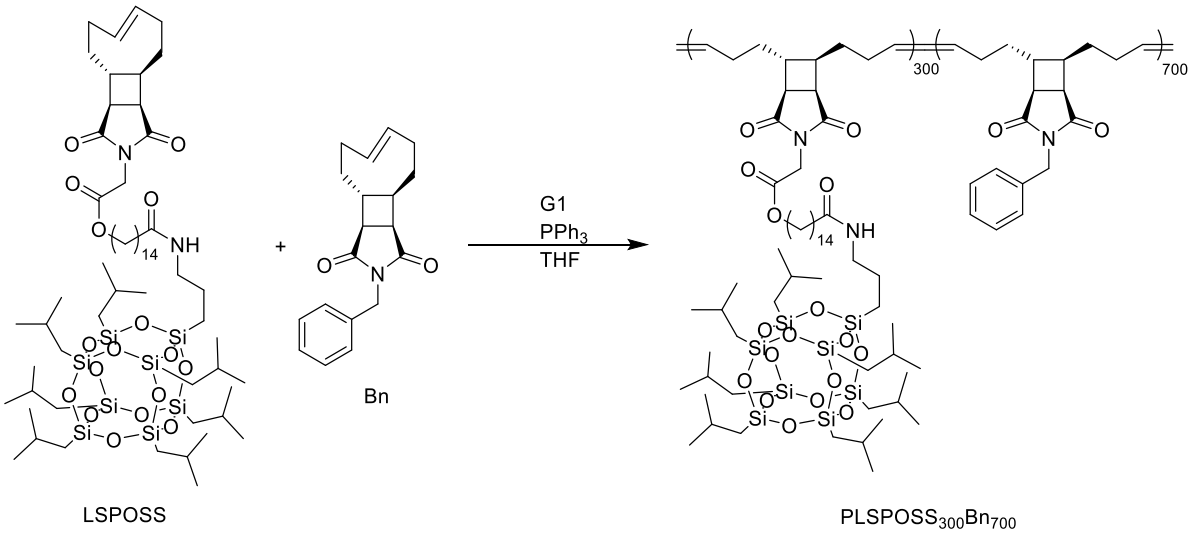

MSPOSS (49.4 mg, 36.3 μmol, 300 eq.) and Bn (25.0 mg, 84.7 μmol, 700.0 eq.) were dissolved in THF (209.8 μL). To this mixture, a 1% PPh_3 solution in THF (95.2 μL, 3.6 μmol, 30.0 eq.) was added. While stirring vigorously, a 5 mM G1 solution in THF (24.2 μL, 0.1 μmol, 1.0 eq.) was introduced. The reaction mixture was stirred for 2 h and then quenched with 100 μL of EVE. The resulting product solution was precipitated into methanol three times, affording $PMSPOSS_{300}Bn_{700}$ as a white powder (conversion: >99%). ^1H NMR analysis confirmed the incorporation ratio (MSPOSS: 30%, Bn: 70%).

NMR Spectra

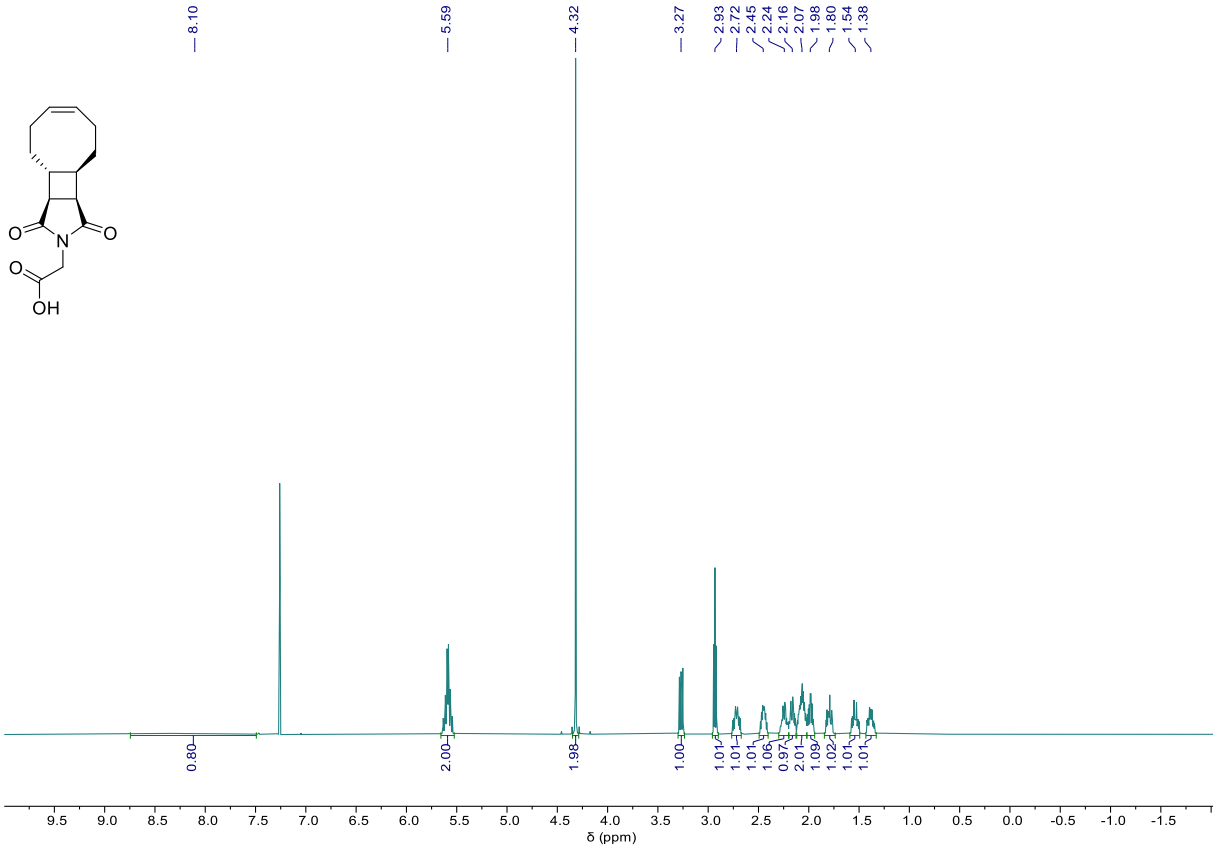

Figure S1. ^{1}H NMR (500 MHz, $CDCl_3$) spectrum of **2**

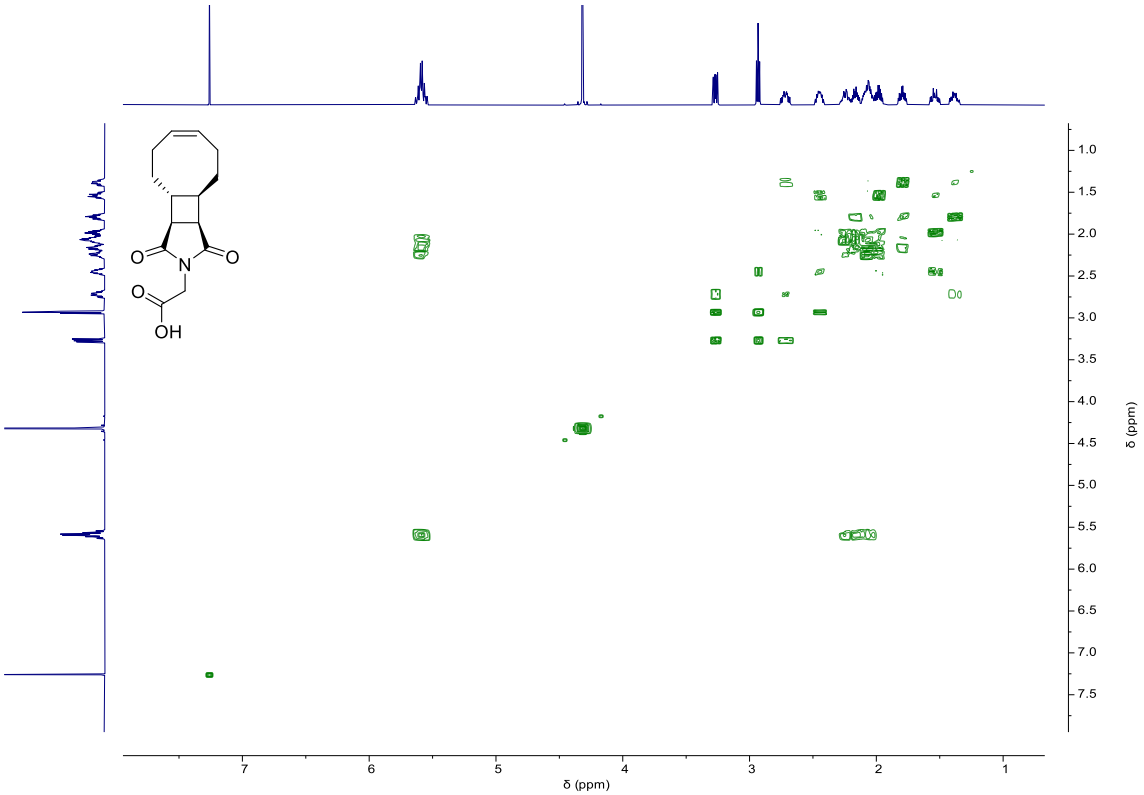

Figure S2. COSY NMR (500 MHz, $CDCl_3$) spectrum of **2**

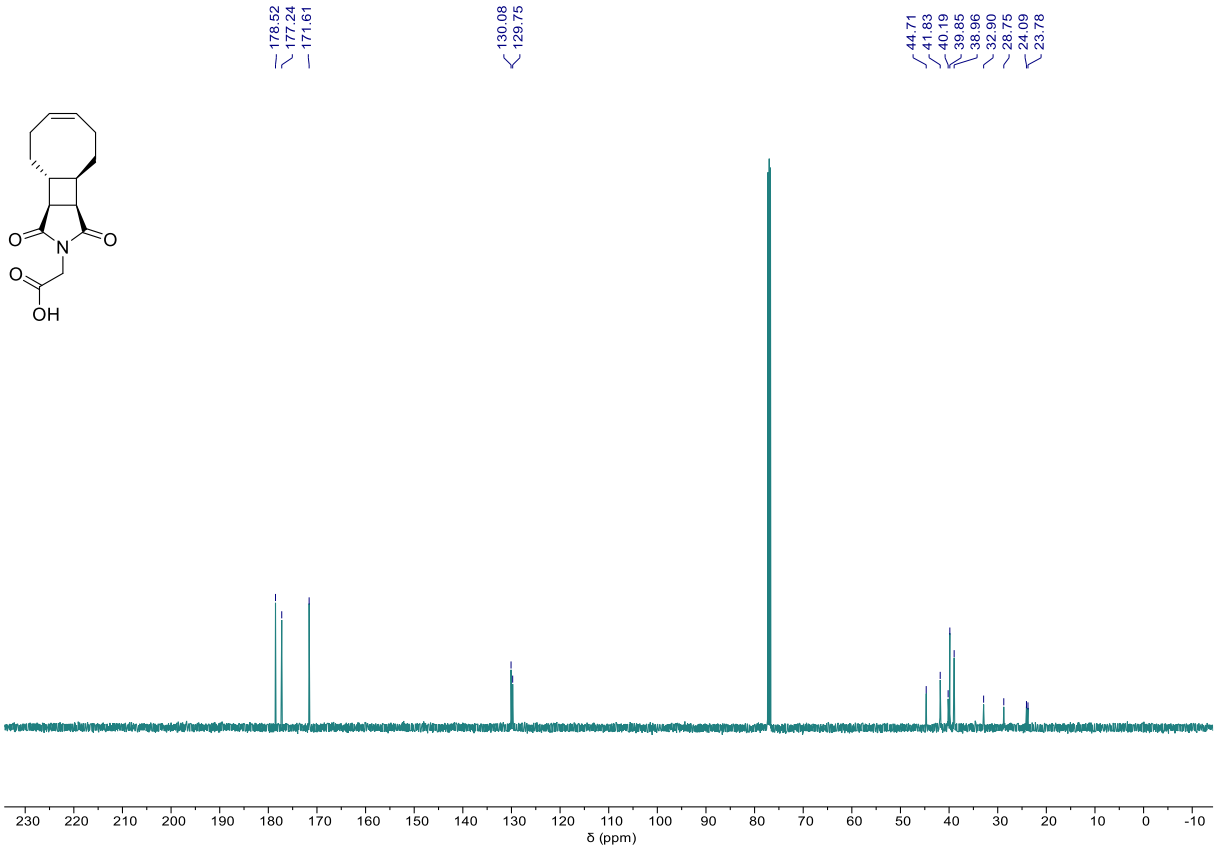

Figure S3. ^{13}C NMR (126 MHz, $CDCl_3$) spectrum of **2**

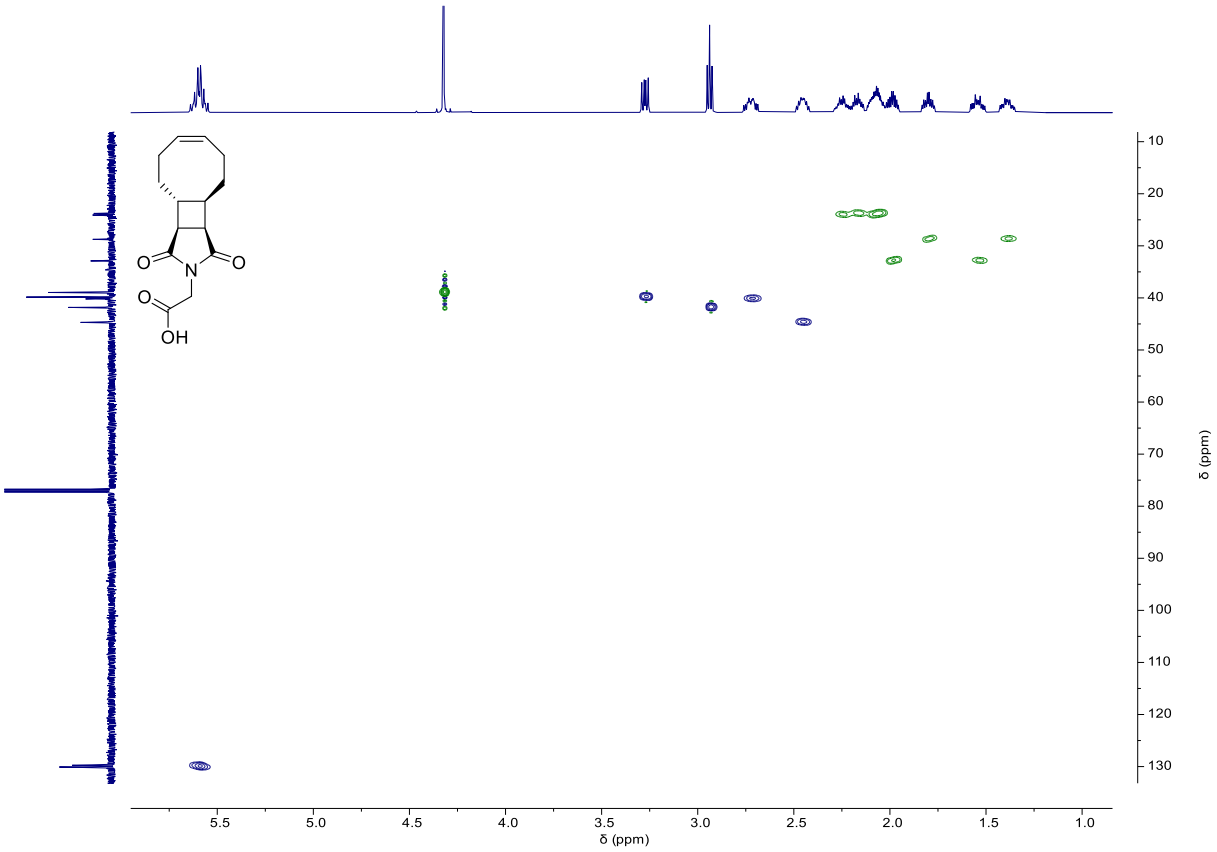

Figure S4. HSQC NMR (500 MHz for ^{1}H, 126 MHz for ^{13}C, $CDCl_3$) spectrum of **2**

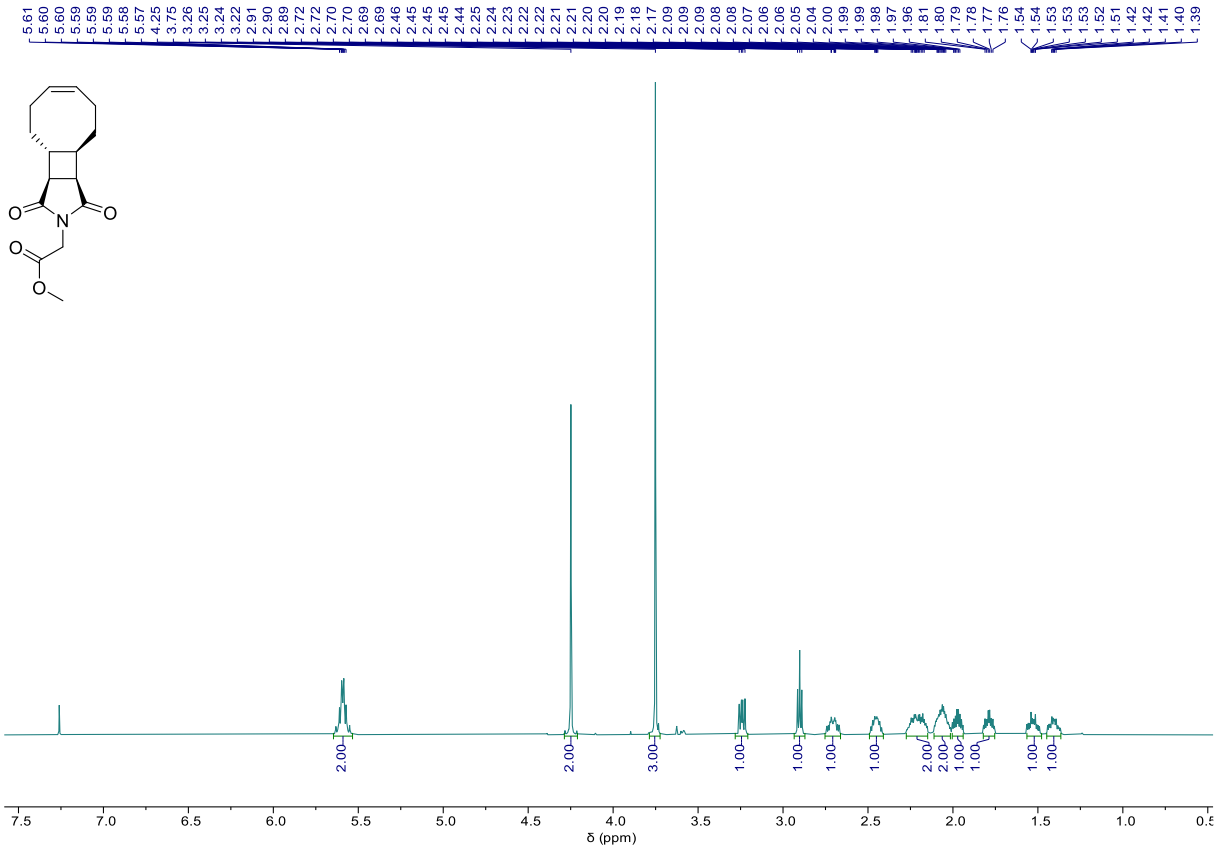

Figure S5. ^{1}H NMR (500 MHz, $CDCl_3$) spectrum of *Z*SS

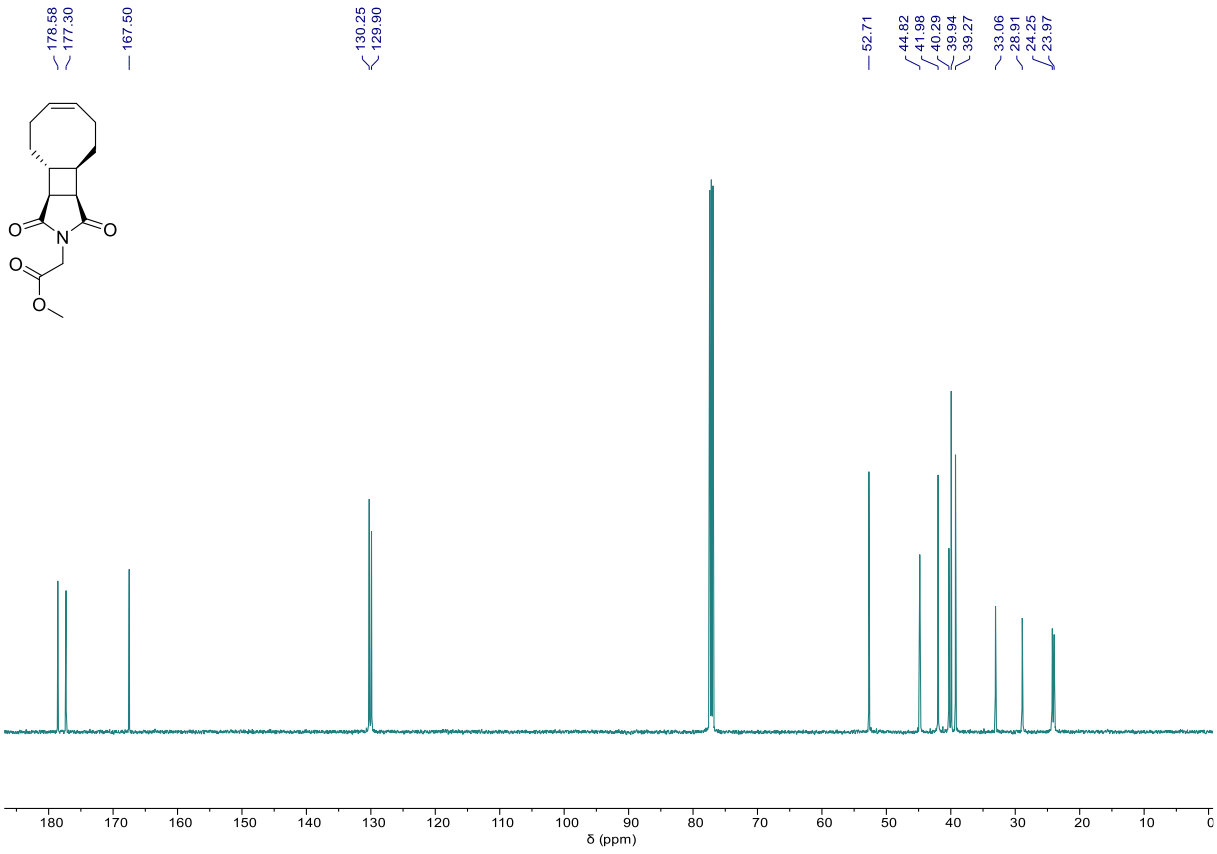

Figure S6. ^{13}C NMR (126 MHz, $CDCl_3$) spectrum of *Z*SS

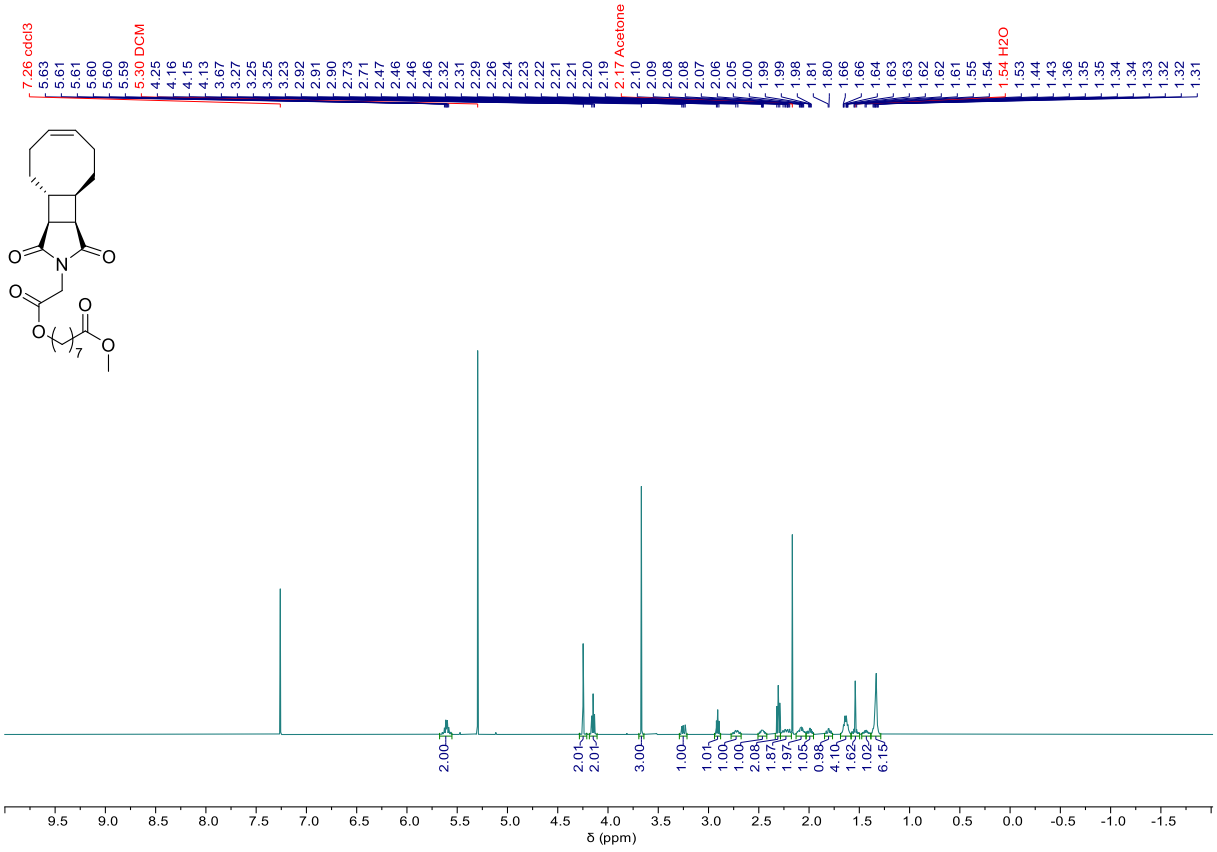

Figure S7. ^{1}H NMR (500 MHz, $CDCl_3$) spectrum of *Z*MS

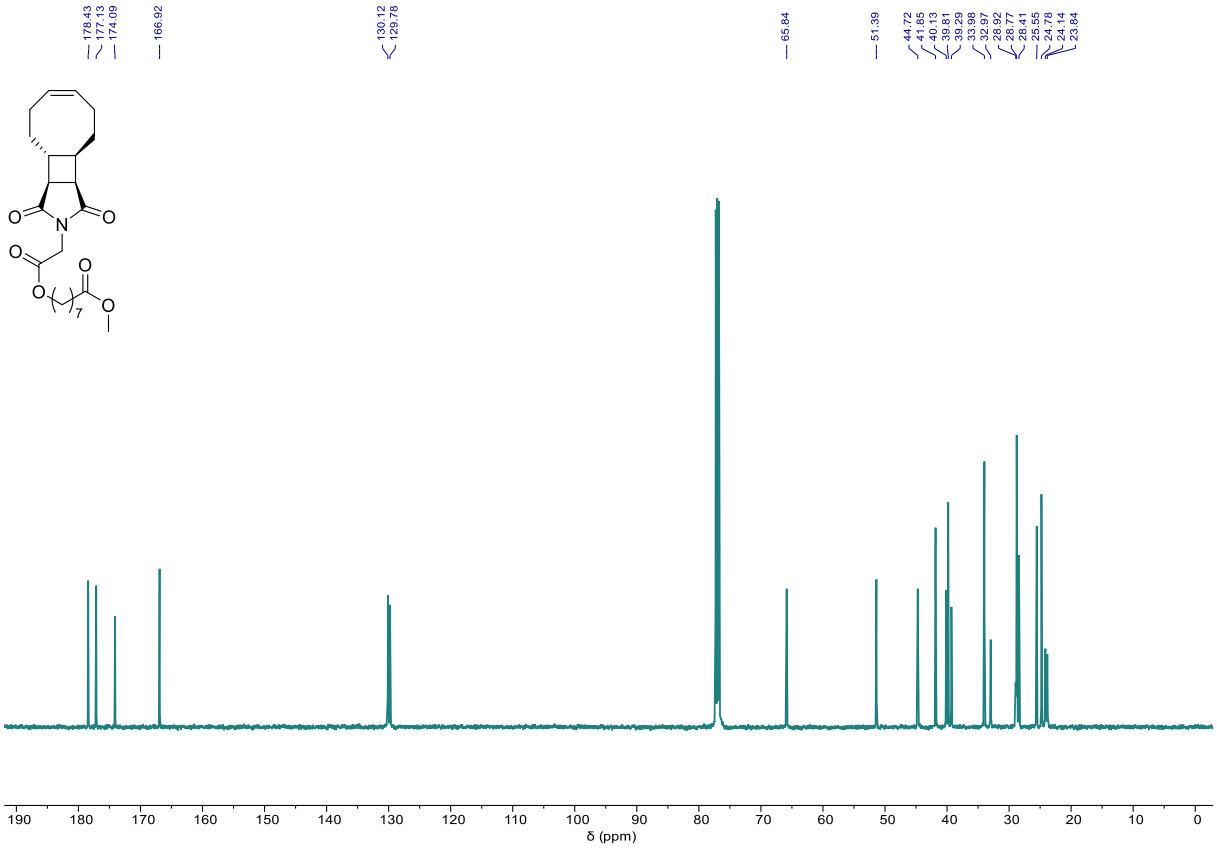

Figure S8. ^{13}C NMR (126 MHz, $CDCl_3$) spectrum of *Z*MS

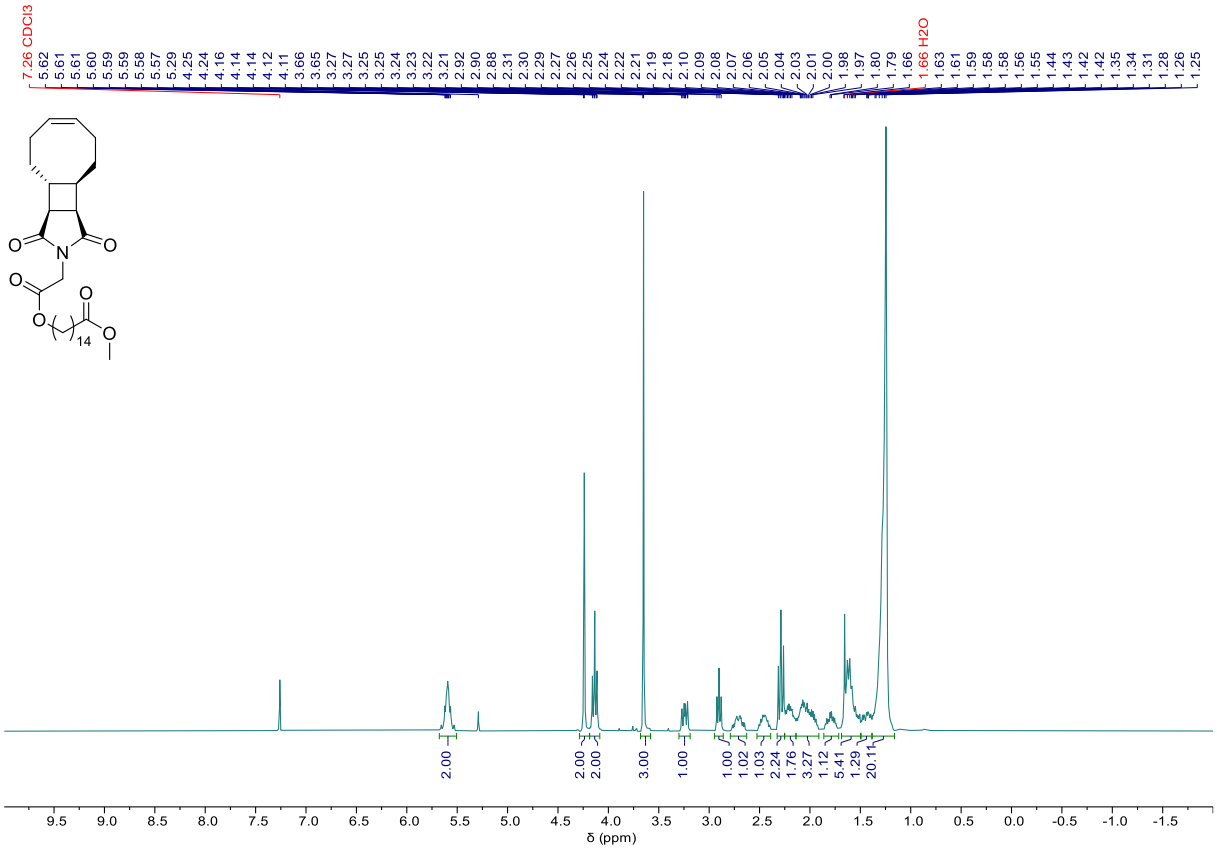

Figure S9. ^{1}H NMR (500 MHz, $CDCl_3$) spectrum of *Z*LS

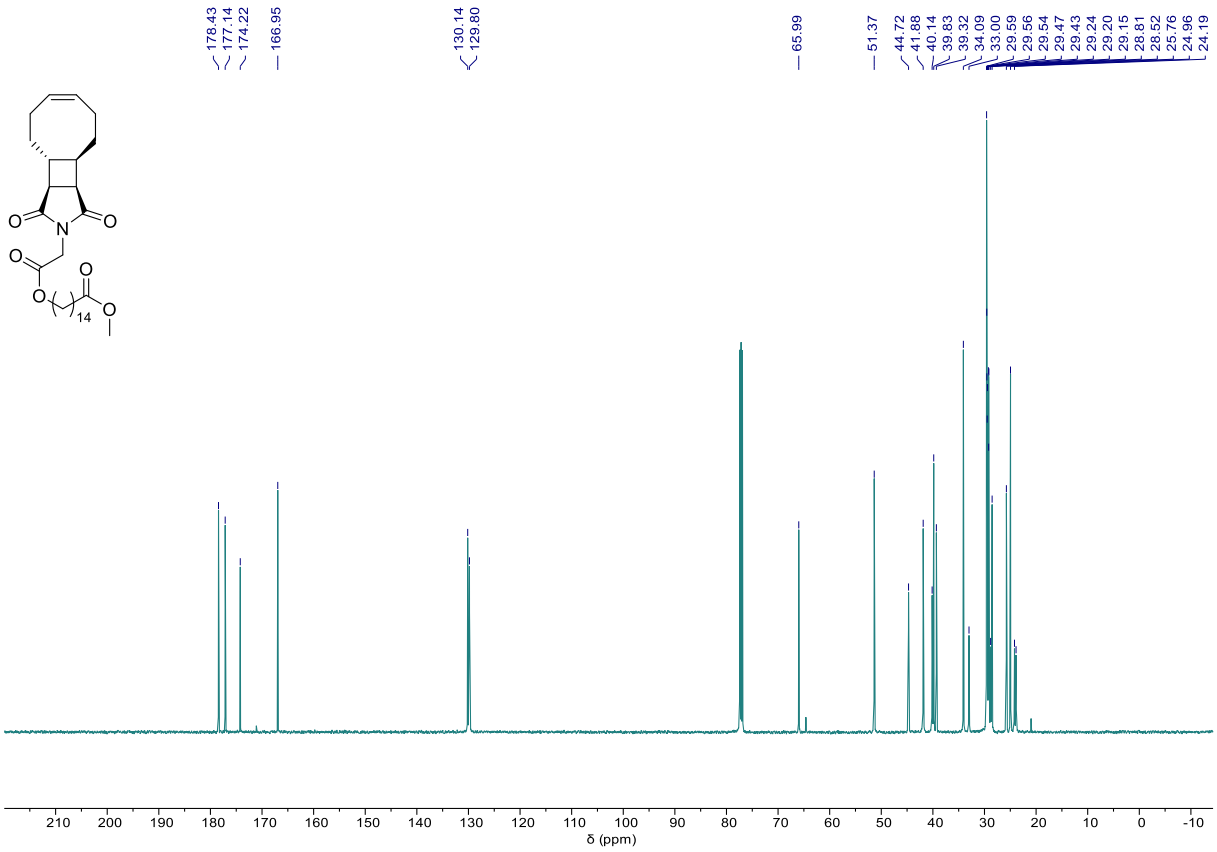

Figure S10. ^{13}C NMR (126 MHz, $CDCl_3$) spectrum of *Z*LS

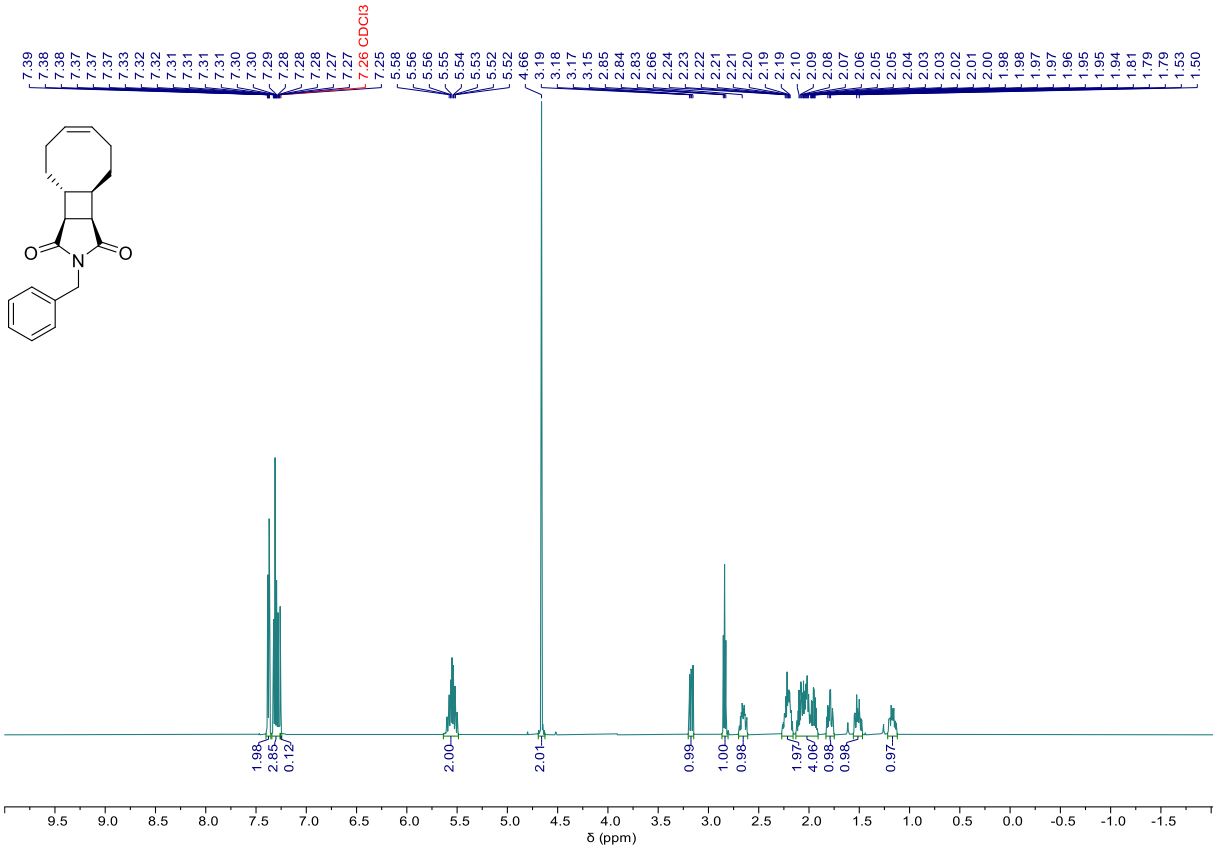

Figure S11. ^{1}H NMR (500 MHz, $CDCl_3$) spectrum of *Z*Bn

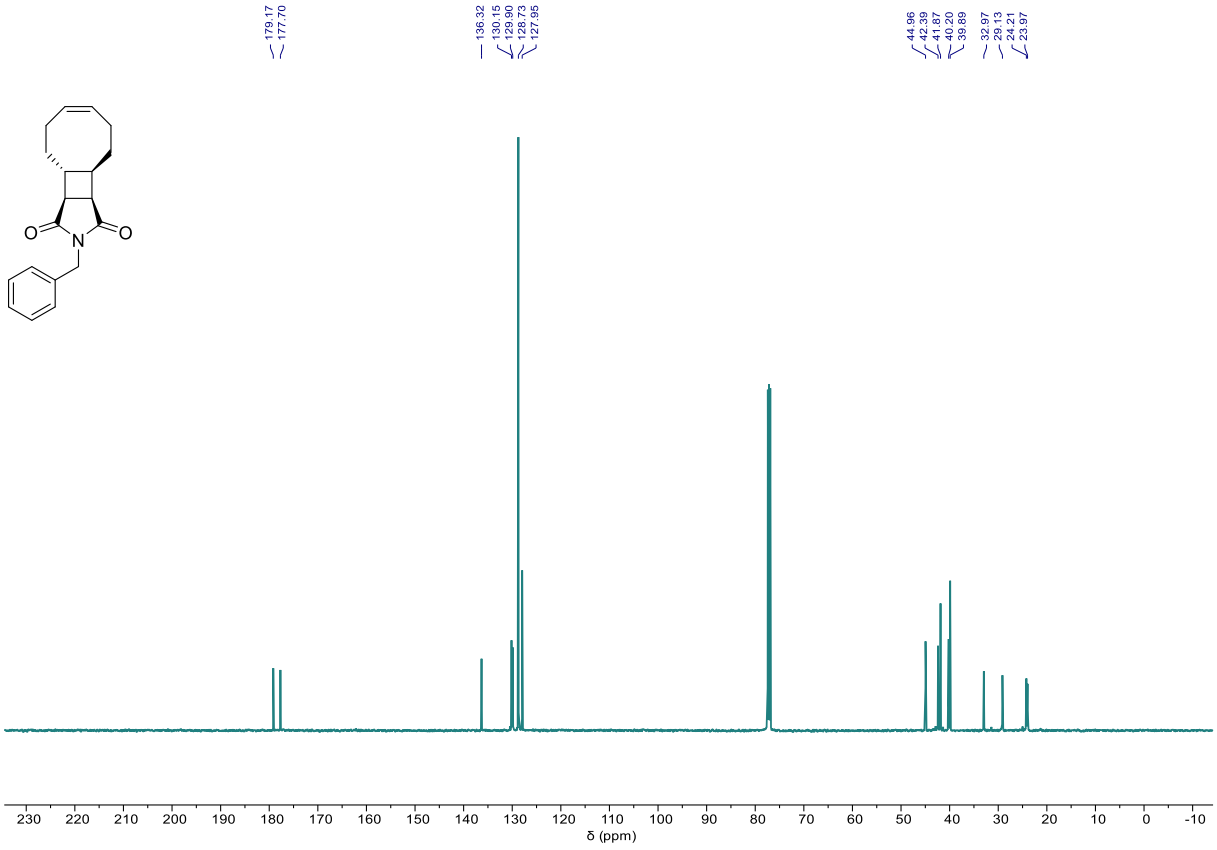

Figure S12. ^{13}C NMR (126 MHz, $CDCl_3$) spectrum of *Z*Bn

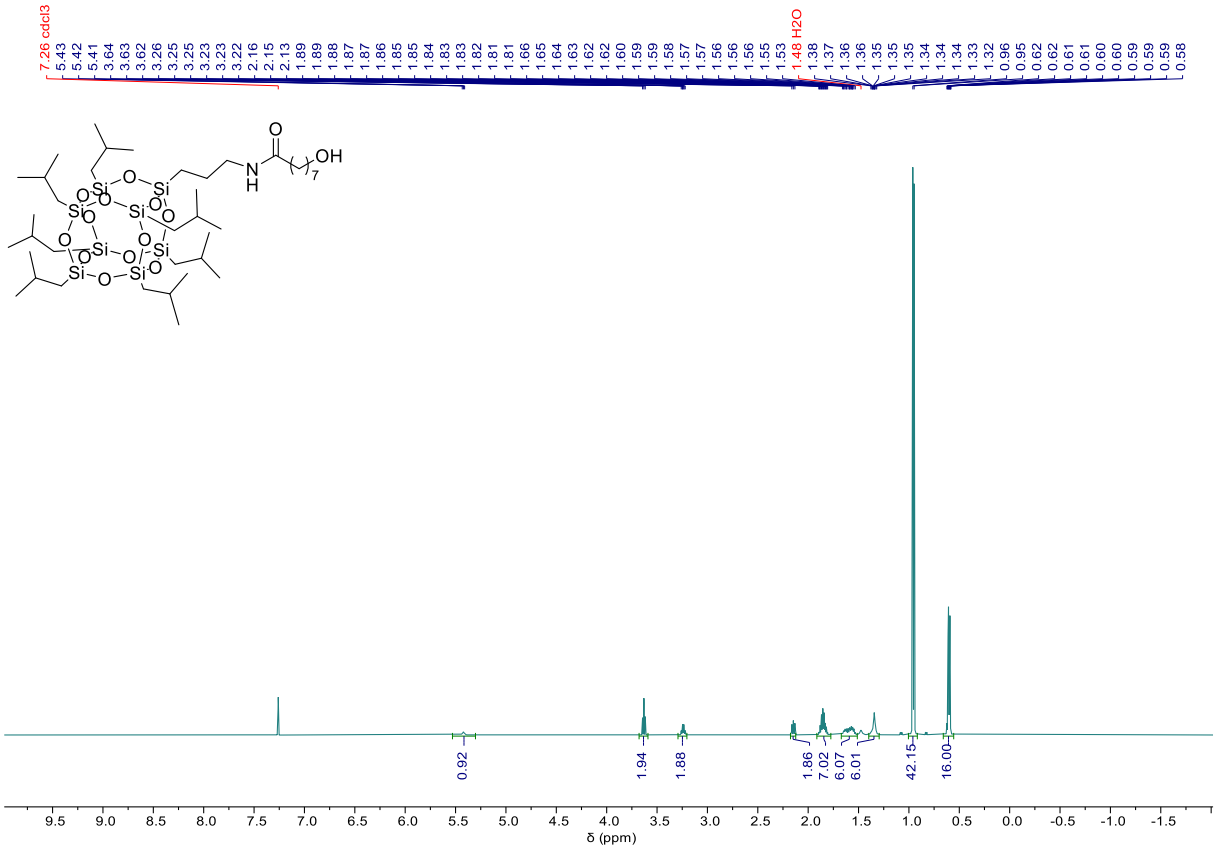

Figure S13. ^{1}H NMR (500 MHz, $CDCl_3$) spectrum of **3**

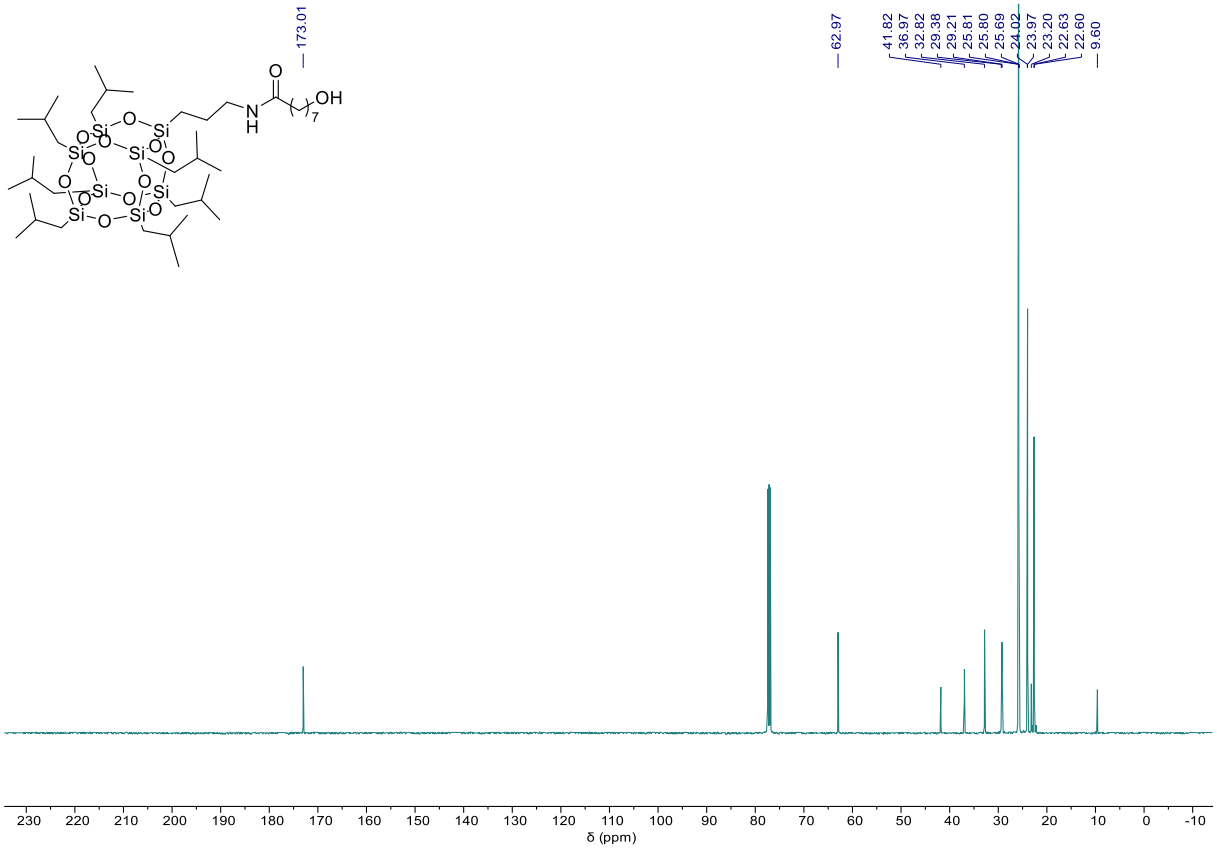

Figure S14. ^{13}C NMR (126 MHz, $CDCl_3$) spectrum of **3**

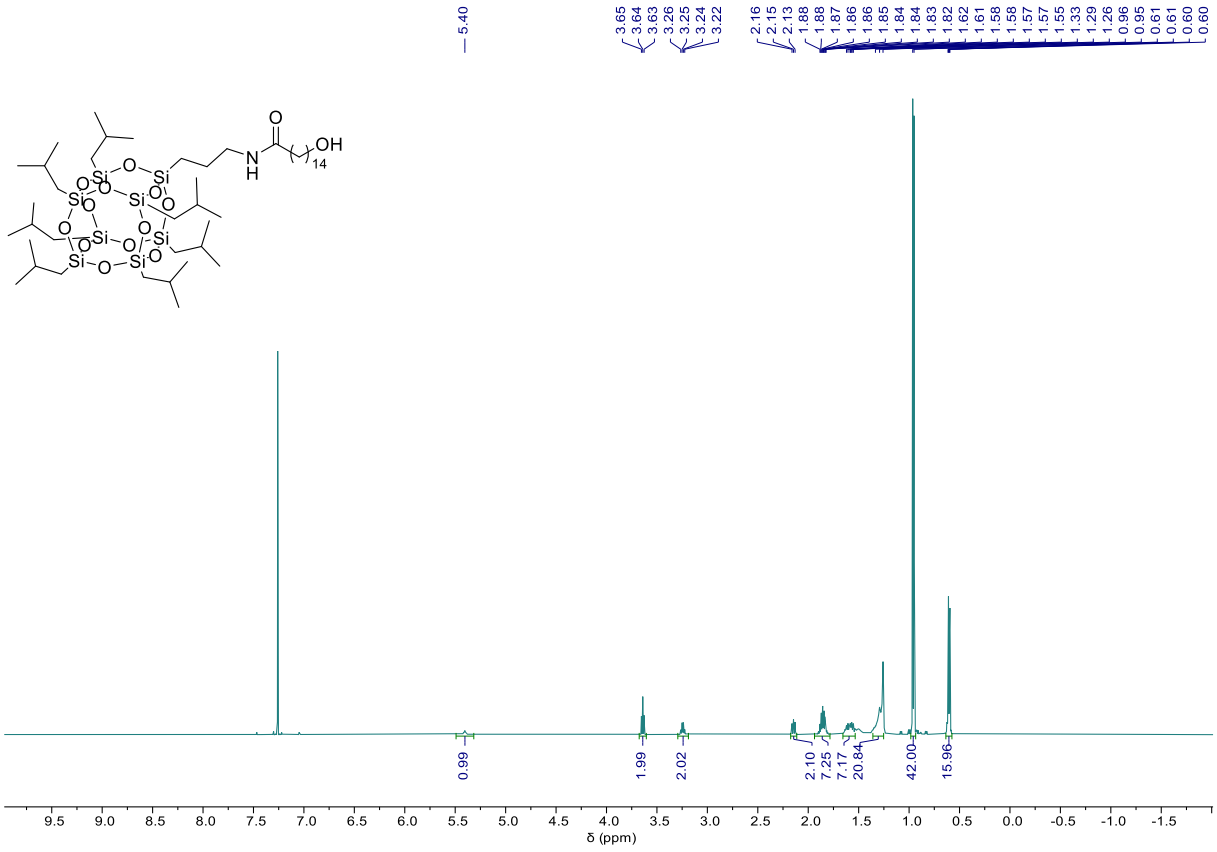

Figure S15. ^{1}H NMR (500 MHz, $CDCl_3$) spectrum of **4**

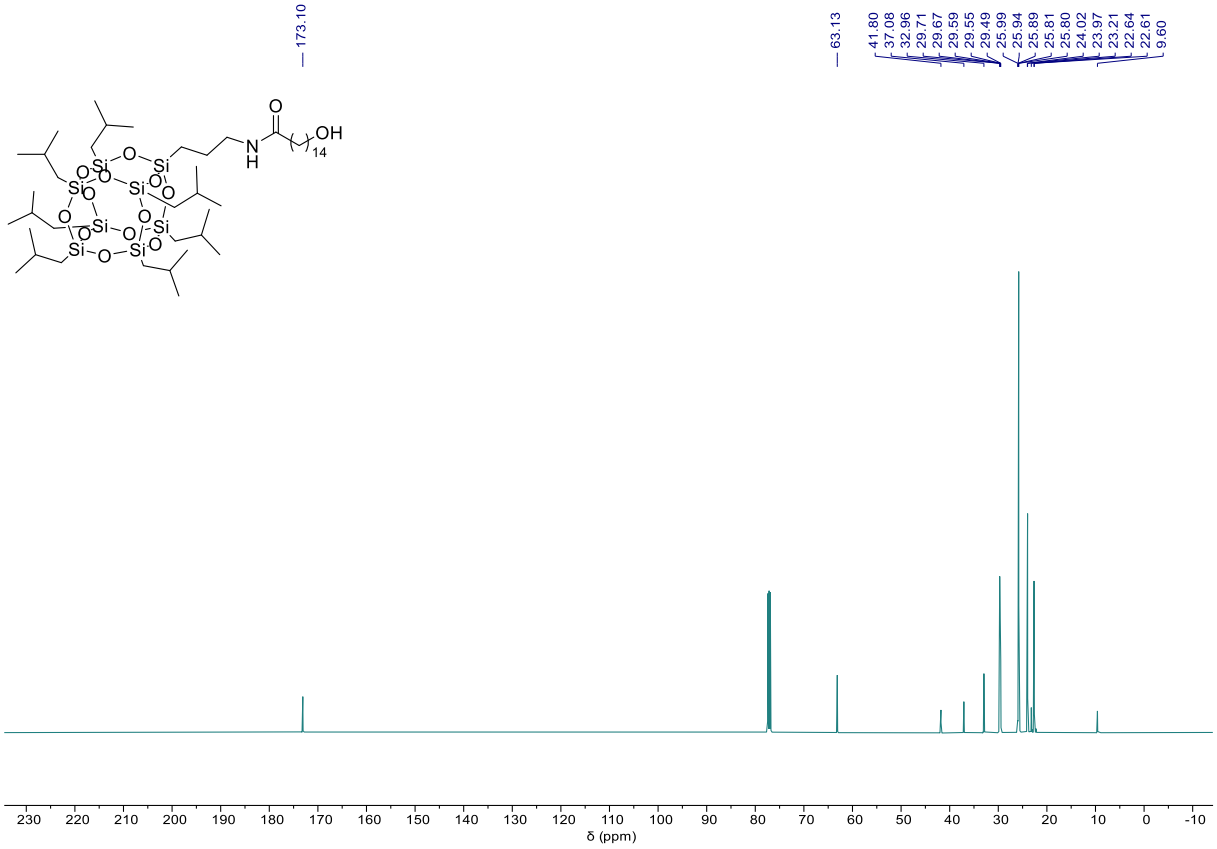

Figure S16. ^{13}C NMR (126 MHz, $CDCl_3$) spectrum of **4**

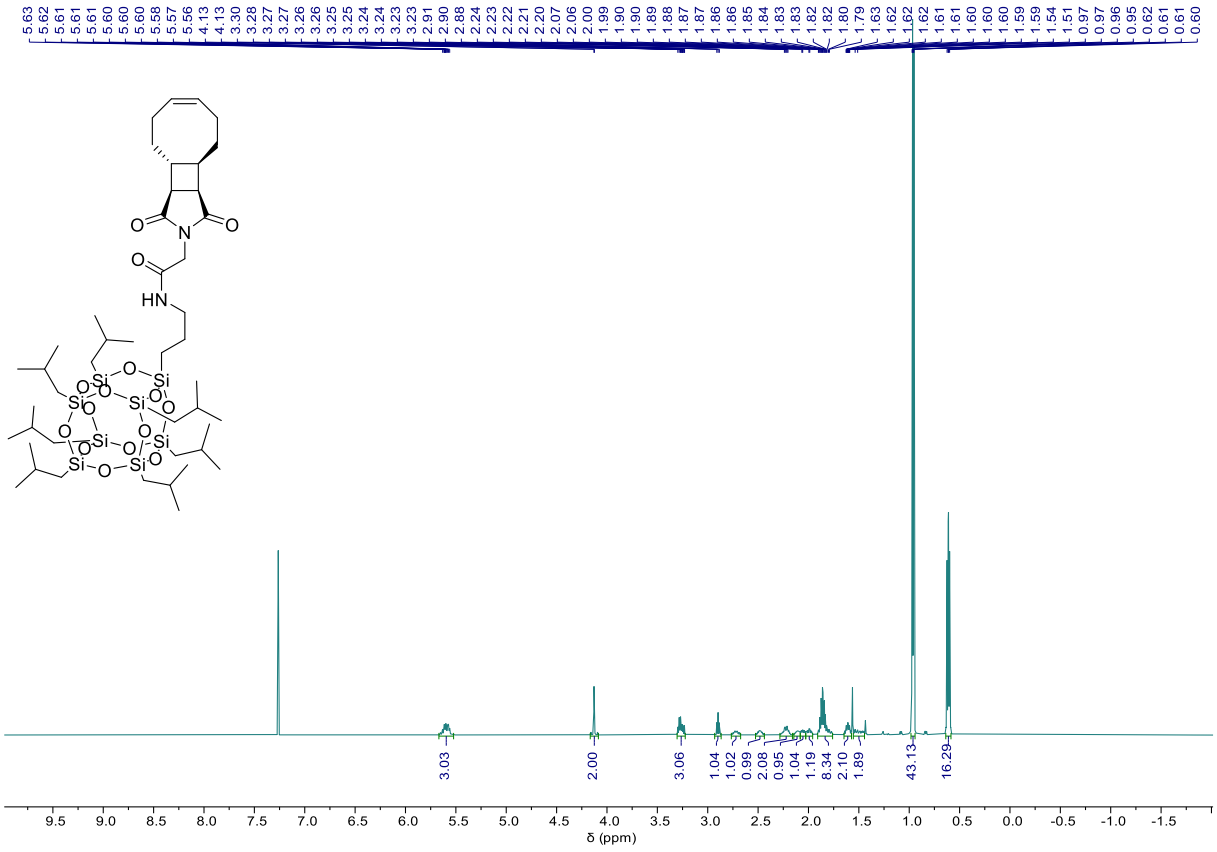

Figure S17. ^{1}H NMR (500 MHz, $CDCl_3$) spectrum of *Z*SSPOSS

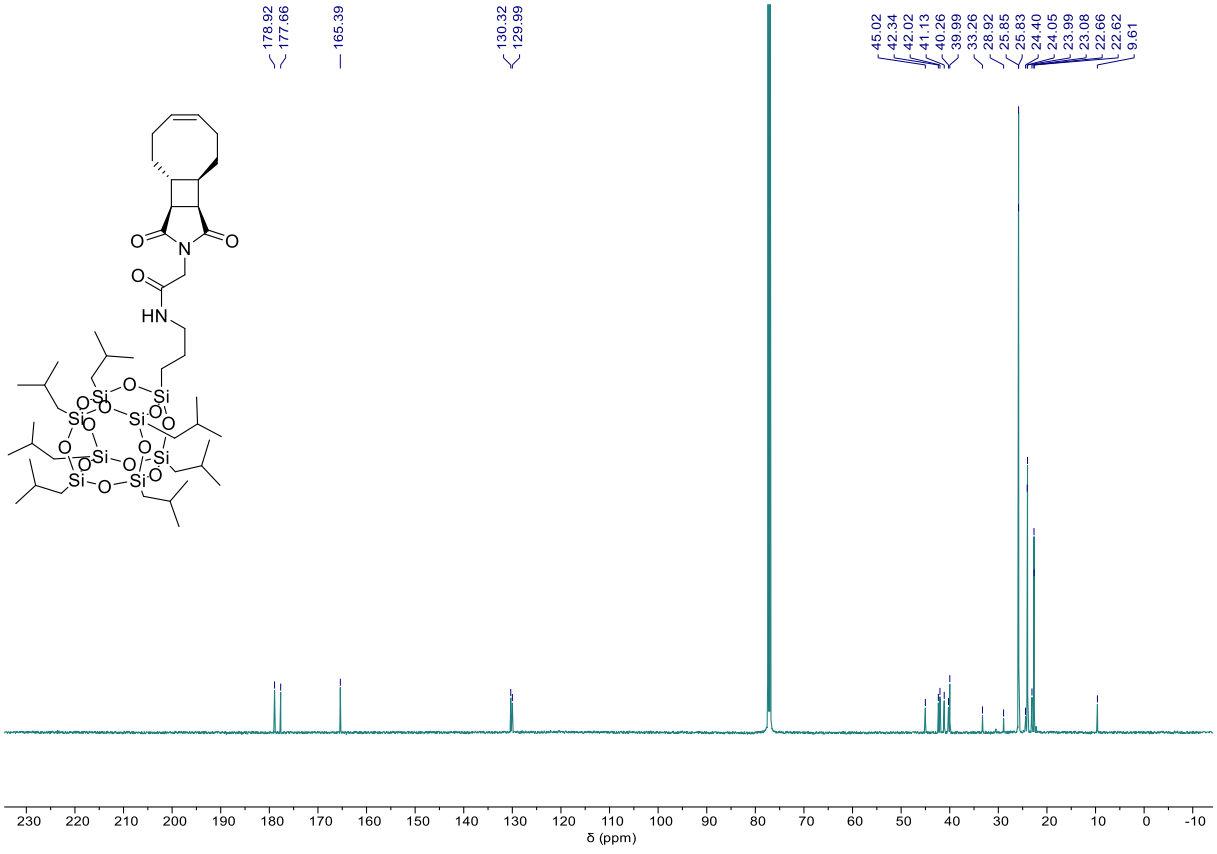

Figure S18. ^{13}C NMR (126 MHz, $CDCl_3$) spectrum of *Z*SSPOSS

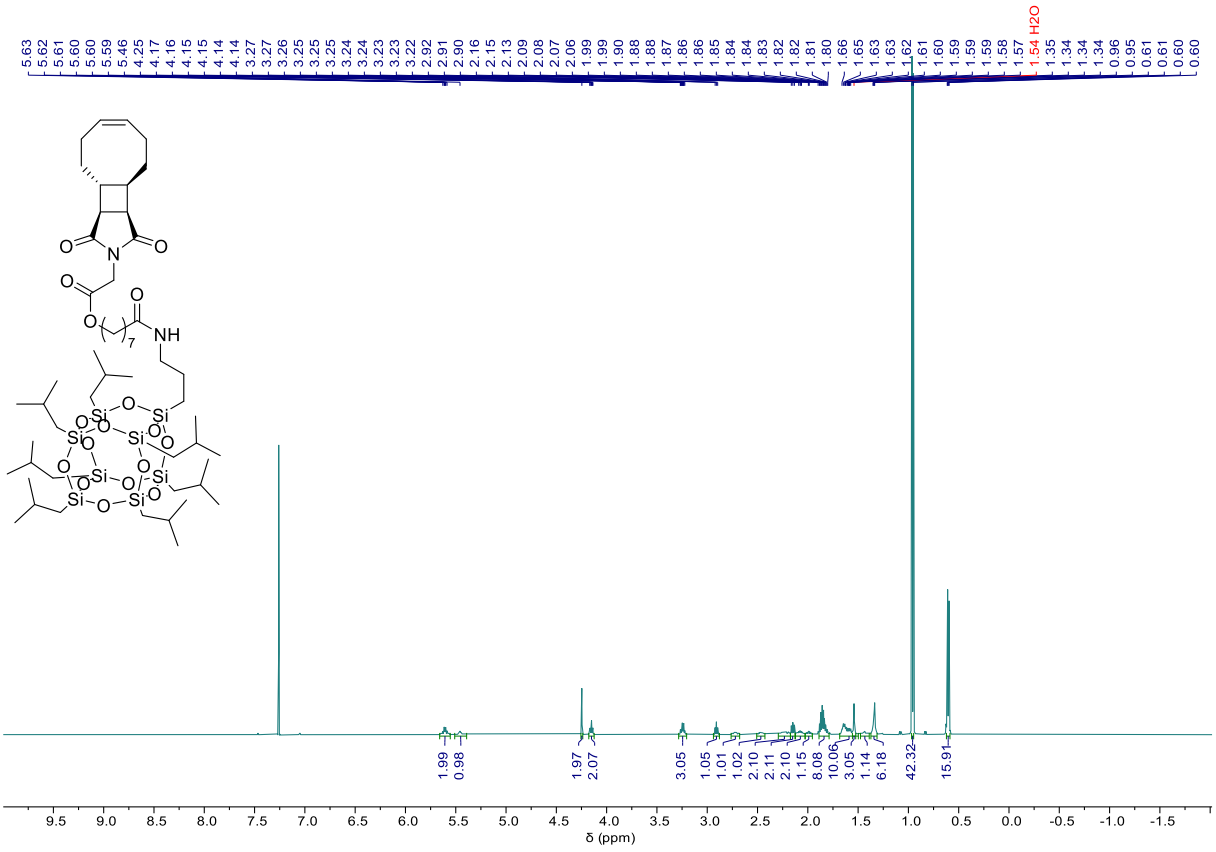

Figure S19. ^{1}H NMR (500 MHz, $CDCl_3$) spectrum of *Z*MSPOSS

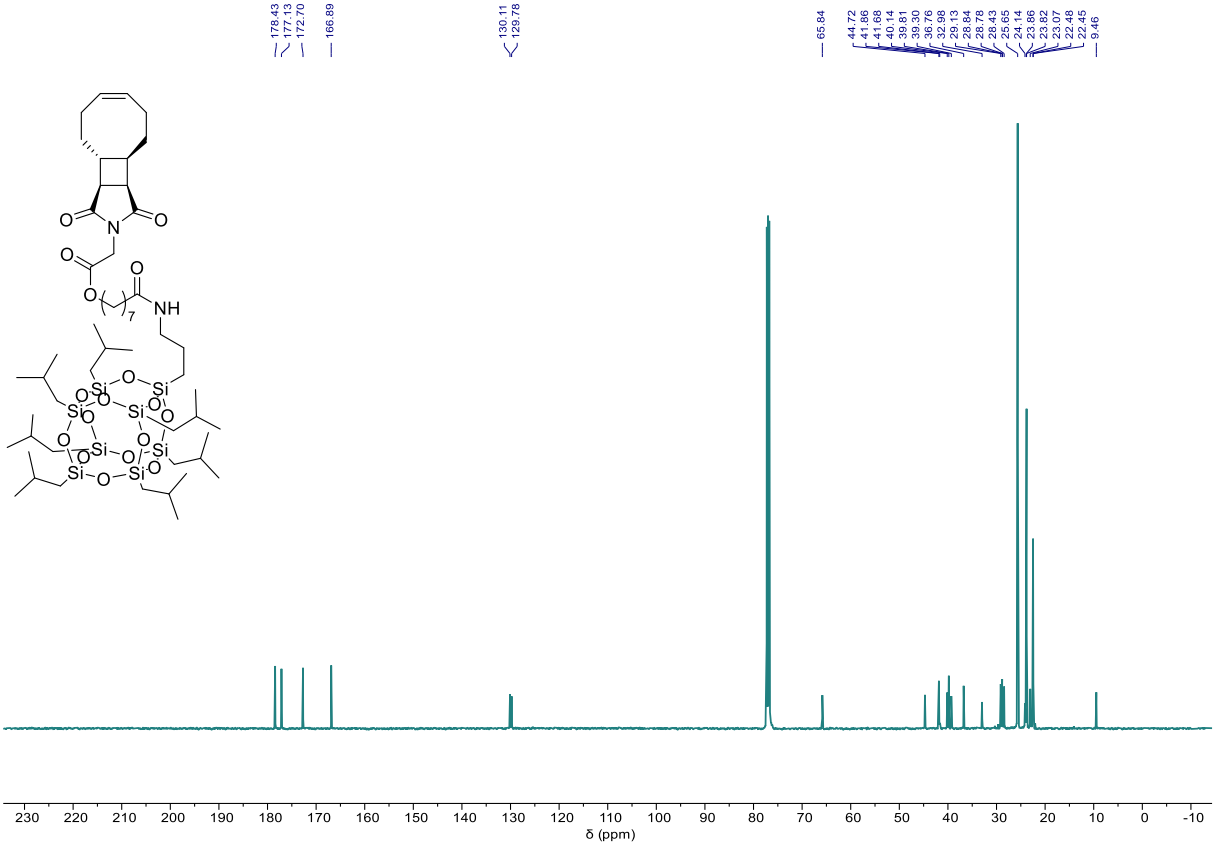

Figure S20. ^{13}C NMR (126 MHz, $CDCl_3$) spectrum of *Z*MSPOSS

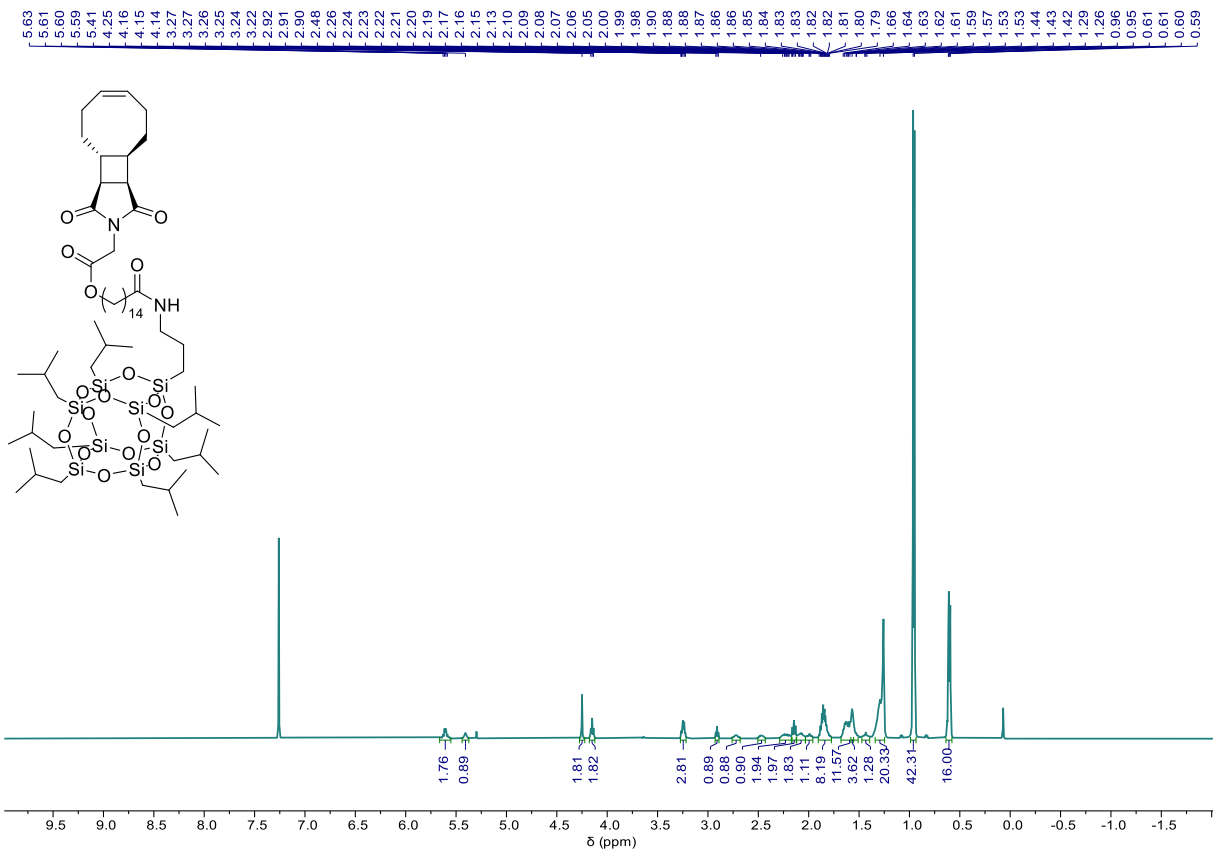

Figure S21. ^{1}H NMR (500 MHz, $CDCl_3$) spectrum of *Z*LSPOSS

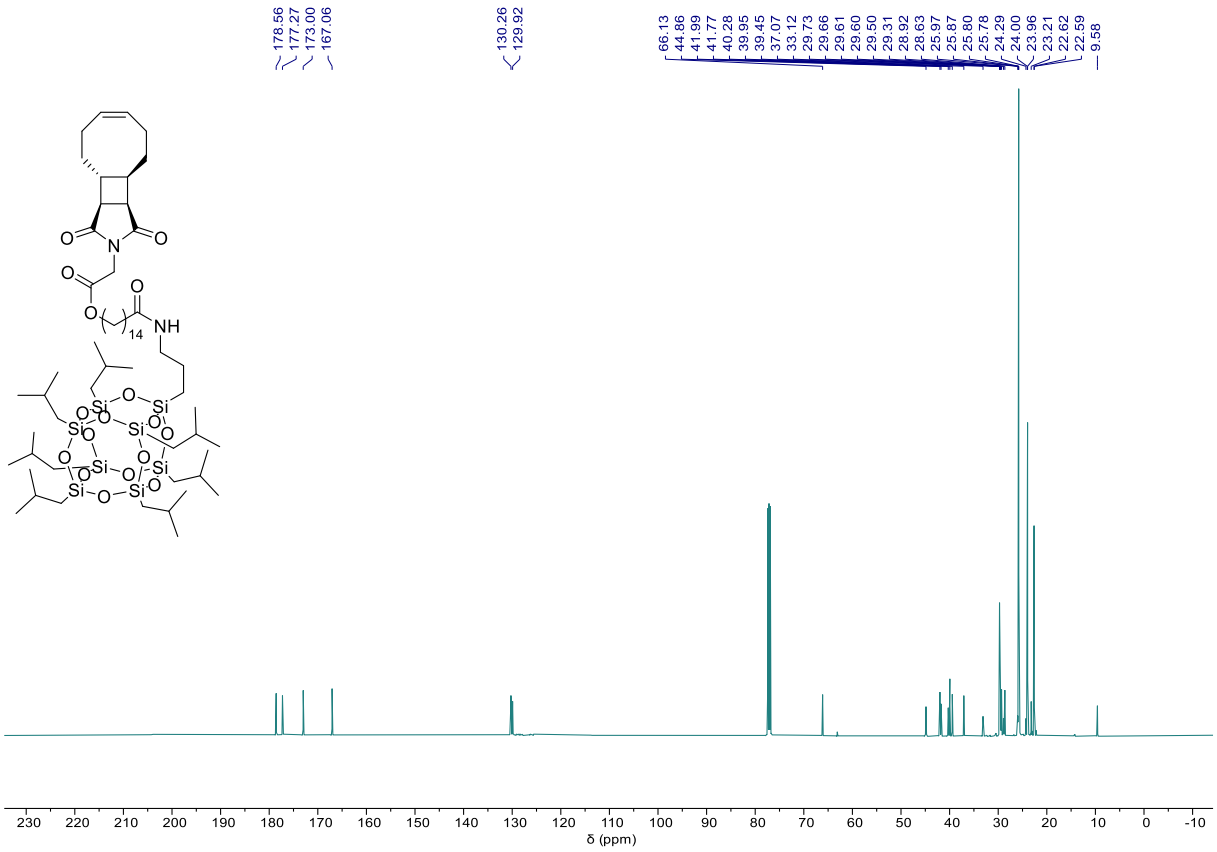

Figure S22. ^{13}C NMR (126 MHz, $CDCl_3$) spectrum of *Z*LSPOSS

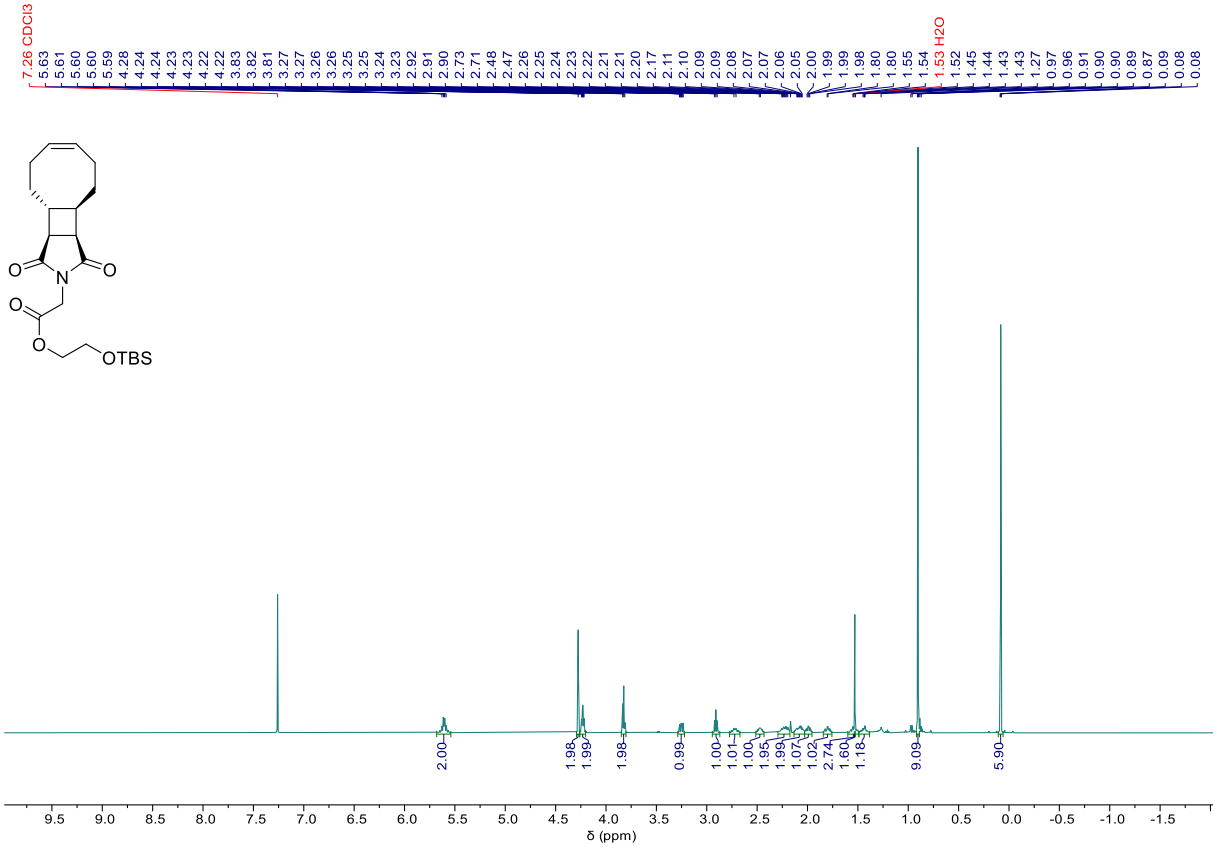

Figure S23. ^{1}H NMR (500 MHz, $CDCl_3$) spectrum of **5**

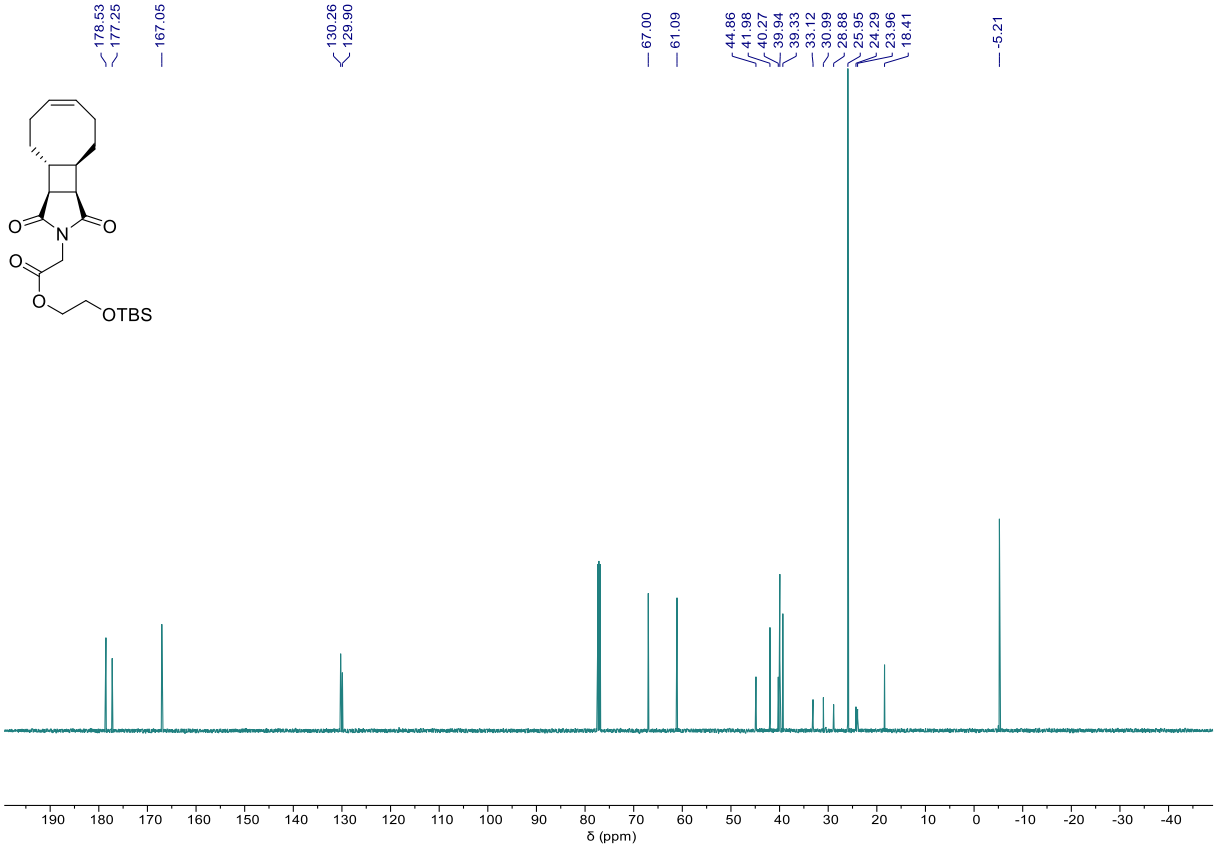

Figure S24. ^{13}C NMR (126 MHz, $CDCl_3$) spectrum of **5**

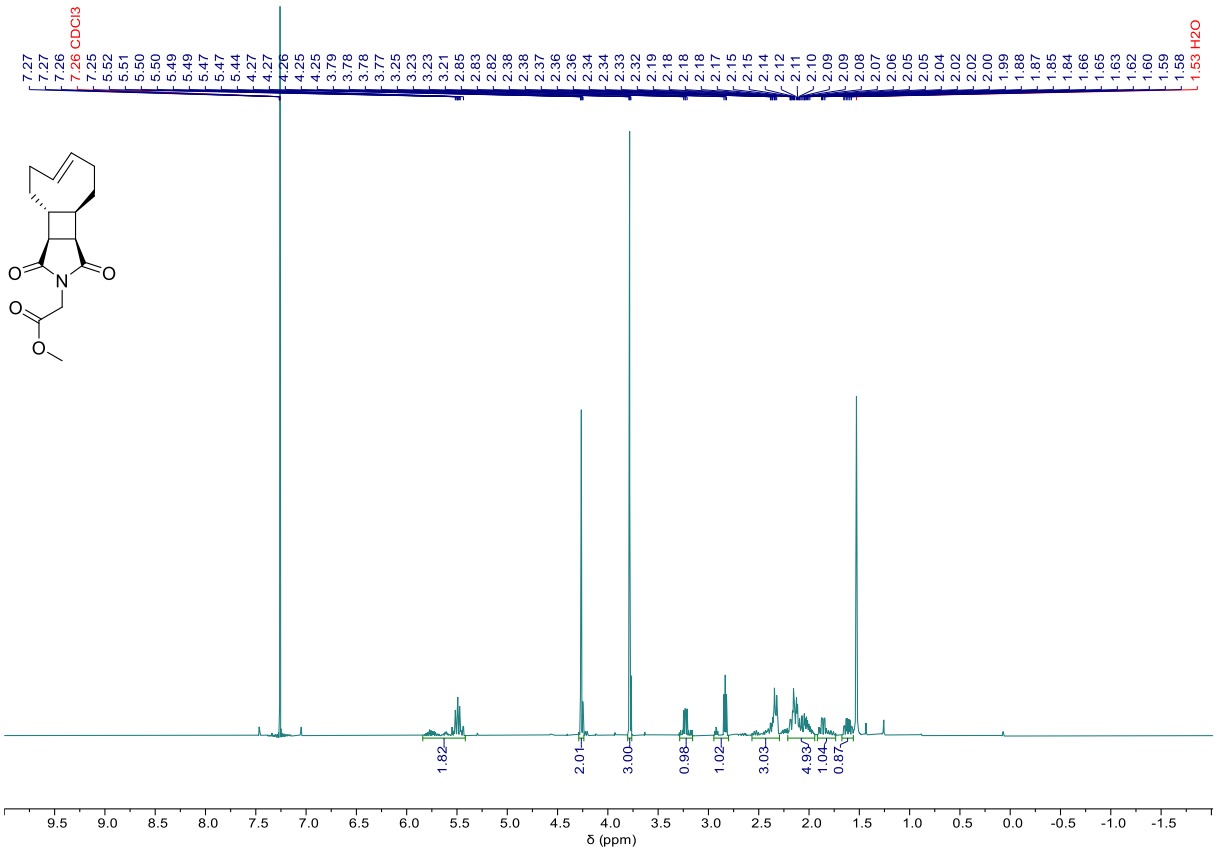

Figure S25. ^{1}H NMR (500 MHz, $CDCl_3$) spectrum of SS

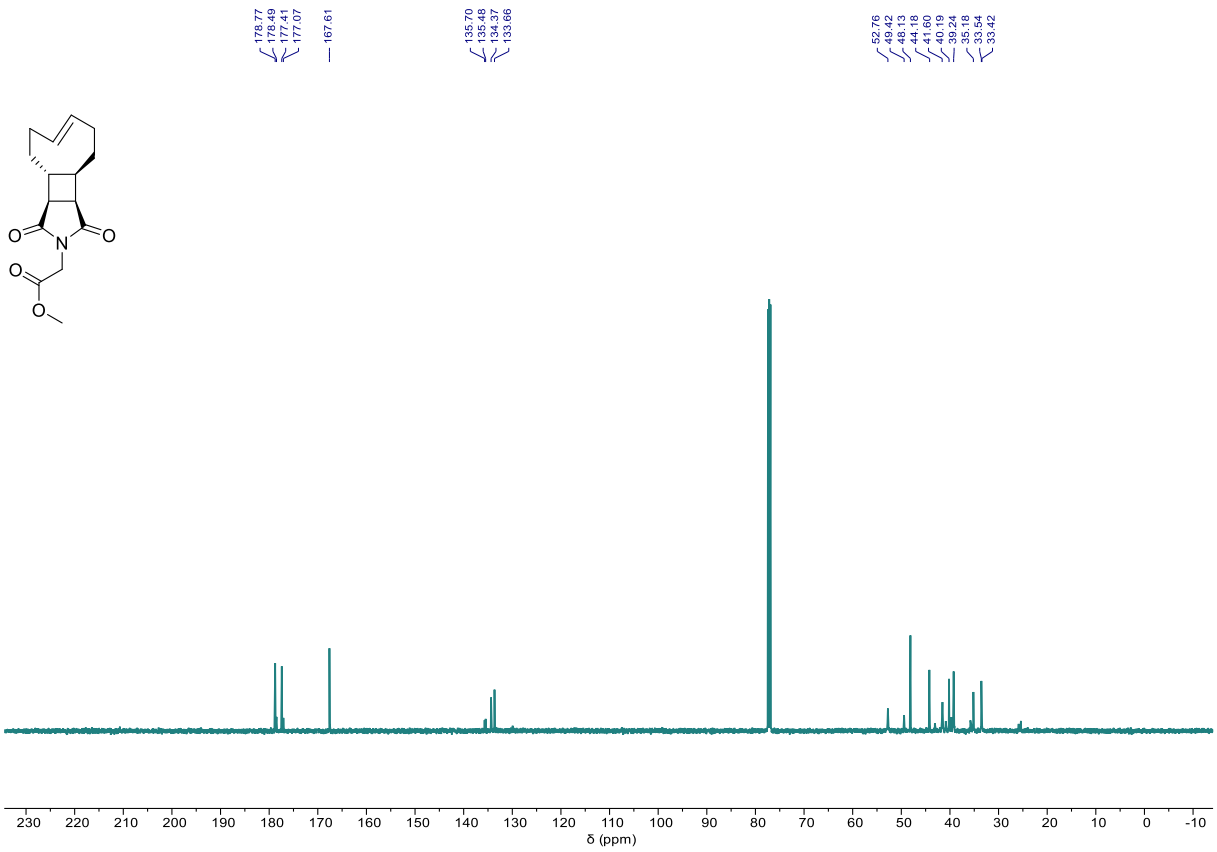

Figure S26. ^{13}C NMR (126 MHz, $CDCl_3$) spectrum of SS

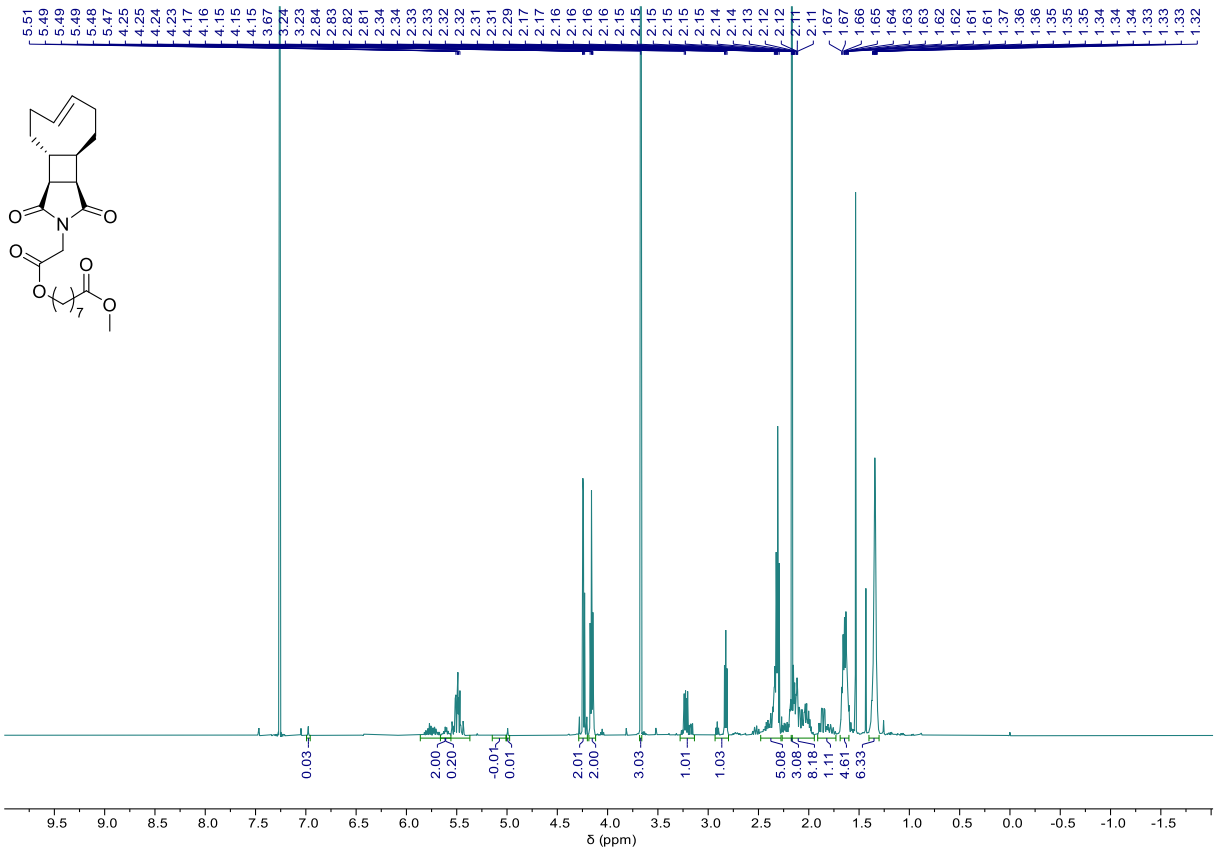

Figure S27. ^{1}H NMR (500 MHz, $CDCl_3$) spectrum of MS

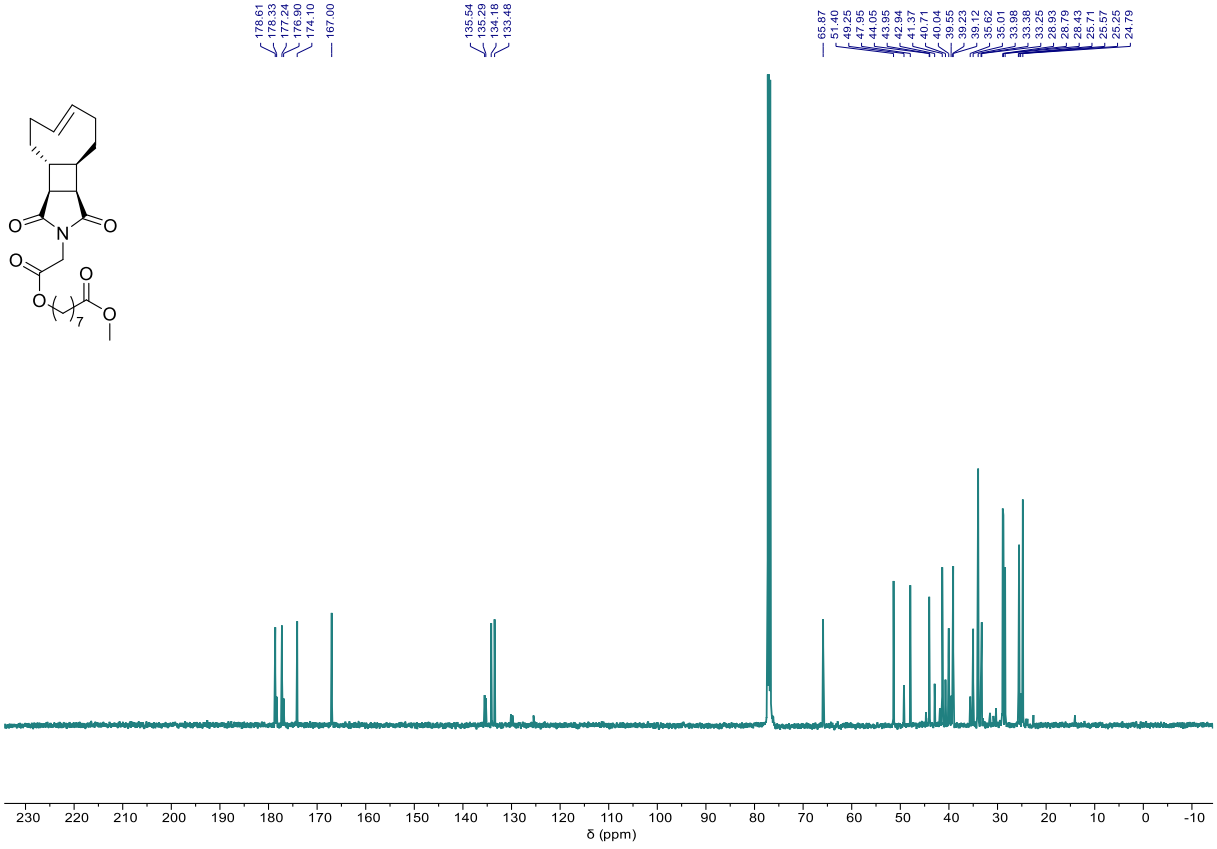

Figure S28. ^{13}C NMR (126 MHz, $CDCl_3$) spectrum of MS

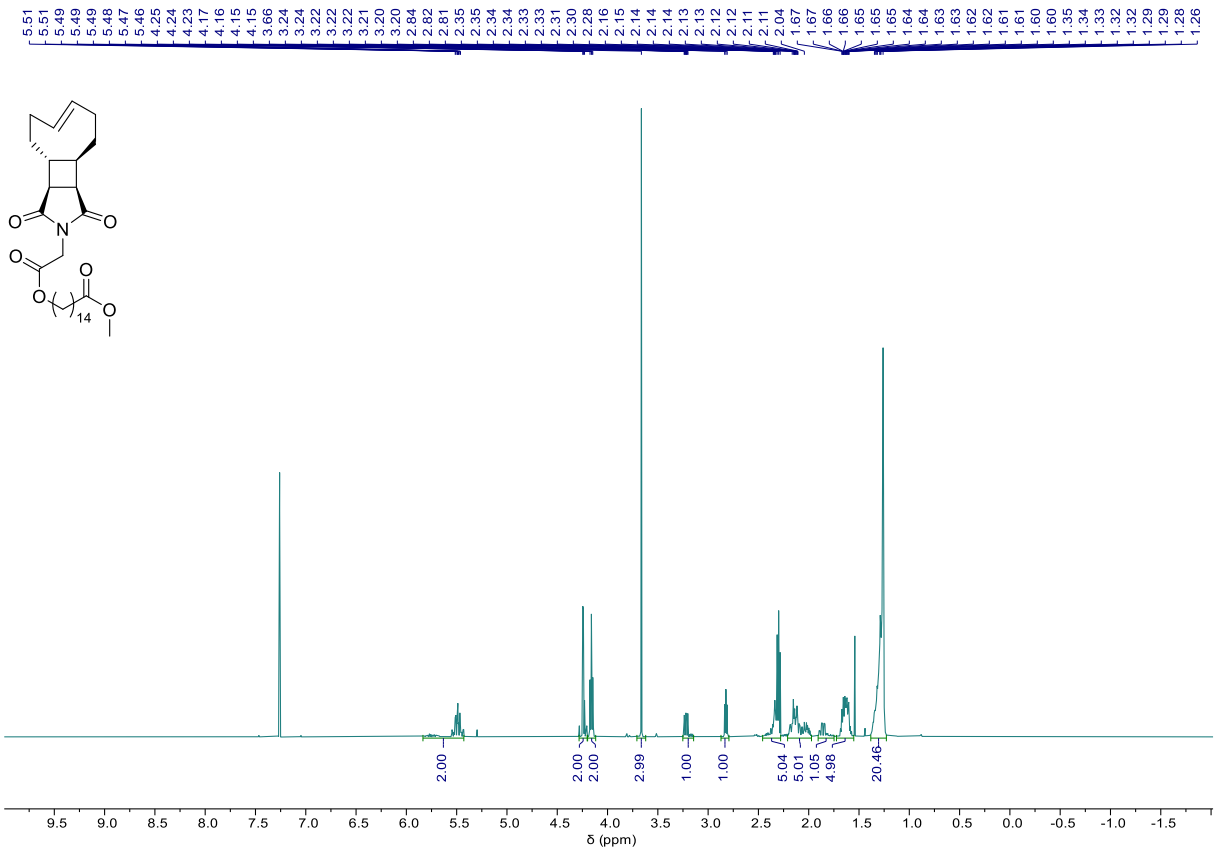

Figure S29. ^{1}H NMR (500 MHz, $CDCl_3$) spectrum of LS

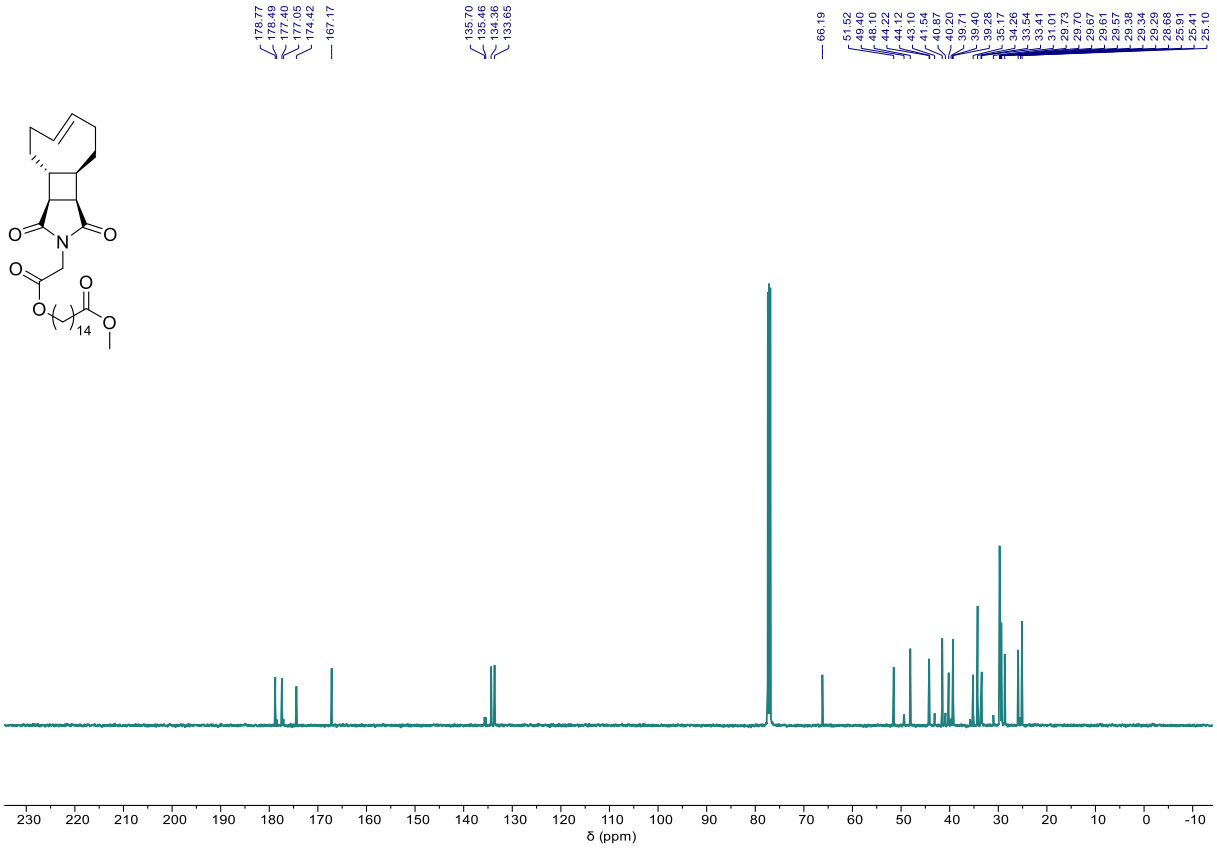

Figure S30. ^{13}C NMR (126 MHz, $CDCl_3$) spectrum of LS

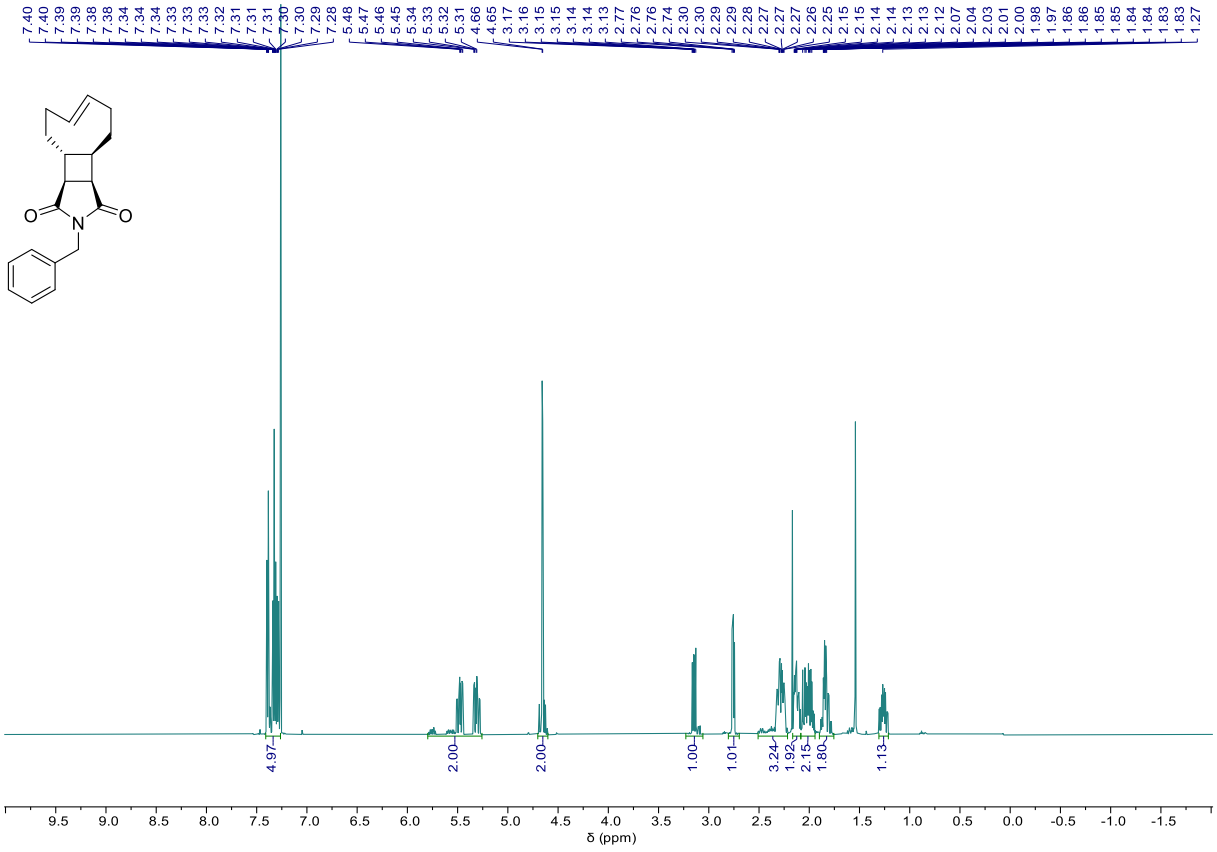

Figure S31. ^{1}H NMR (500 MHz, $CDCl_3$) spectrum of Bn

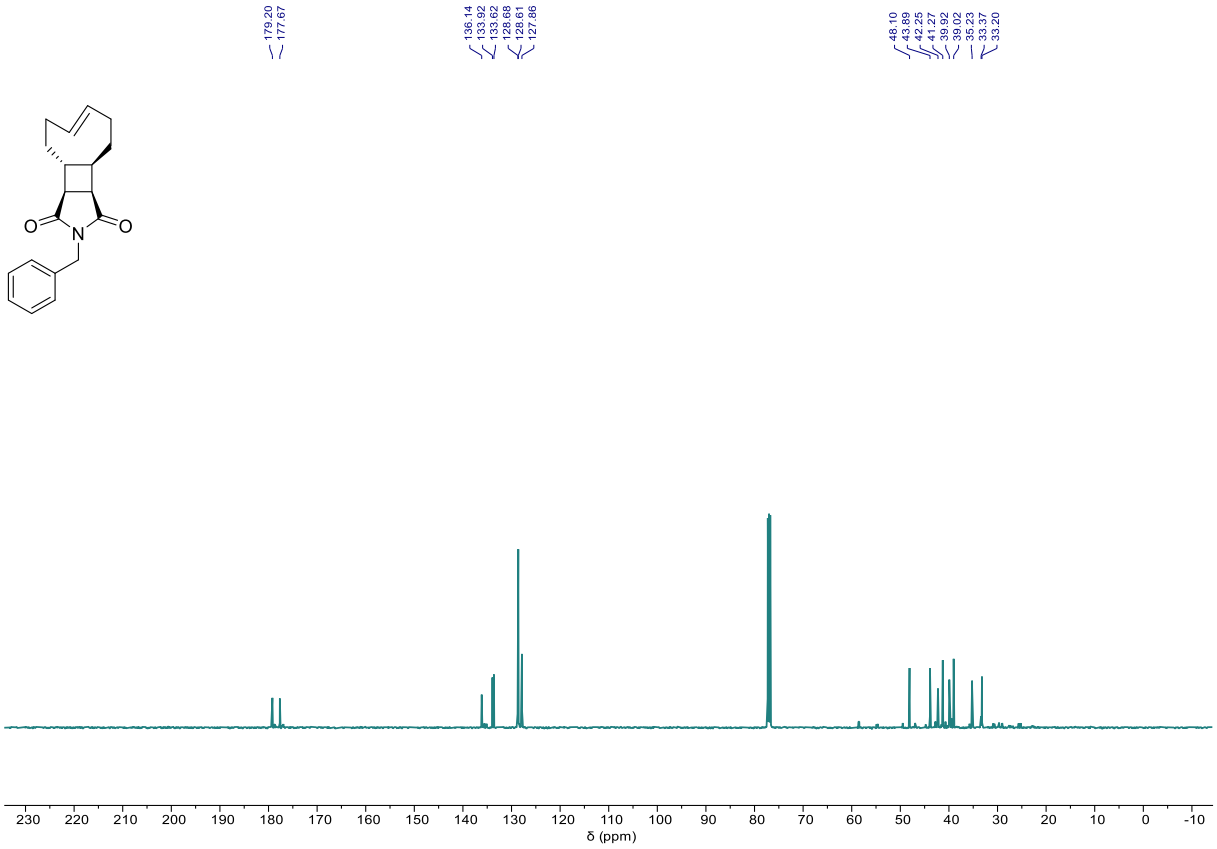

Figure S32. ^{13}C NMR (126 MHz, $CDCl_3$) spectrum of Bn

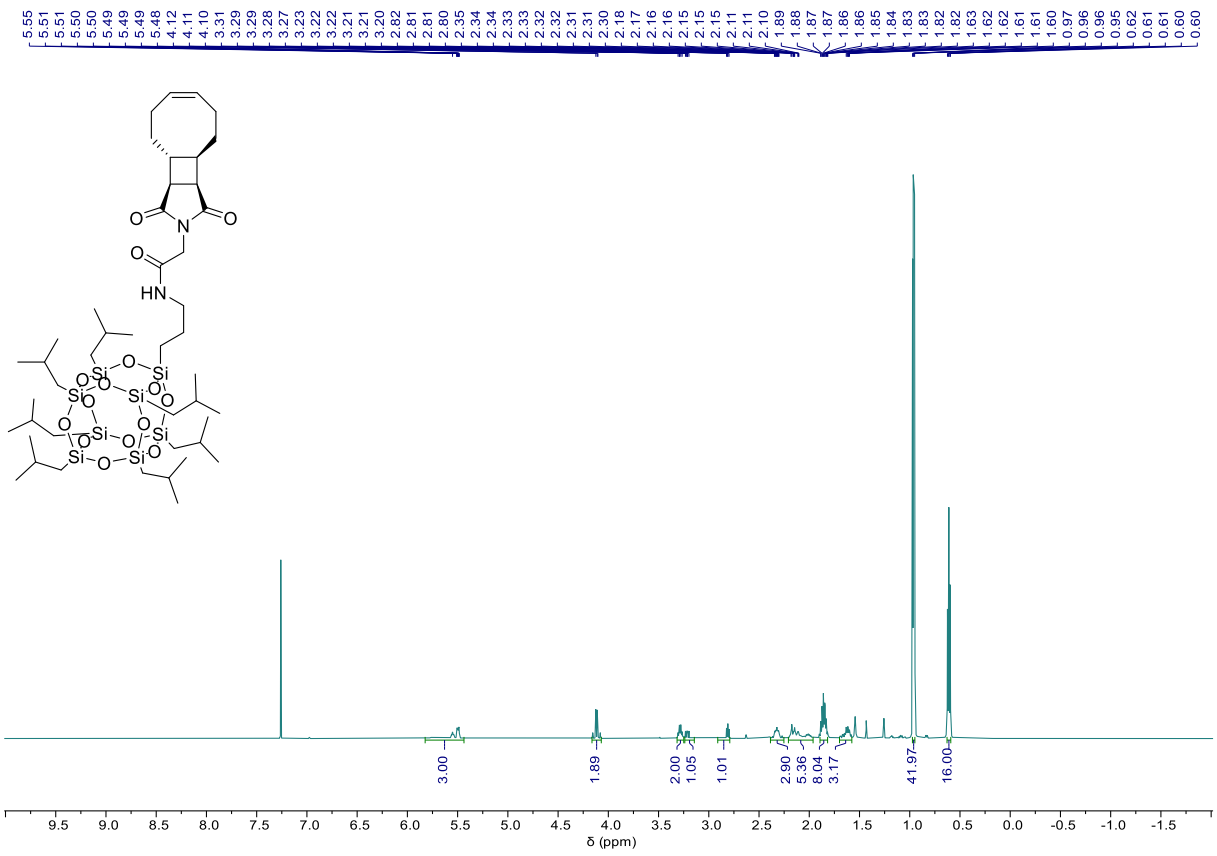

Figure S33. ^{1}H NMR (500 MHz, $CDCl_3$) spectrum of SSPOSS

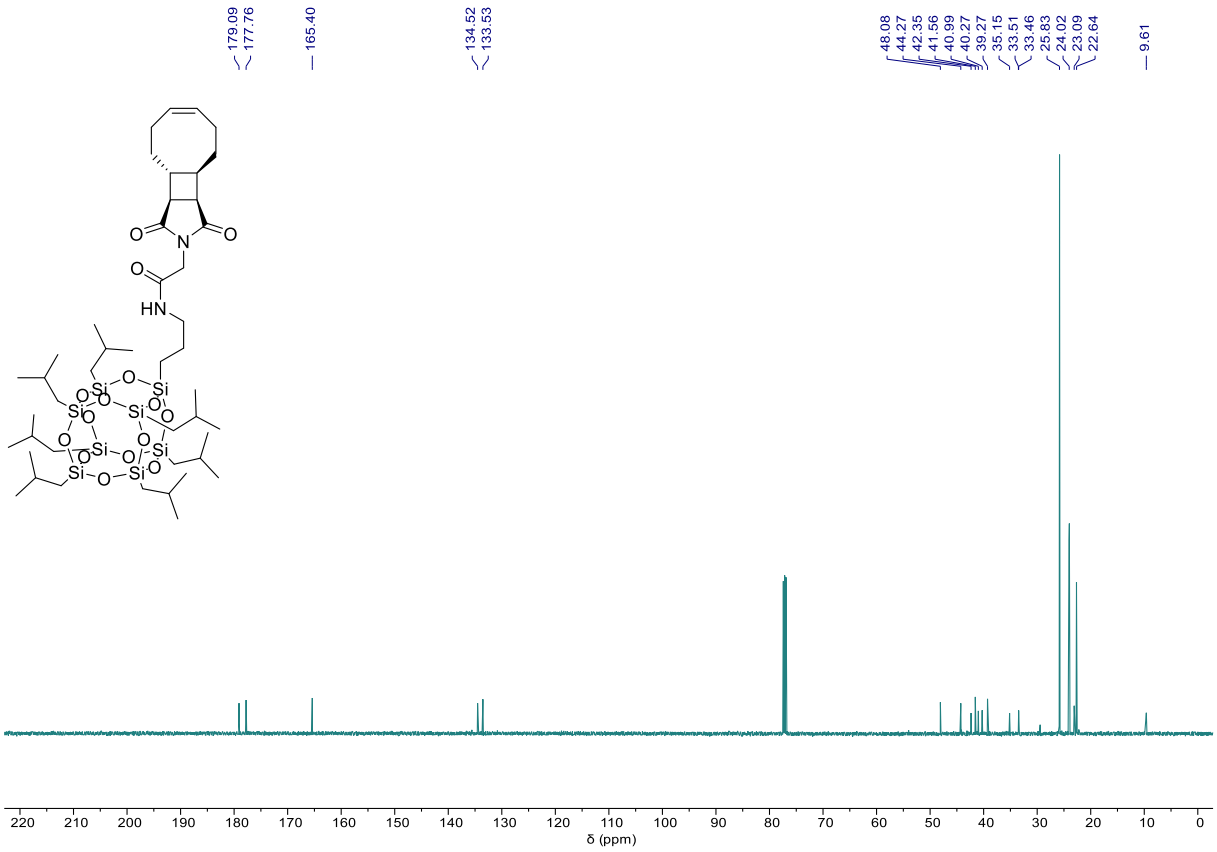

Figure S34. ^{13}C NMR (126 MHz, $CDCl_3$) spectrum of SSPOSS

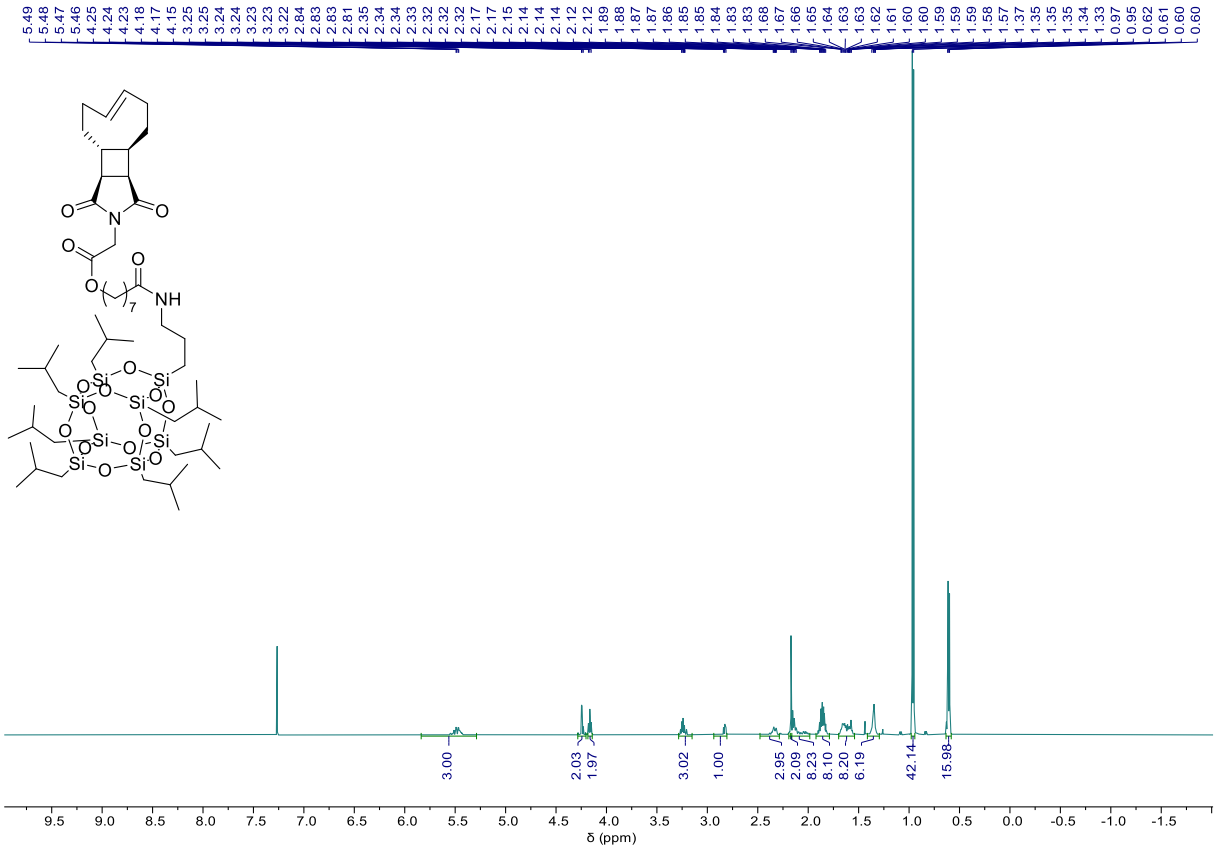

Figure S35. ^{1}H NMR (500 MHz, $CDCl_3$) spectrum of MSPOSS

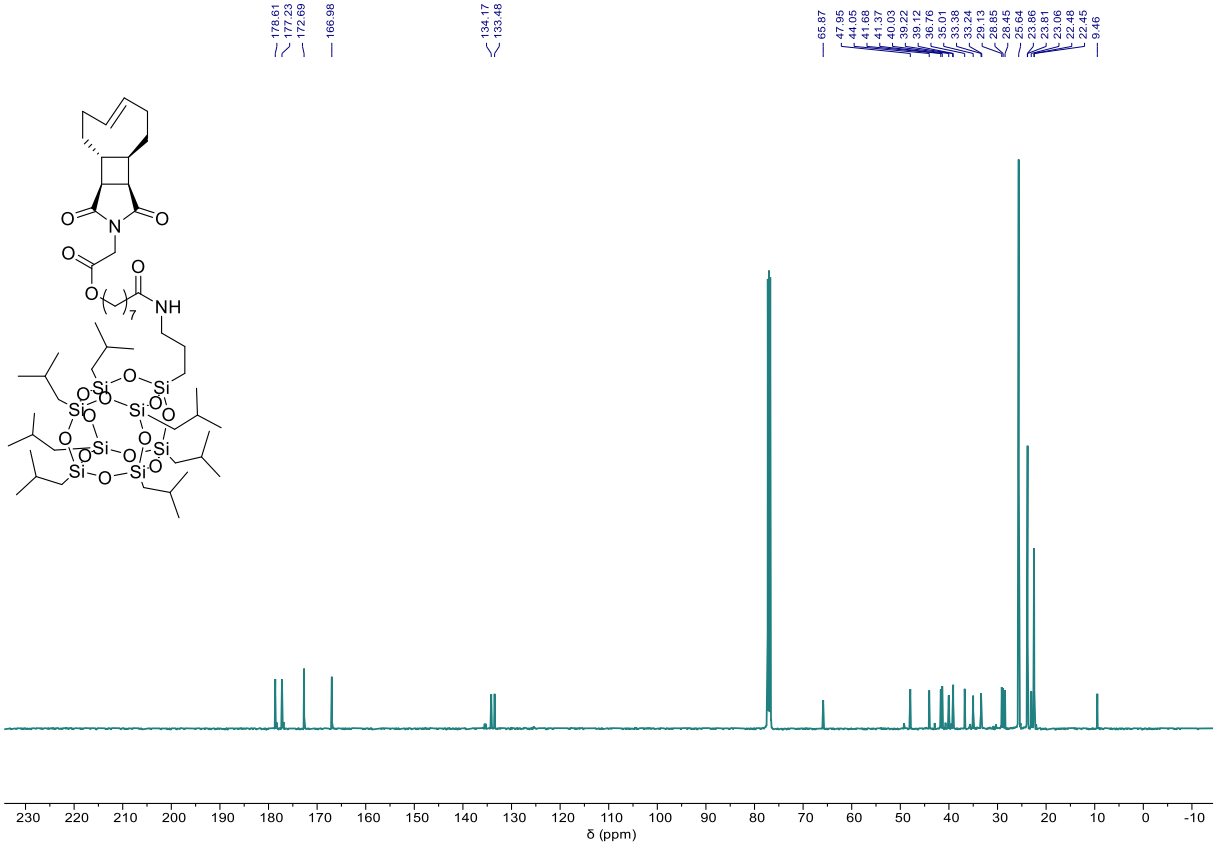

Figure S36. ^{13}C NMR (126 MHz, $CDCl_3$) spectrum of MSPOSS

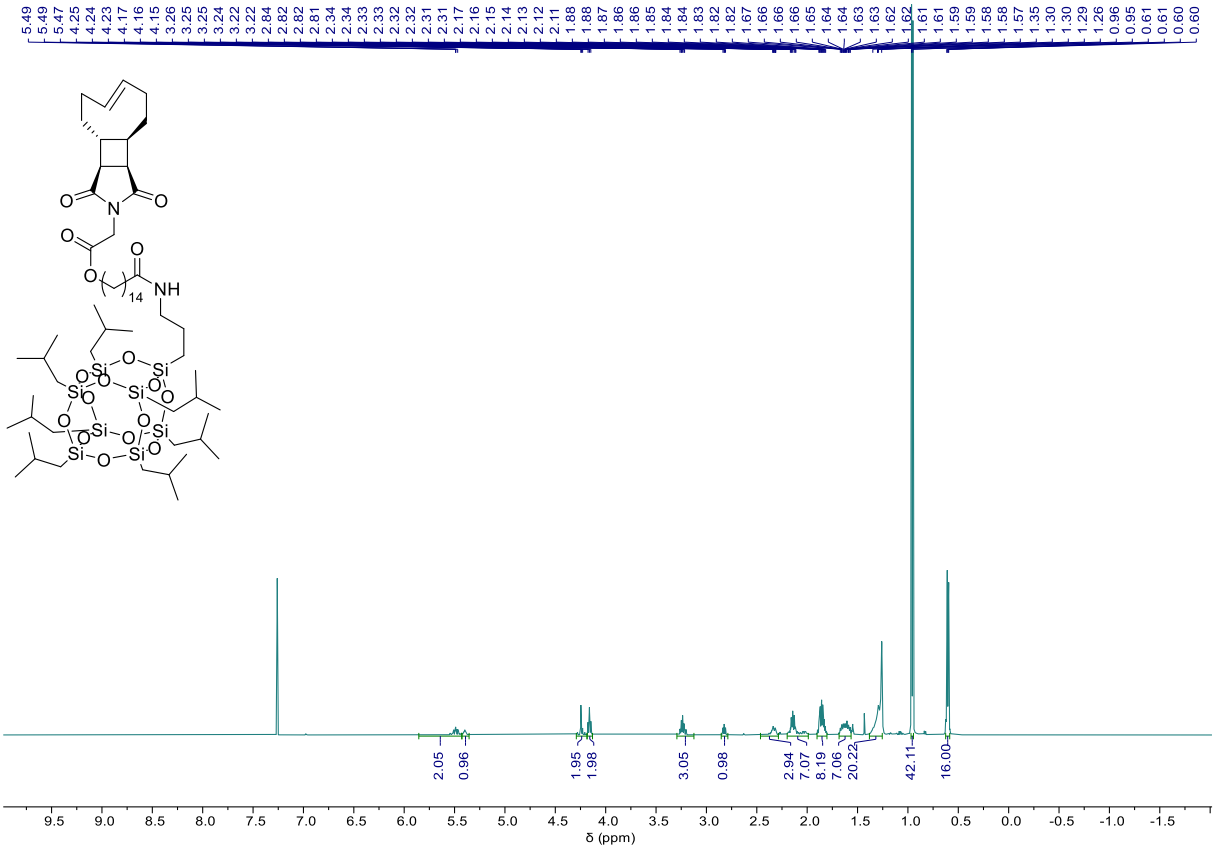

Figure S37. ^{1}H NMR (500 MHz, $CDCl_3$) spectrum of LSPOSS

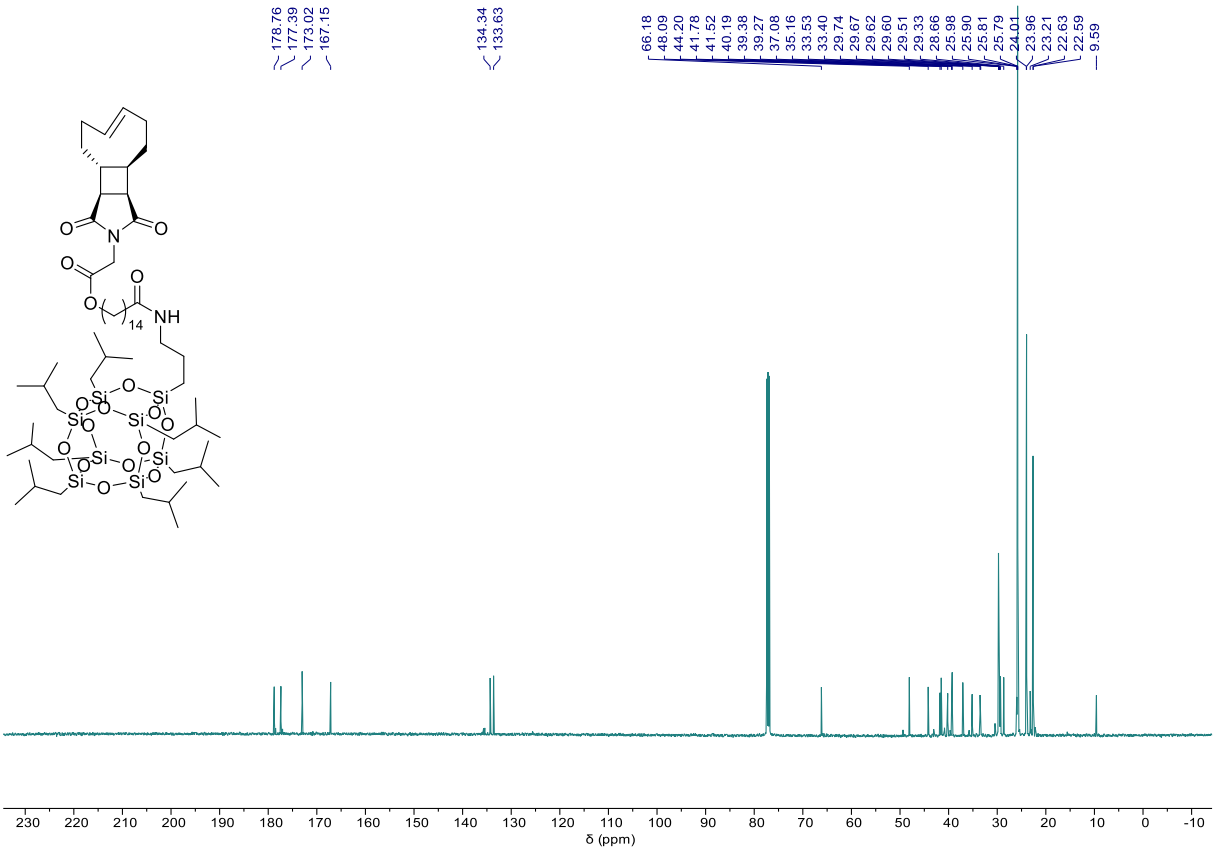

Figure S38. ^{13}C NMR (126 MHz, $CDCl_3$) spectrum of LSPOSS

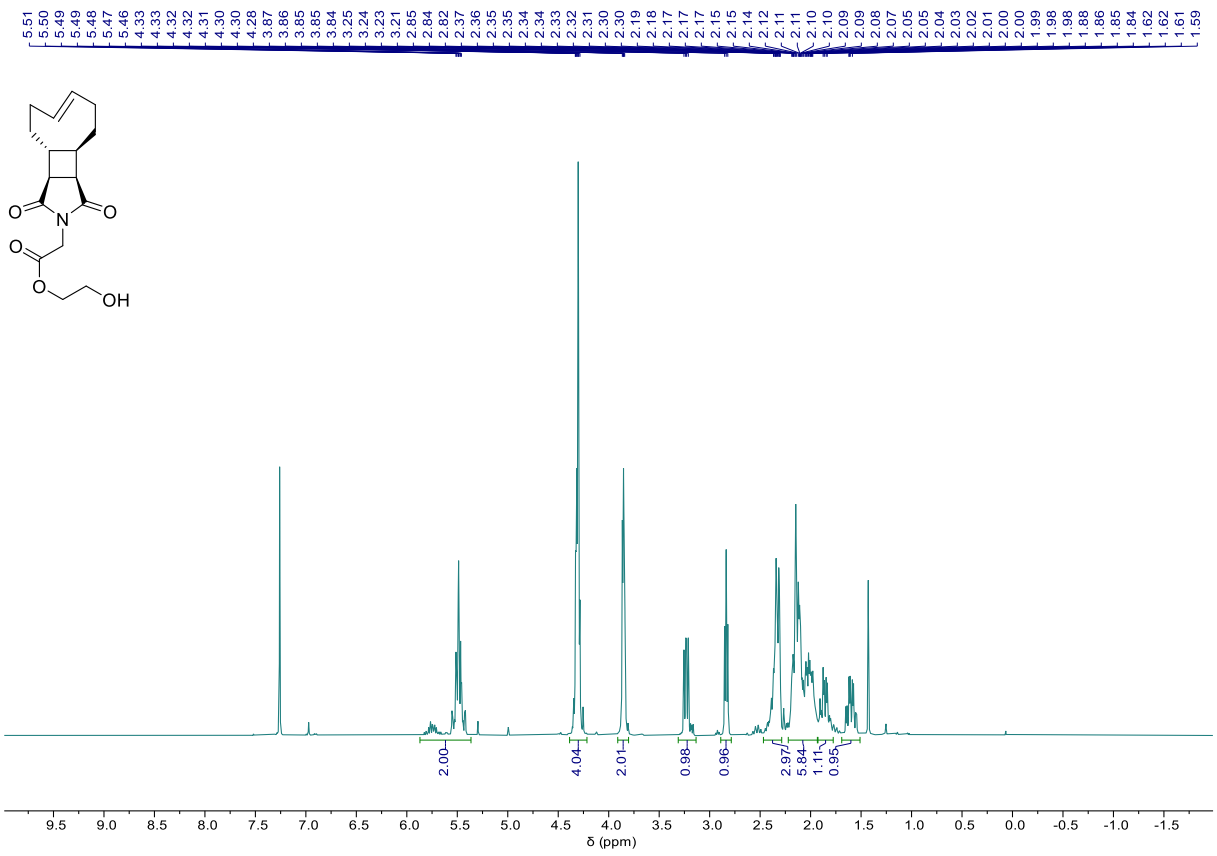

Figure S39. ^{1}H NMR (500 MHz, $CDCl_3$) spectrum of **6**

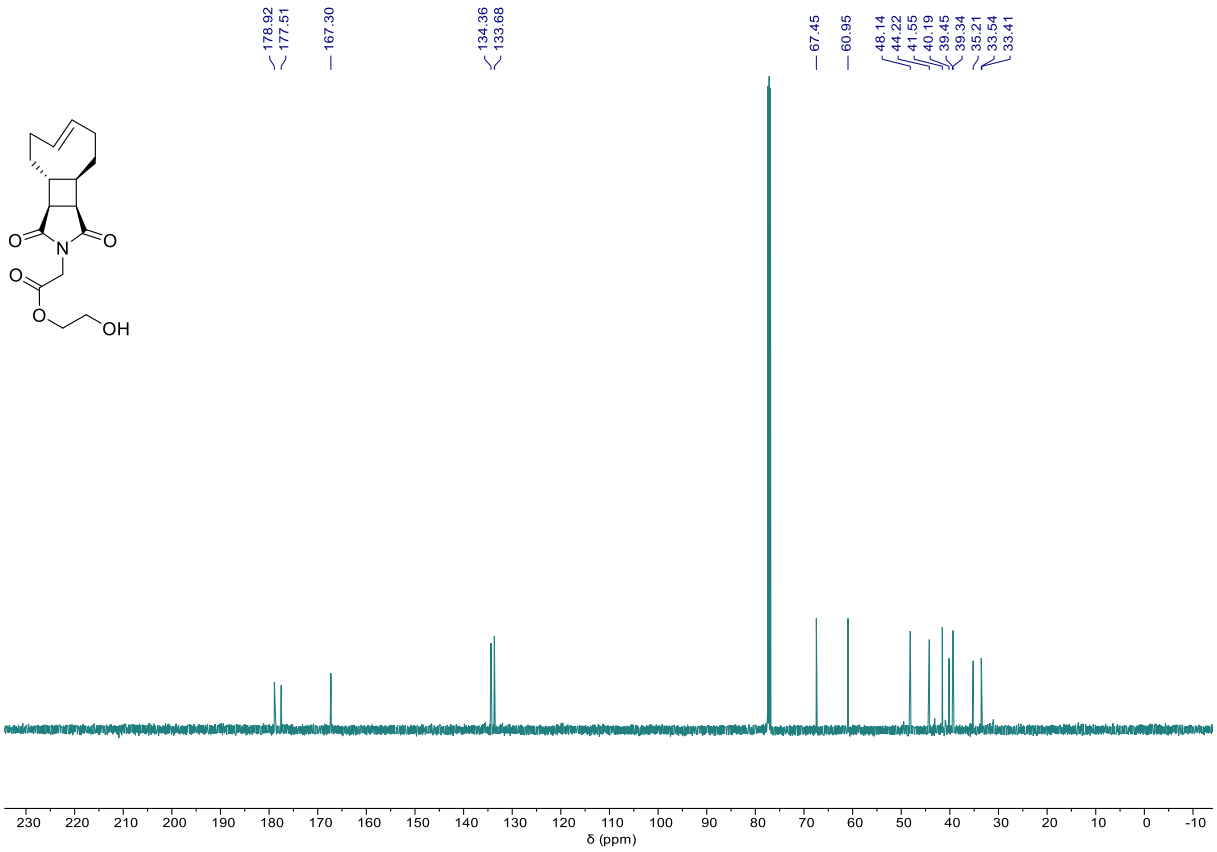

Figure S40. ^{13}C NMR (126 MHz, $CDCl_3$) spectrum of **6**

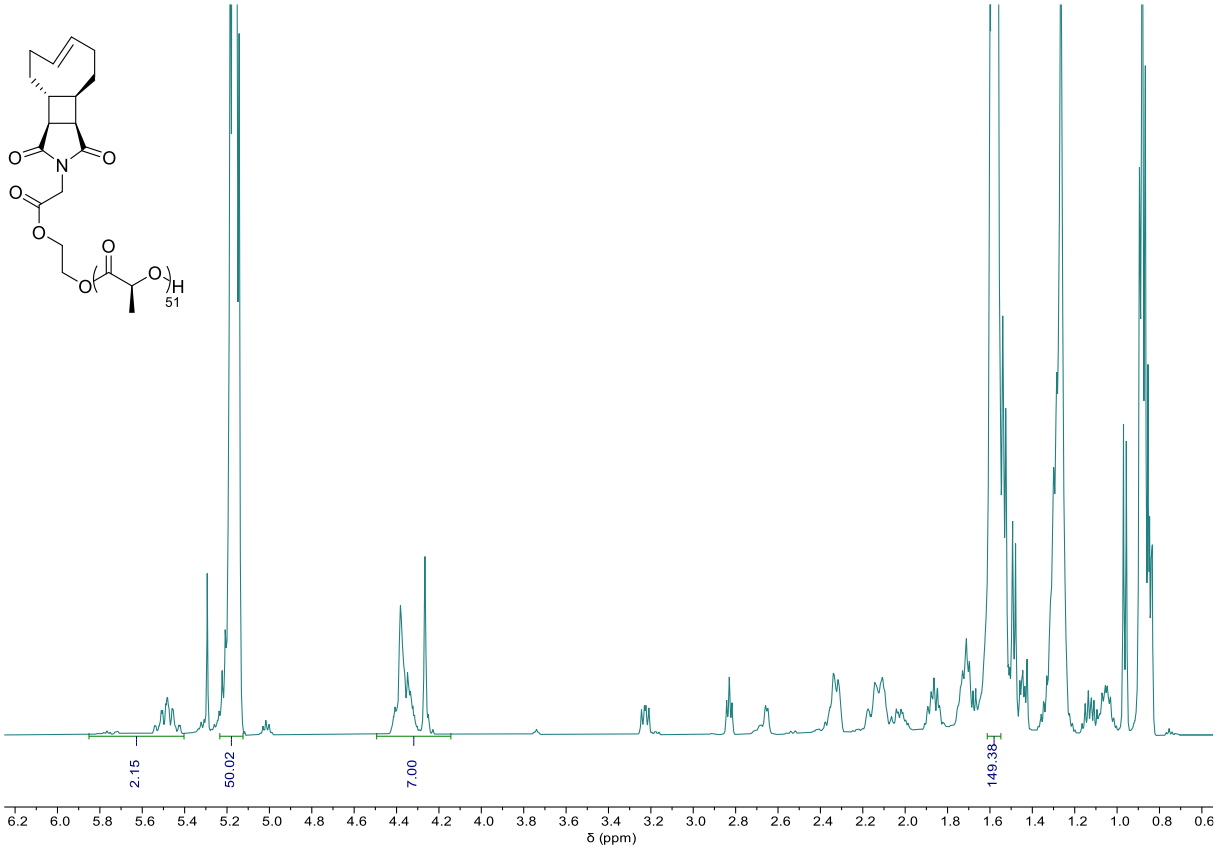

Figure S41. ^{1}H NMR (500 MHz, $CDCl_3$) spectrum of PLLA

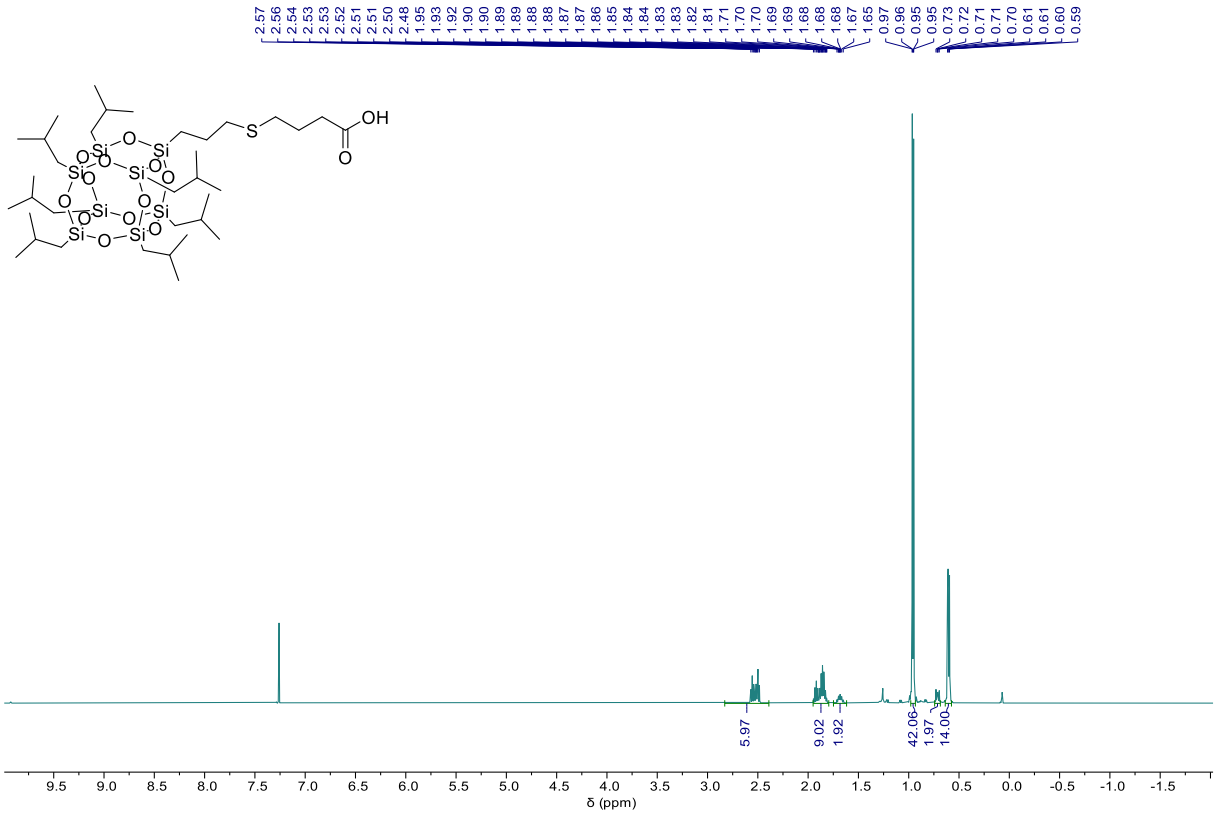

Figure S42. ^{1}H NMR (500 MHz, $CDCl_3$) spectrum of **7**

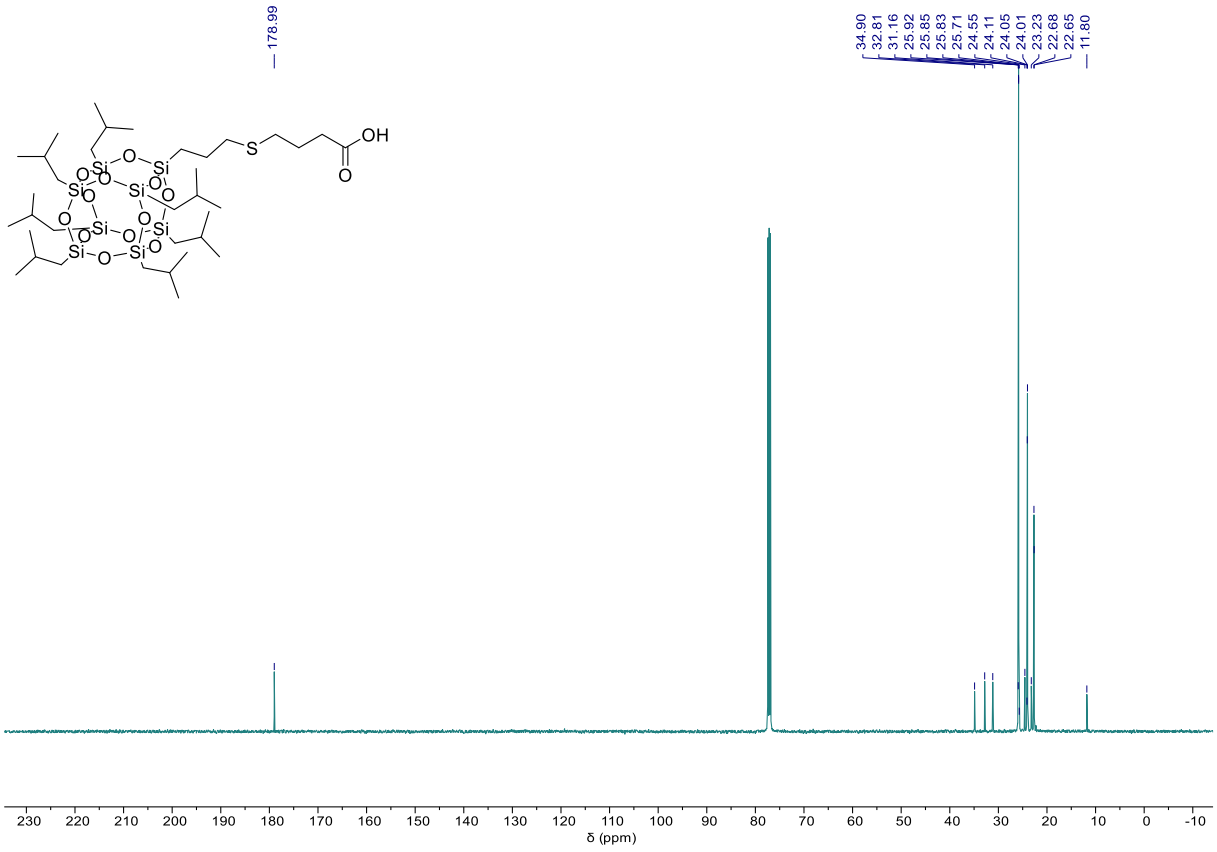

Figure S43. ^{13}C NMR (126 MHz, $CDCl_3$) spectrum of **7**

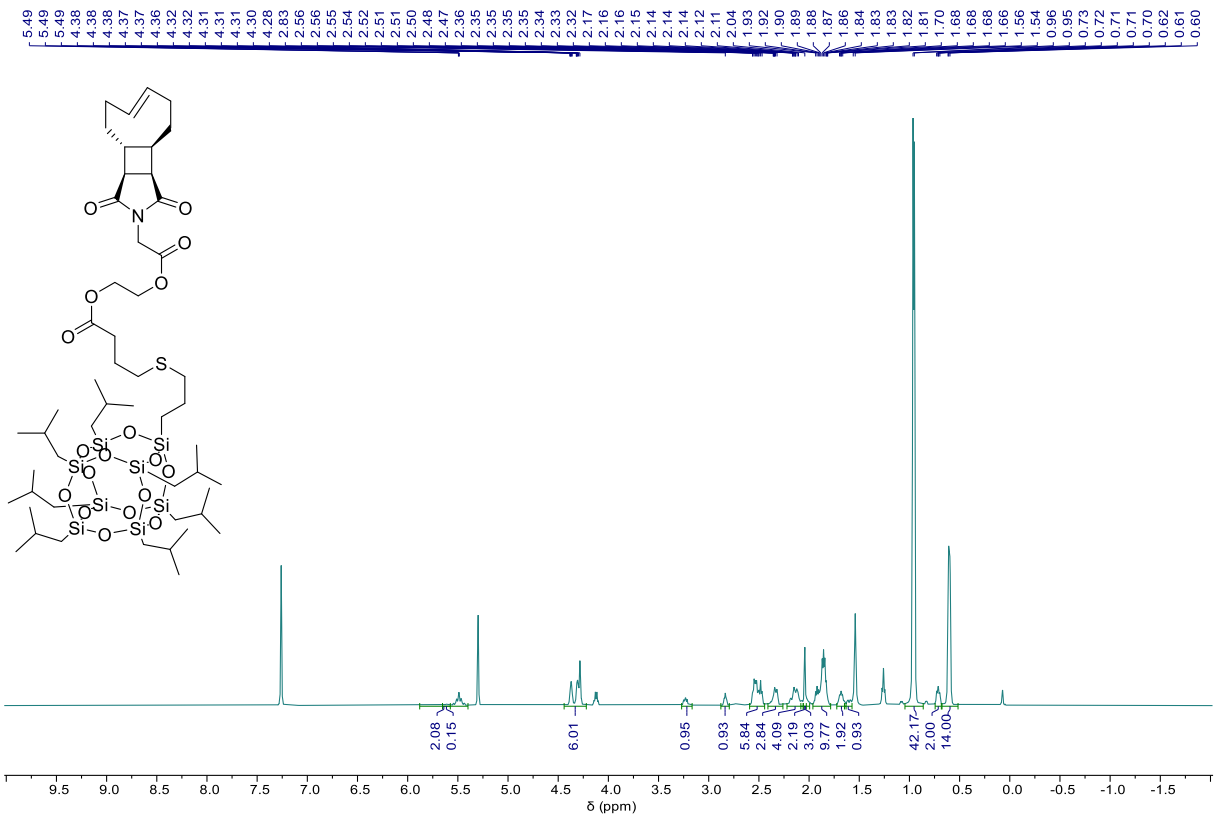

Figure S44. ^{1}H NMR (500 MHz, $CDCl_3$) spectrum of M'SPOSS

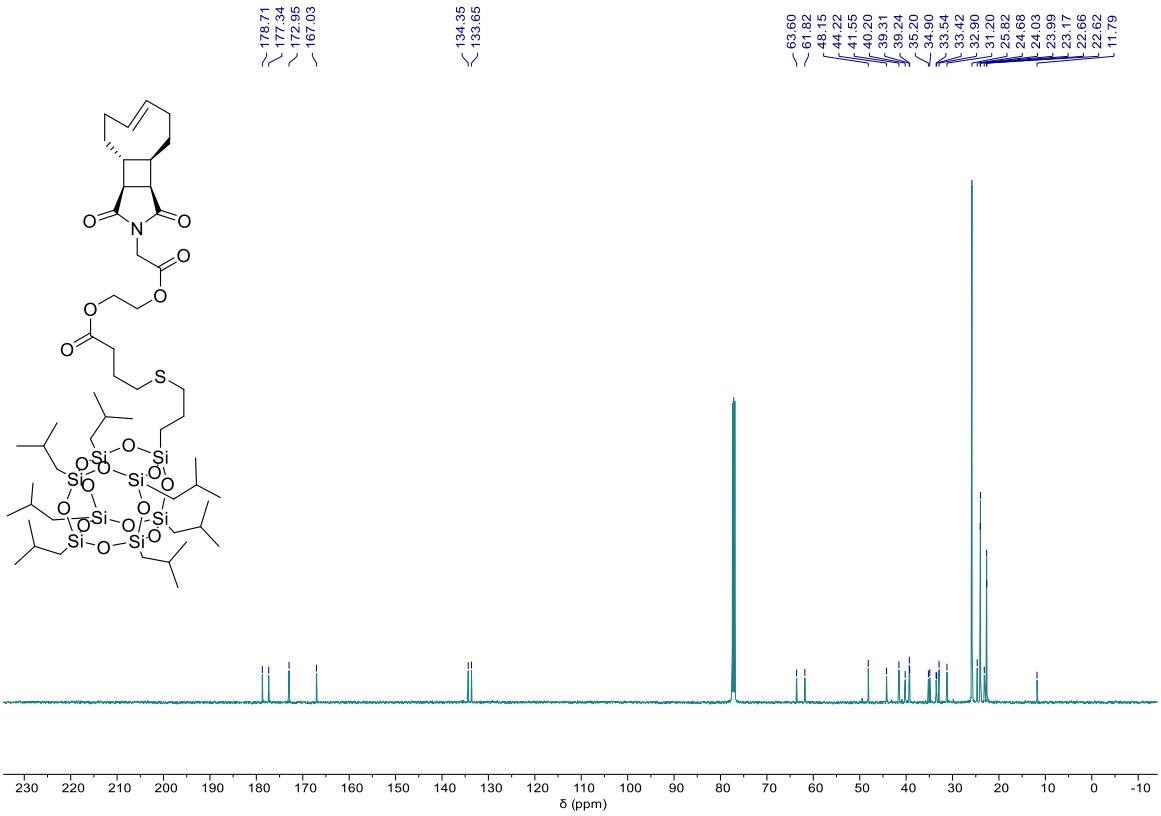

Figure S45. ^{13}C NMR (126 MHz, $CDCl_3$) spectrum of M'SPOSS

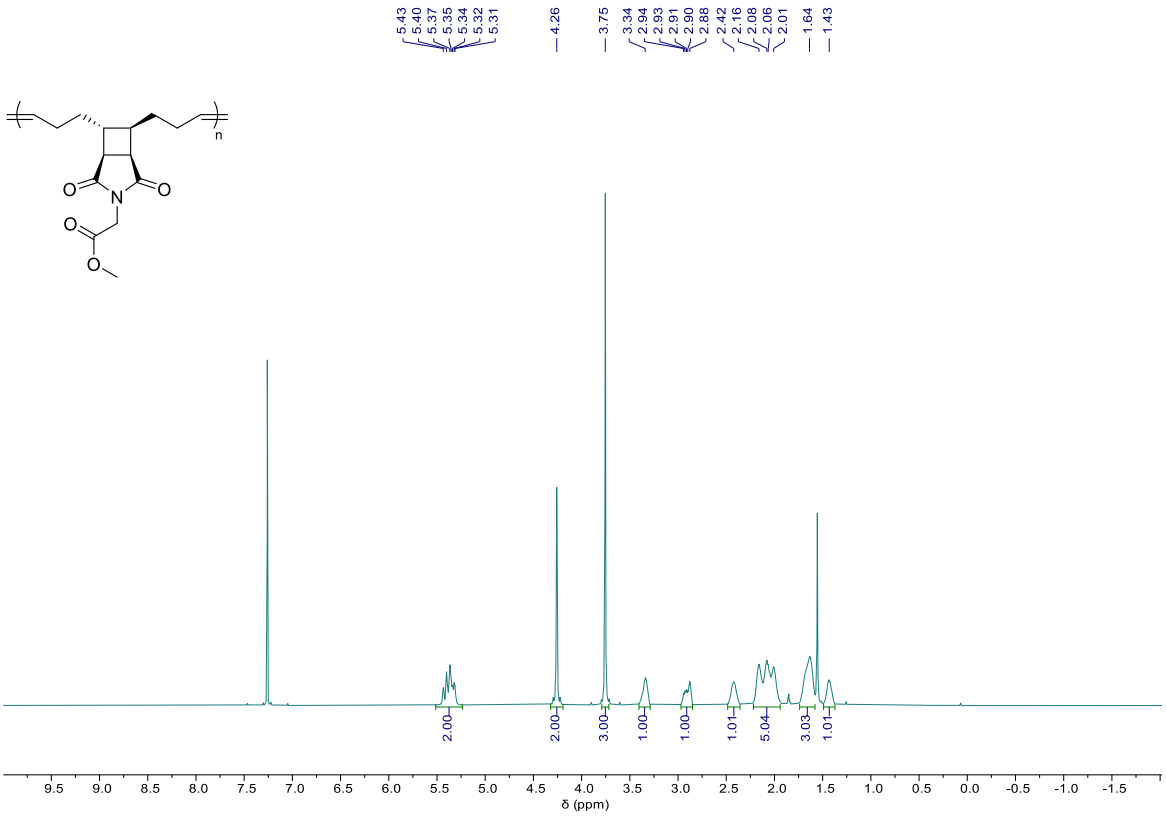

Figure S46. ^{1}H NMR (500 MHz, $CDCl_3$) spectrum of PSS

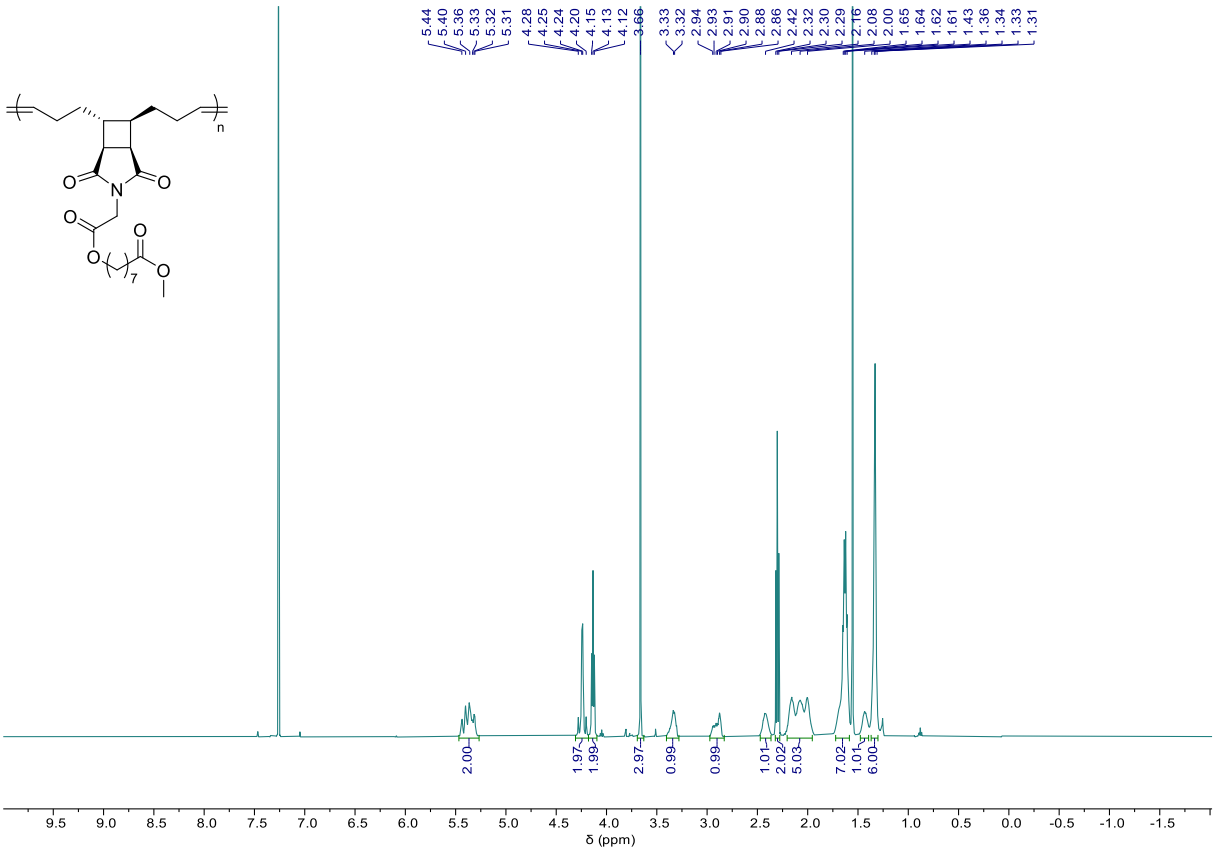

Figure S47. ^{1}H NMR (500 MHz, $CDCl_3$) spectrum of PMS

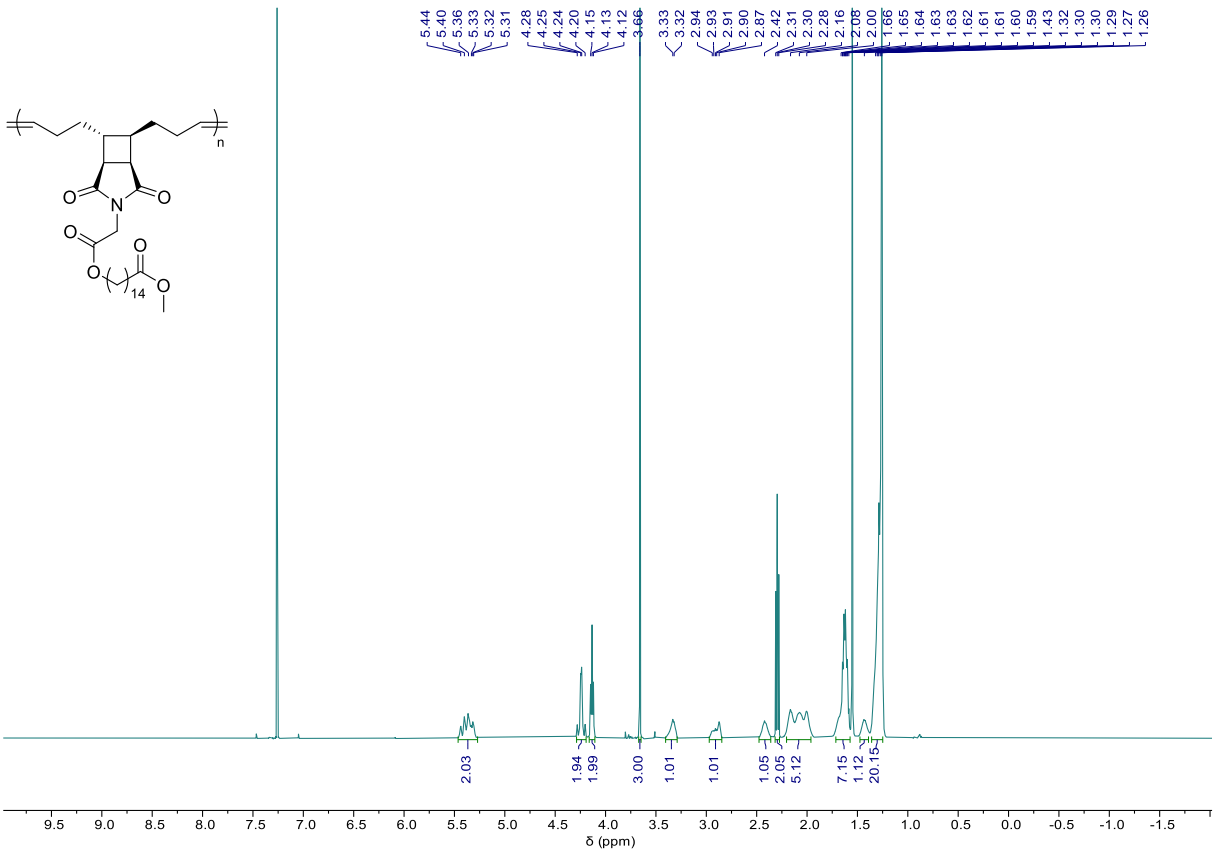

Figure S48. ^{1}H NMR (500 MHz, $CDCl_3$) spectrum of PLS

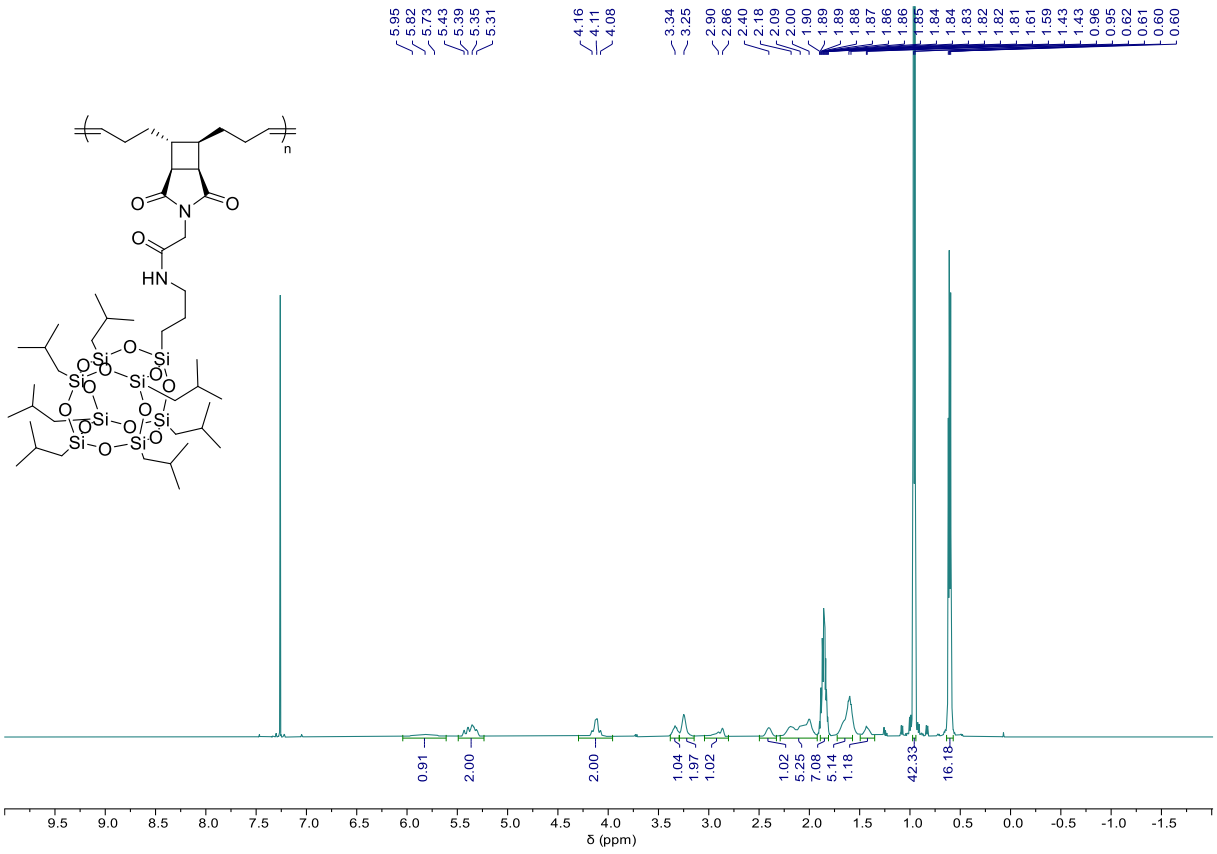

Figure S49. ^{1}H NMR (500 MHz, $CDCl_3$) spectrum of PSSPOSS

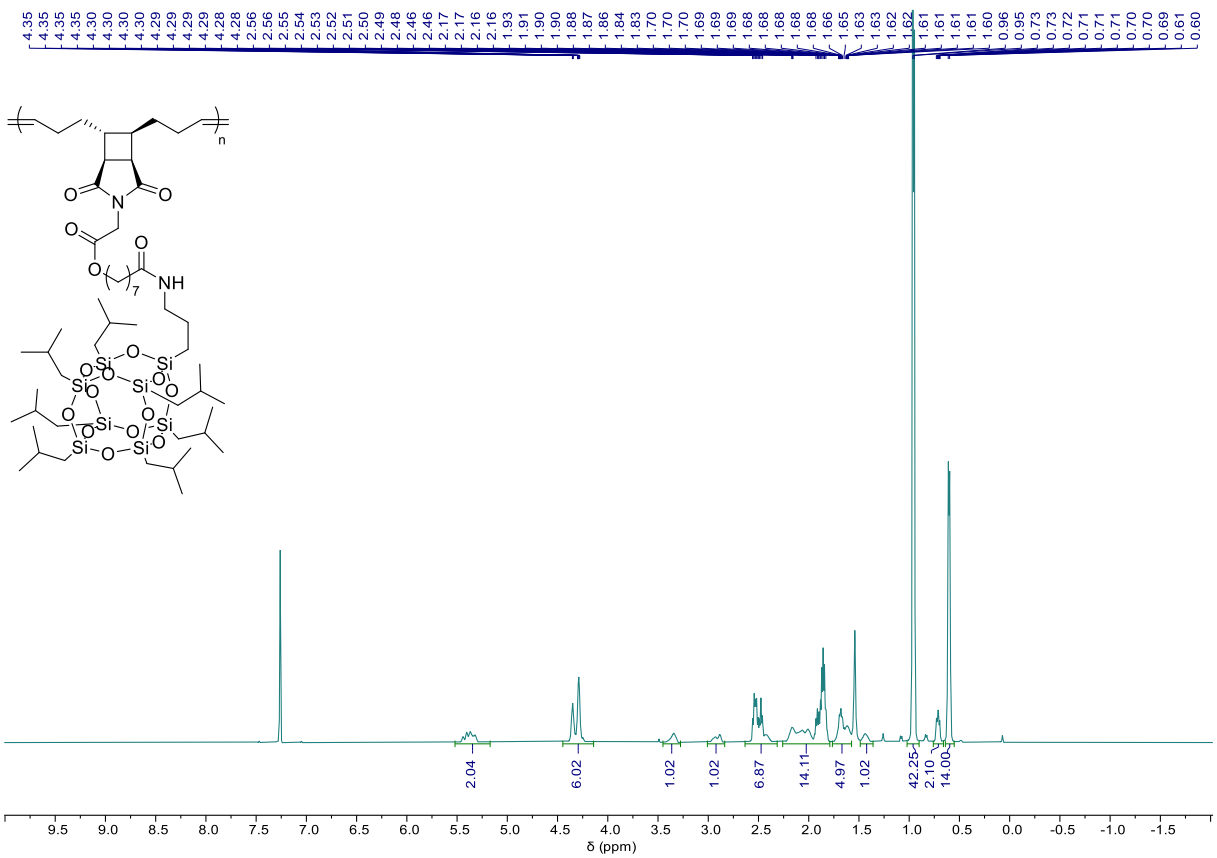

Figure S50. ^{1}H NMR (500 MHz, $CDCl_3$) spectrum of PMSPOSS

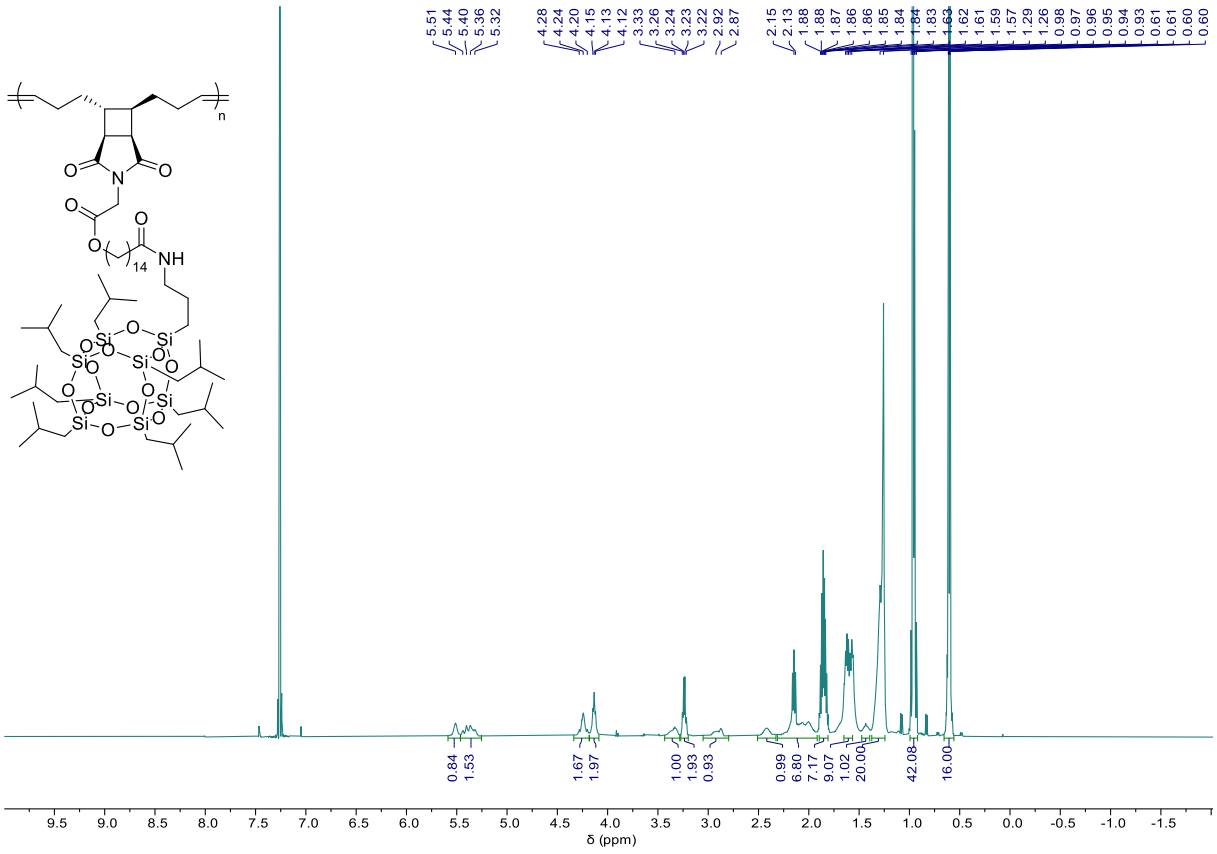

Figure S51. ^{1}H NMR (500 MHz, $CDCl_3$) spectrum of PLSPOSS

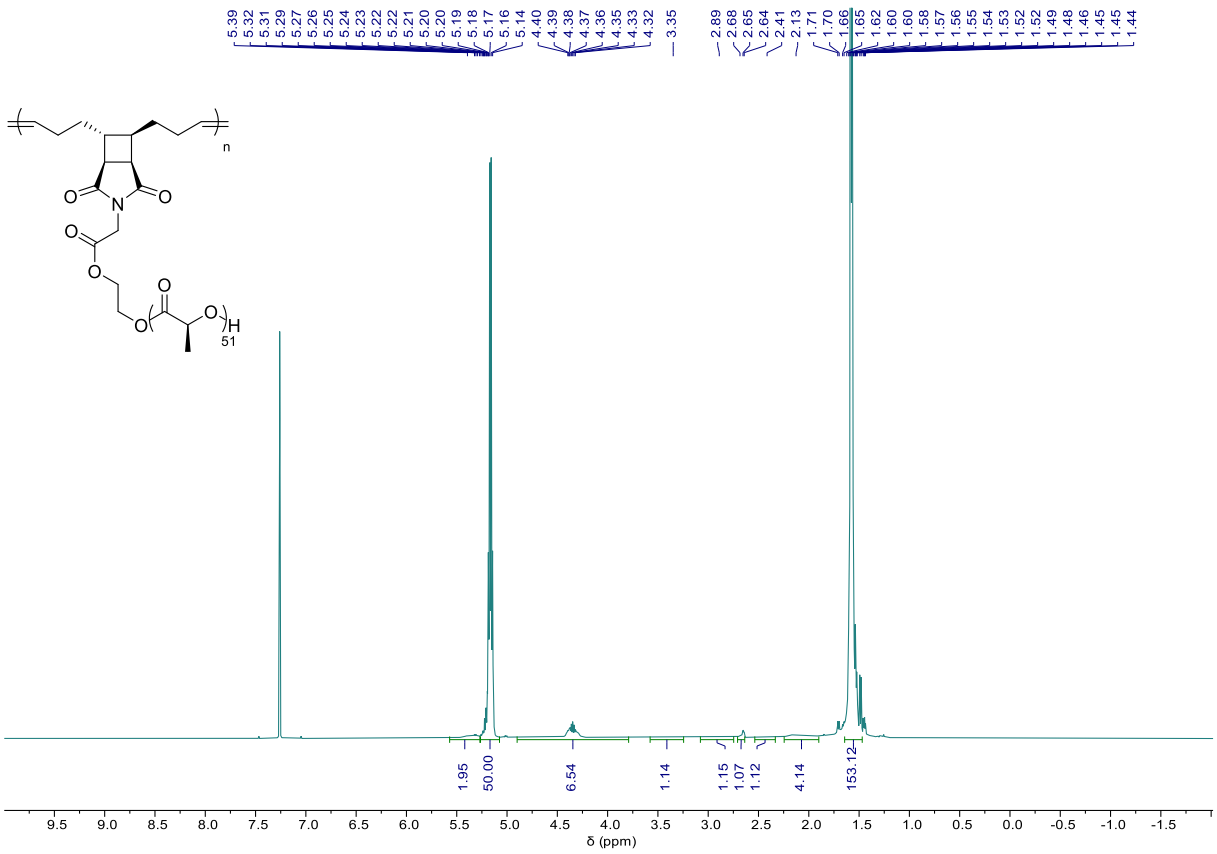

Figure S52. ^{1}H NMR (500 MHz, $CDCl_3$) spectrum of PPLLA

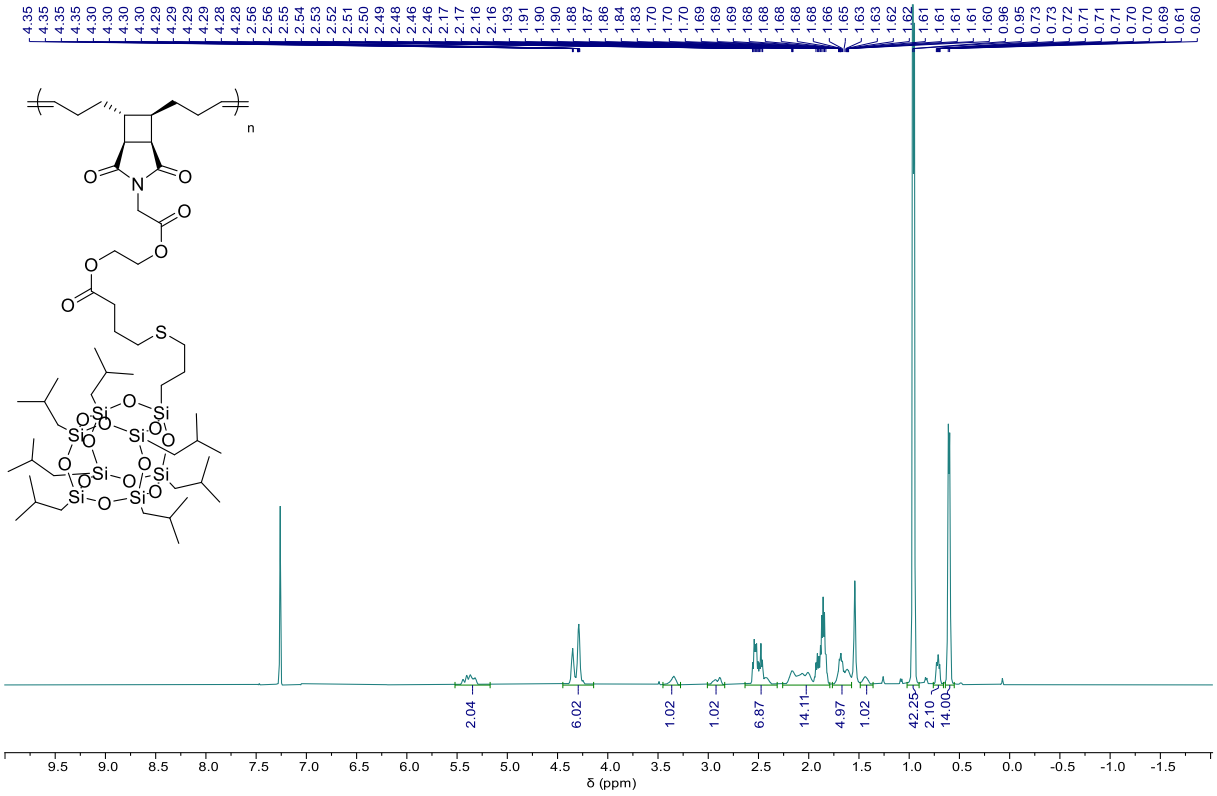

Figure S53. ^{1}H NMR (500 MHz, $CDCl_3$) spectrum of PM'SPOSS

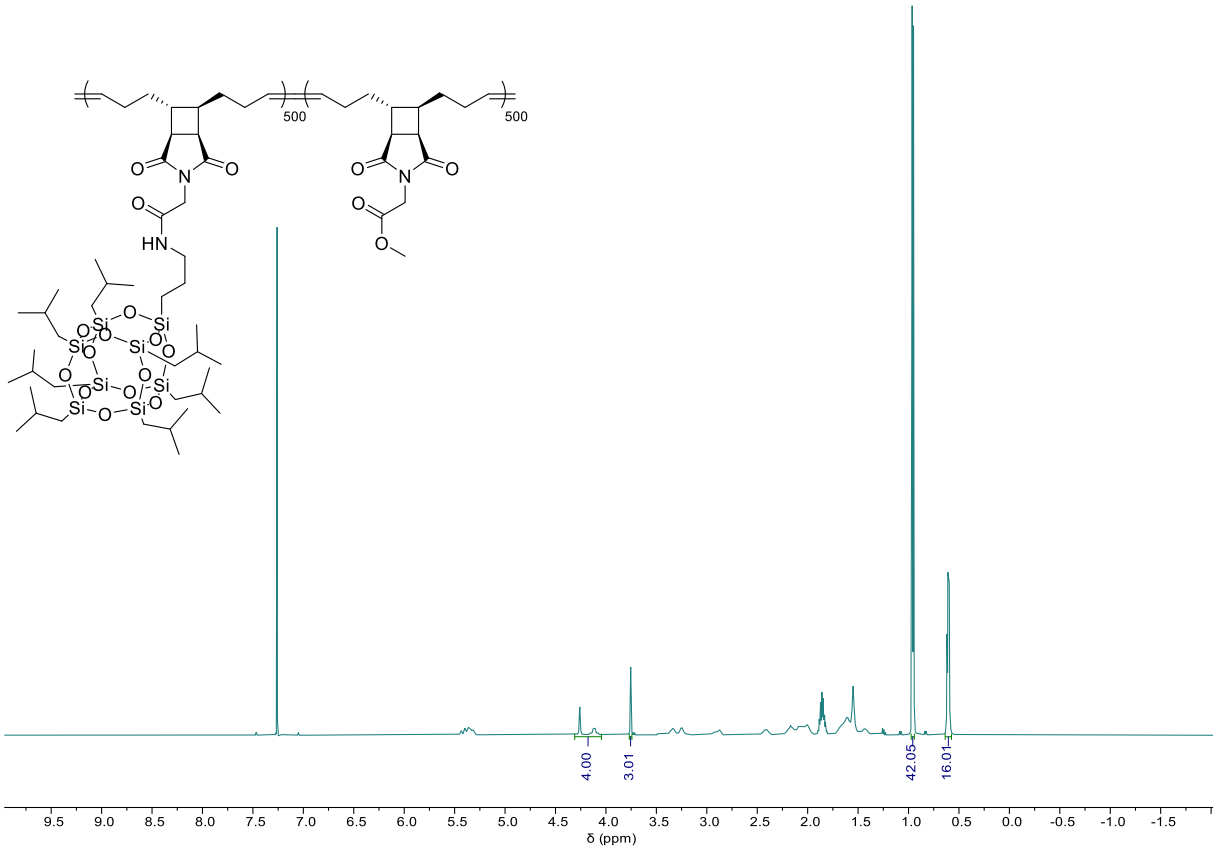

Figure S54. ^{1}H NMR (500 MHz, $CDCl_3$) spectrum of $PSSPOSS_{500}SS_{500}$

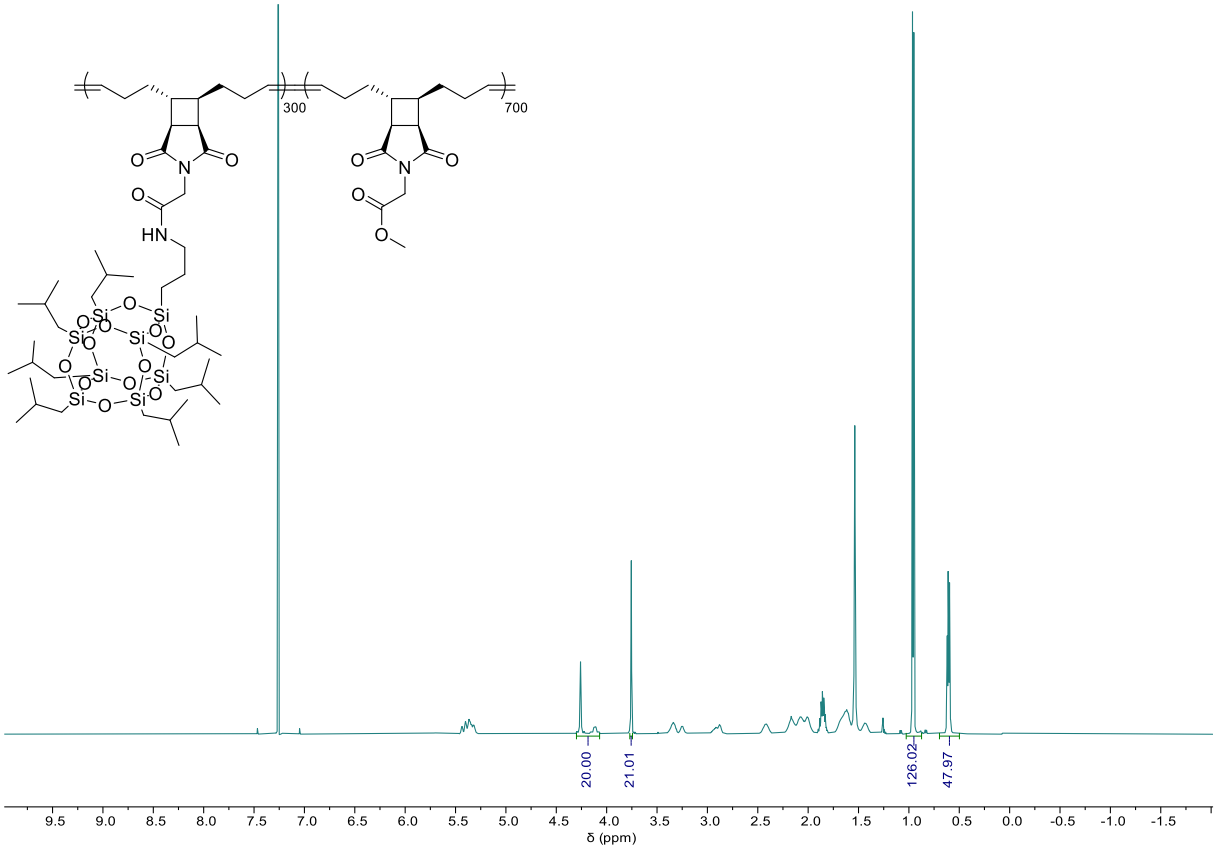

Figure S55. ^{1}H NMR (500 MHz, $CDCl_3$) spectrum of $PSSPOSS_{300}SS_{700}$

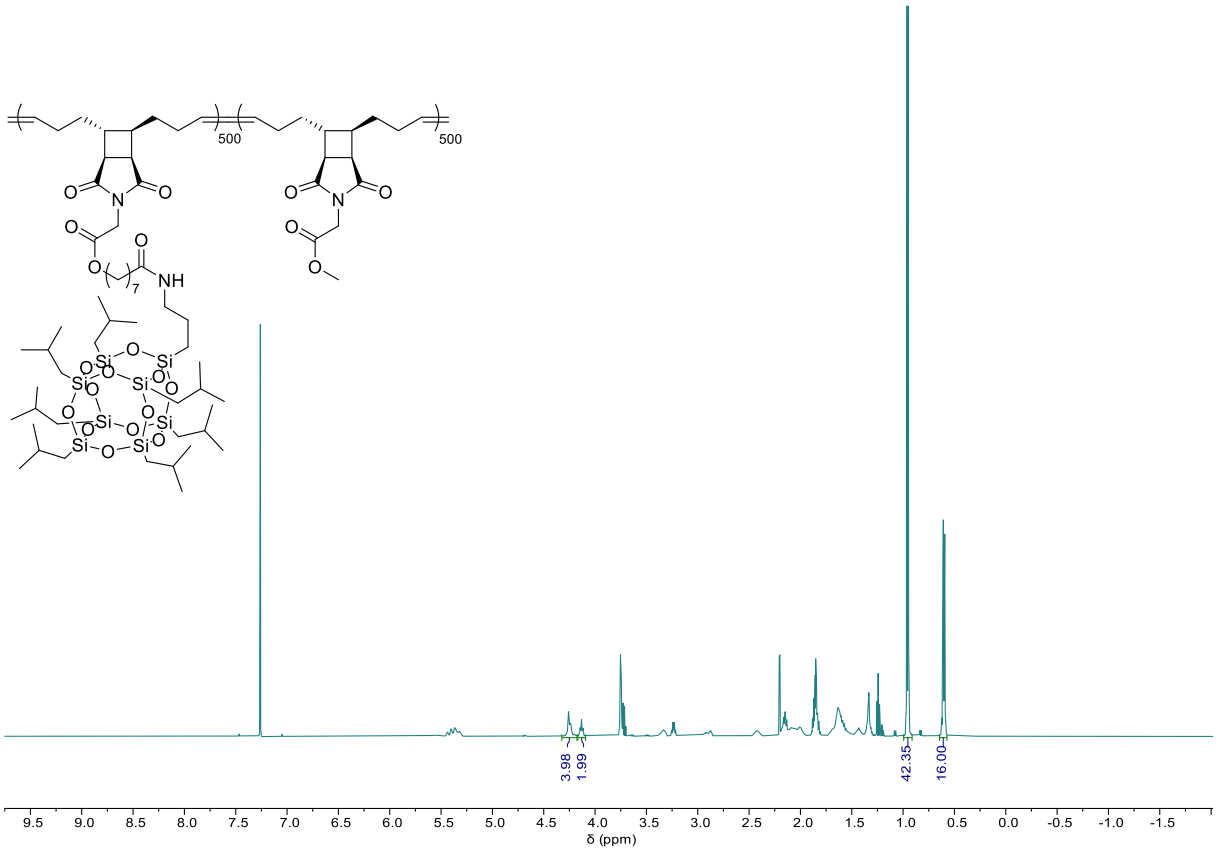

Figure S56. ^{1}H NMR (500 MHz, $CDCl_3$) spectrum of $PMSPOSS_{500}SS_{500}$

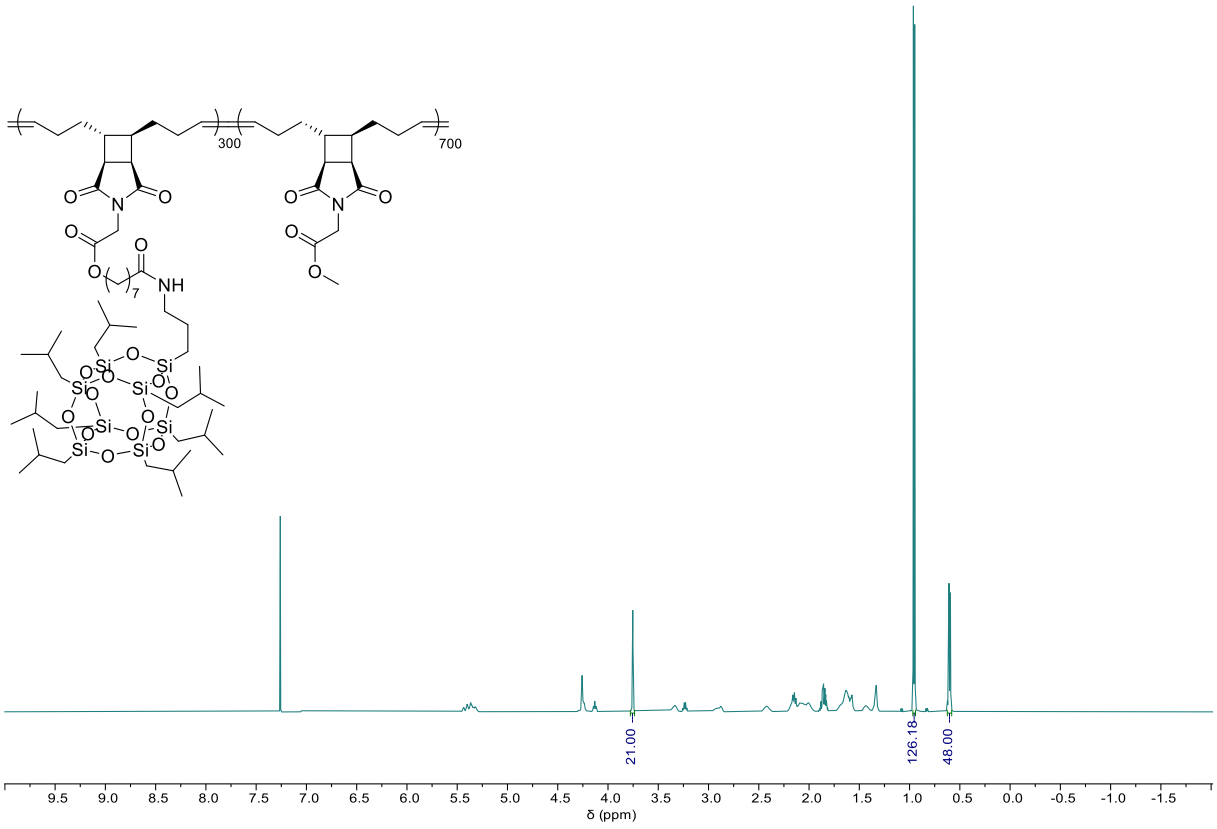

Figure S57. ^{1}H NMR (500 MHz, $CDCl_3$) spectrum of $PMSPOSS_{300}SS_{700}$

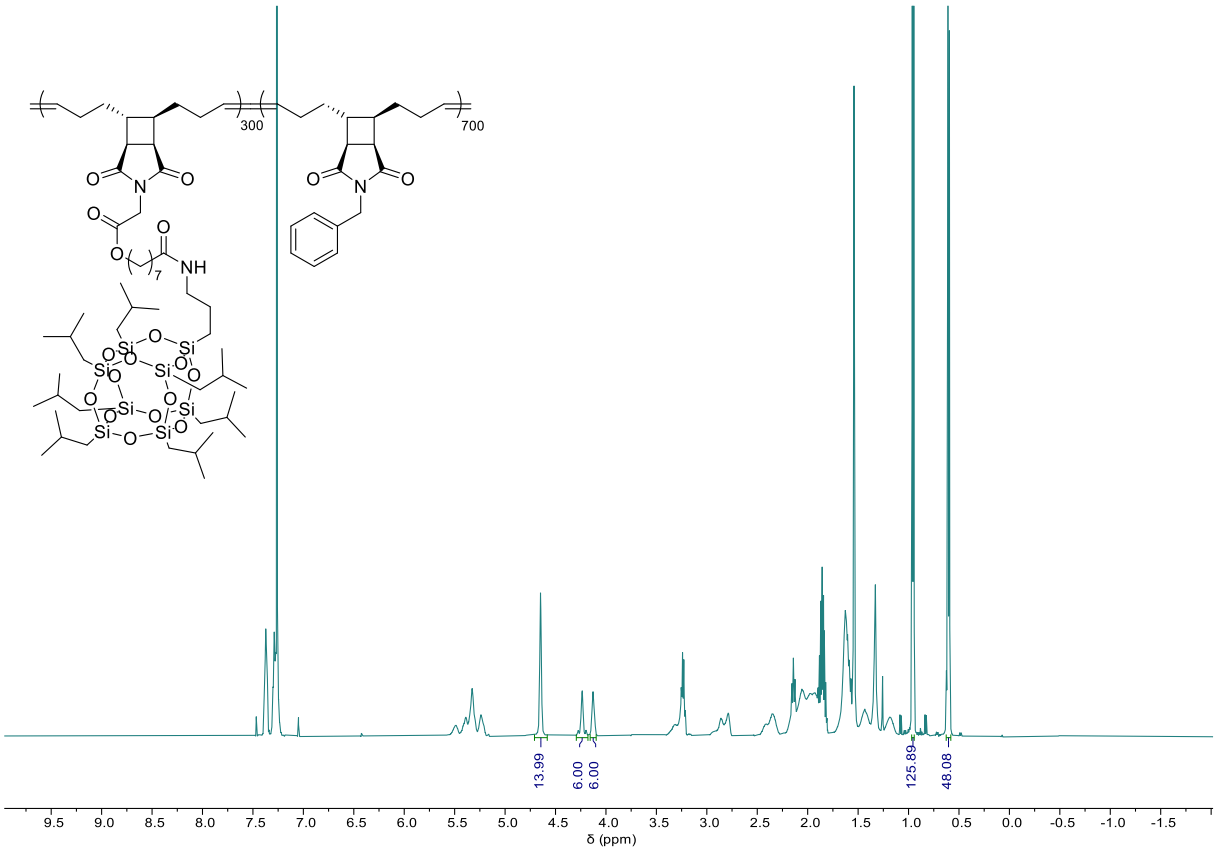

Figure S58. ^{1}H NMR (500 MHz, $CDCl_3$) spectrum of $PMSPOSS_{300}Bn_{700}$

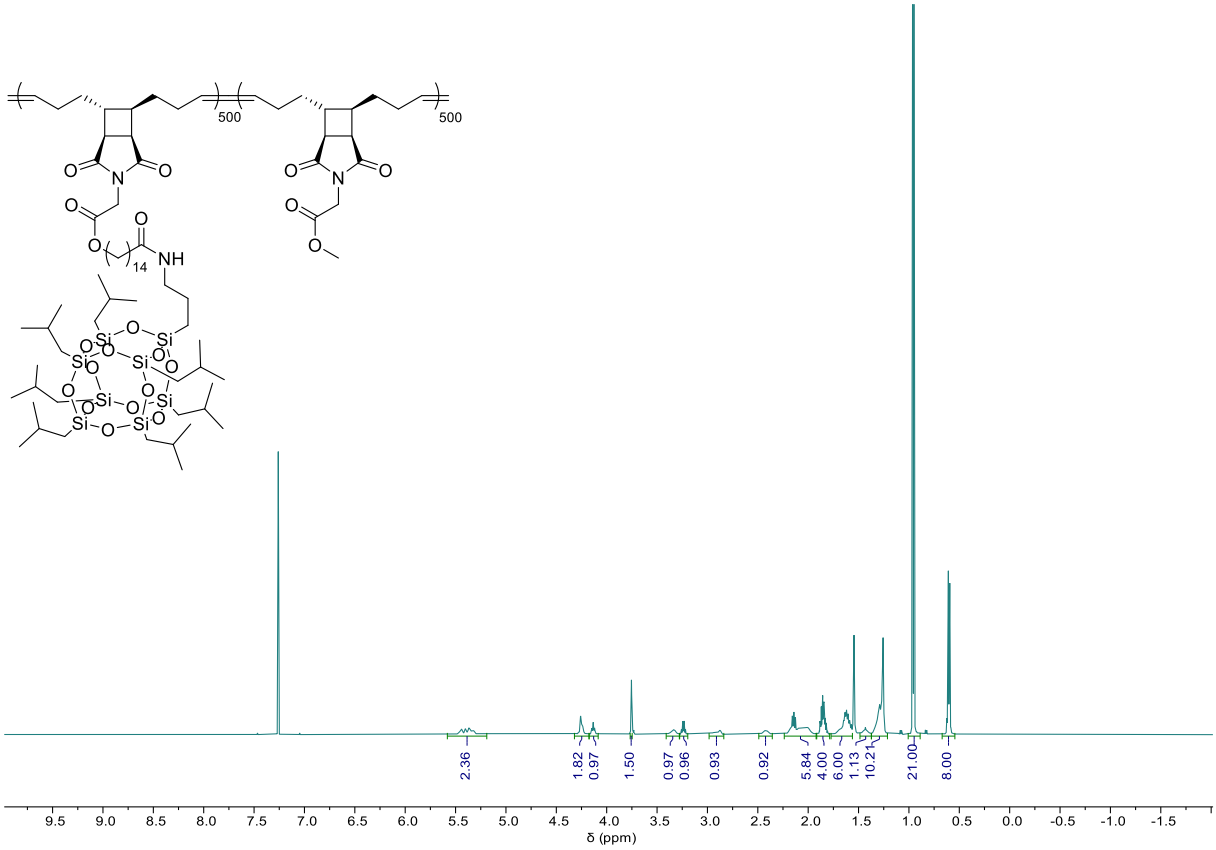

Figure S59. ^{1}H NMR (500 MHz, $CDCl_3$) spectrum of $PLSPOSS_{500}SS_{500}$

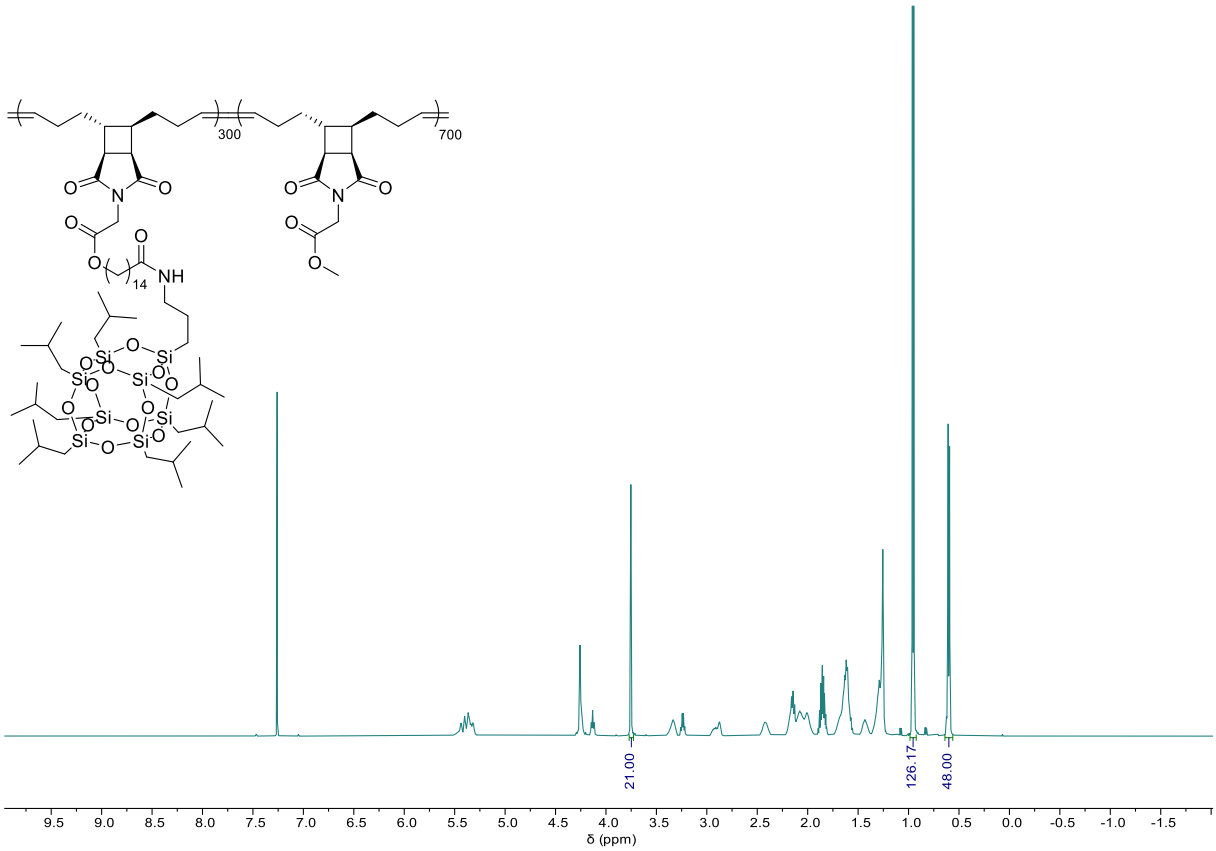

Figure S60. ^{1}H NMR (500 MHz, $CDCl_3$) spectrum of $PLSPOSS_{300}SS_{700}$

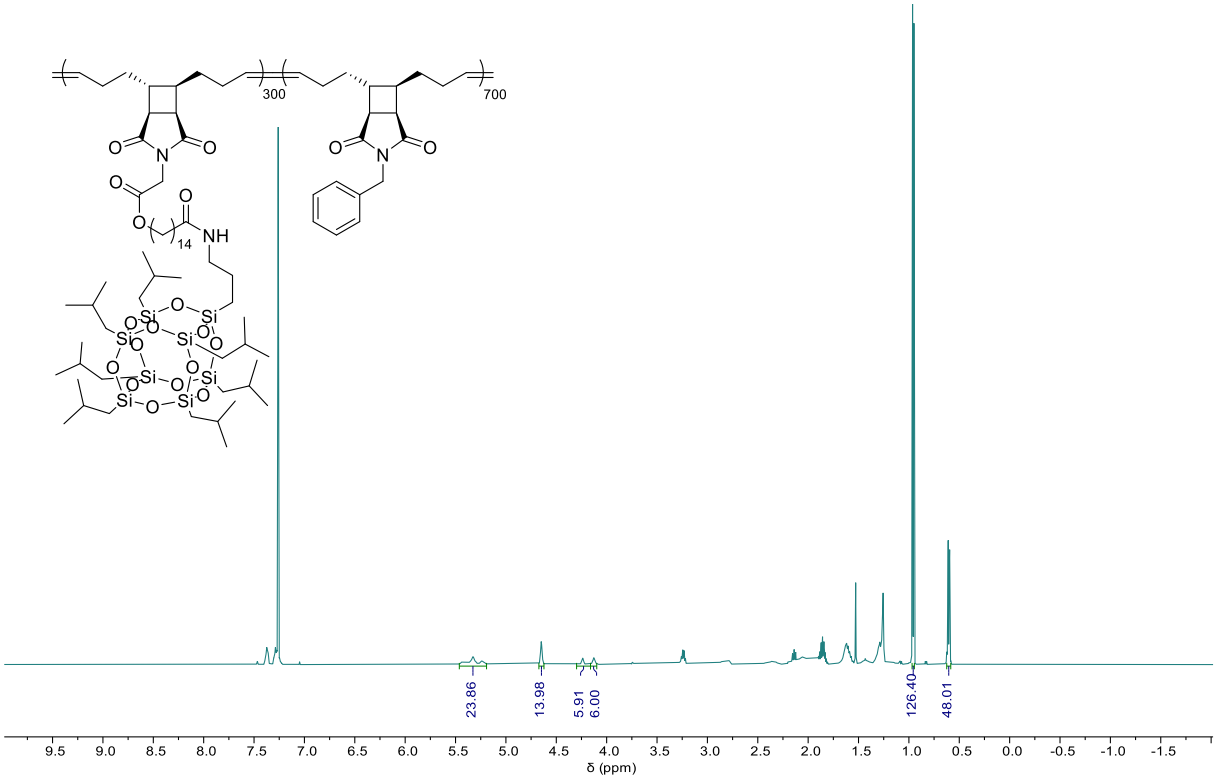

Figure S61. ^{1}H NMR (500 MHz, $CDCl_3$) spectrum of $PLSPOSS_{300}Bn_{700}$

Polymer Backbone Length Control

To investigate the polymerizability and scaling factor of POSS containing polymers, PSSPOSSS, PMSPOSS and PLSPOSS with range of molar masses were synthesized by changing the monomer to G1 ratio.

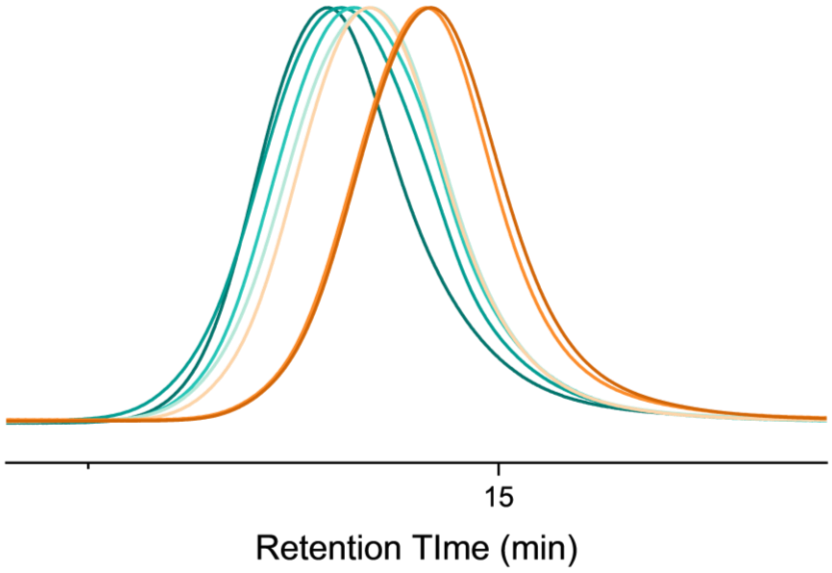

Figure S62. GPC traces of PSSPOSS with different molar masses.

Table S1. PSSPOSS molar mass characterization determined by GPC-MALS

Entry	M_n (kDa)	M_w (kDa)	M_w/M_n
1	973.4	1098	1.13
2	1096	1208	1.10
3	1598	1836	1.15
4	1816	2082	1.15
5	2030	2320	1.14
6	2327	2743	1.18
7	2424	2891	1.19

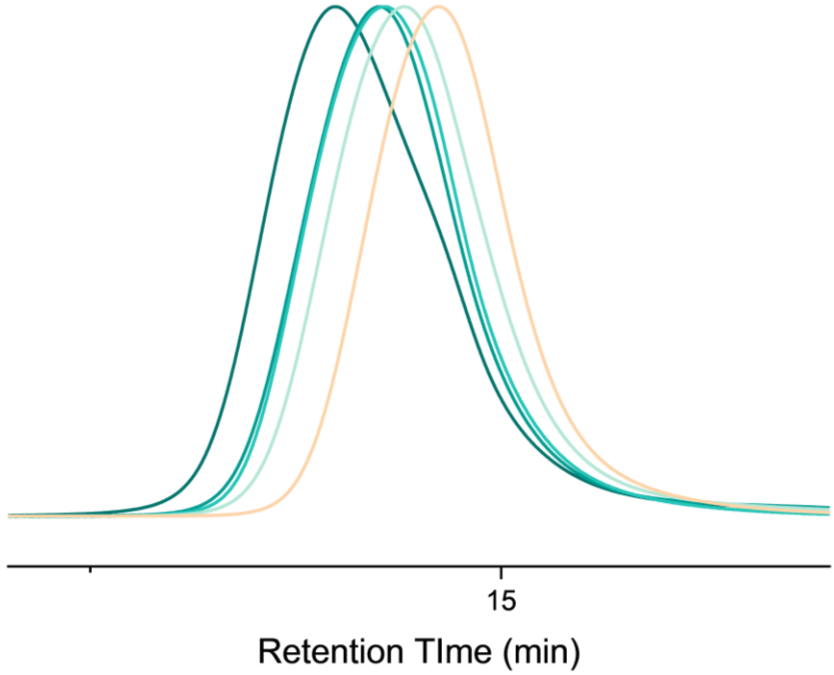

Figure S63. GPC traces of PMSPOSS with different molar masses

Table S2. PMSPOSS molar mass characterization determined by GPC-MALS

Entry	M_n (kDa)	M_w (kDa)	M_w/M_n
1	876.8	939.8	1.07
2	1317	1484	1.13
3	1532	1648	1.08
4	1742	1893	1.09
5	2380	2635	1.11

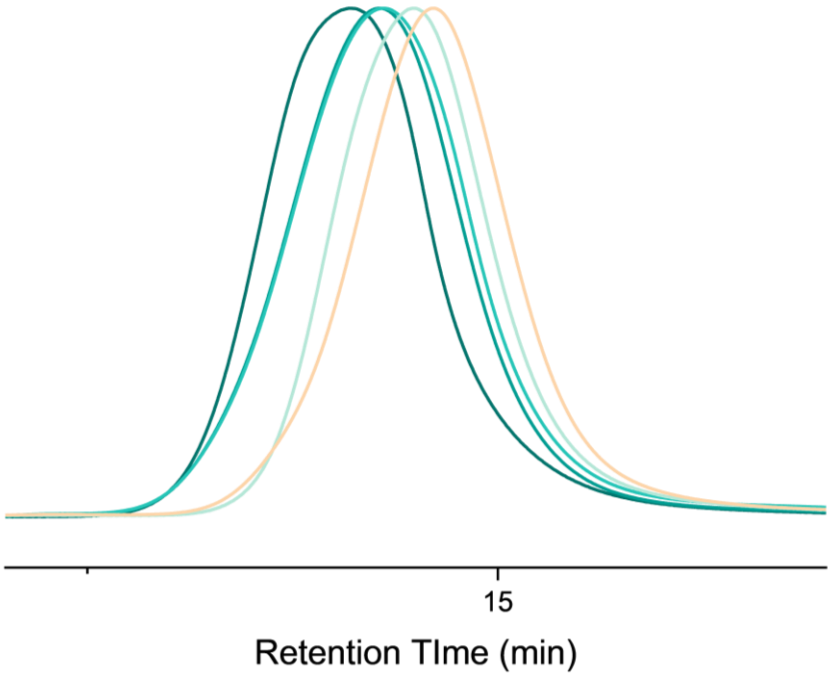

Figure S64. GPC traces of PMSPOSS with different molar masses

Table S3. PLSPOSS molar mass characterization determined by GPC-MALS

Entry	M_n (kDa)	M_w (kDa)	M_w/M_n
1	1133	1306	1.15
2	1339	1459	1.09
3	1861	2261	1.21
4	2024	2430	1.20
5	2334	2637	1.13

Conformation Analysis

Light Scattering

PSSPOSS, PMSPOSS and PLSPOSS with different molar masses were dissolved in THF to make 1 mg/mL solutions. Then the solutions were filtered through Aura MT Syringe Filters with PTFE 13 mm filter with 0.22 μm pore size three times for removal of insoluble particles. The solution obtained was then further filtered into a precleaned 4 mL glass tube by passing the solution through a 0.45 μm pore-size hydrophobic PTFE membrane filter to remove any dust.

The SLS measurements were performed at scattered angles (θ) between 30° to 120°, at 2° intervals. The measured ranges of scattered angles vary depending on the specific sample sizes to ensure $q \cdot R_g < 1$. The collected scattering intensities from different angles were further analyzed by a partial Zimm plot derived from the Rayleigh-Gans-Debye equation through the Particle Explorer software (Brookhaven Instruments, USA) to get the radius of gyration (R_g) of particles.

For DLS measurement, it monitors the rate of fluctuation of the scattered light intensity over its average value to get the correlation function. The average apparent translational diffusion coefficient D_{app} could be obtained by $D_{app} = \Gamma/q^2$, in which Γ was calculated by the constrained regularized CONTIN method. The hydrodynamic radius (R_{h}) is related to D via the Stokes–Einstein equation: $R_h = k_B T/6\pi\eta D$, where k_B is the Boltzmann constant, and η is the viscosity of the solvent at temperature T. Here, DLS measurements were performed up to five different scattering angles (90°, 75°, 60°, 45° and 30°). The final $R_{\mathrm{h},0}$ values of the particles are obtained by extrapolating $R_{h,app}$ to zero scattering angle.

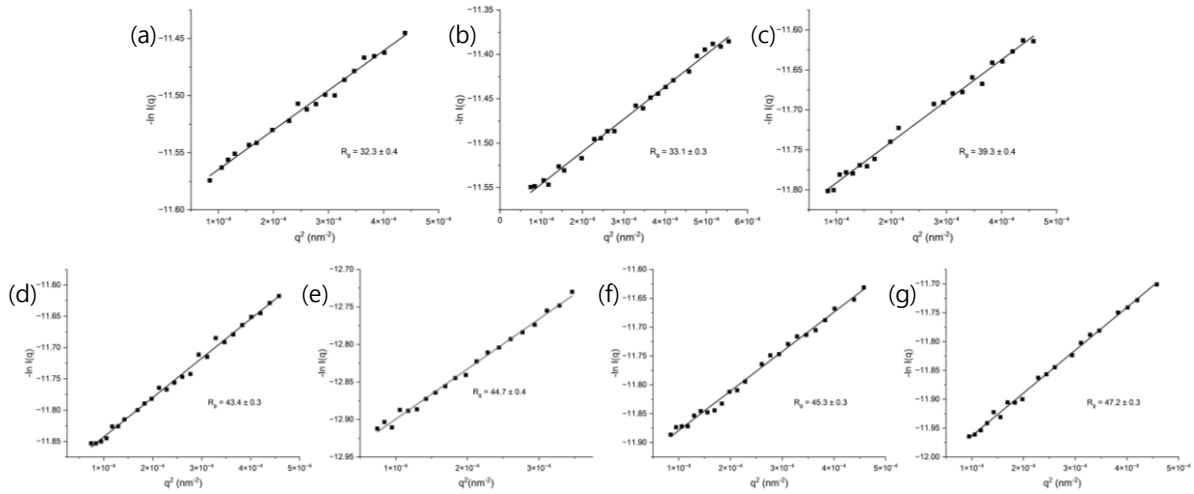

Figure S65. Guinier plots of the scattering intensity for PSSPOSS with M_{w} of (a) 1098, (b) 1208, (c) 1836, (d) 2082, (e) 2320, (f) 2743, (g) 2891 kDa. An apparent R_{g} value from linear regression is reported in each figure.

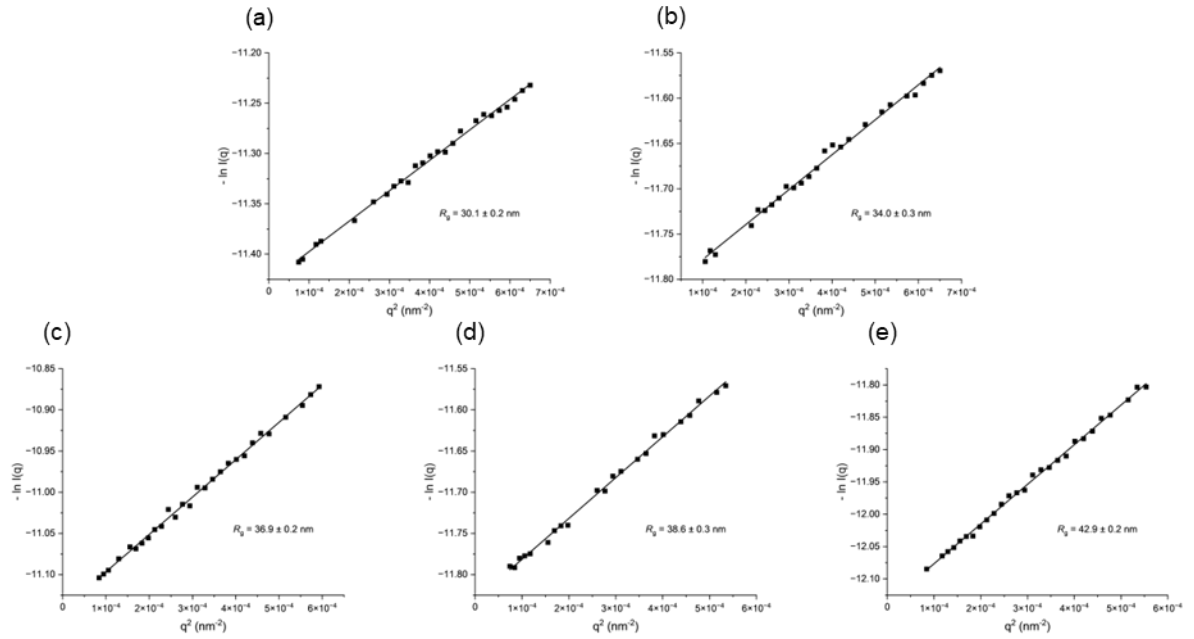

Figure S66. Guinier plots of the scattering intensity for PMSPOSS with M_{w} of (a) 939.8, (b) 1484, (c) 1648, (d) 1893, (e) 2635 kDa. An apparent R_{g} value from linear

regression is reported in each figure.

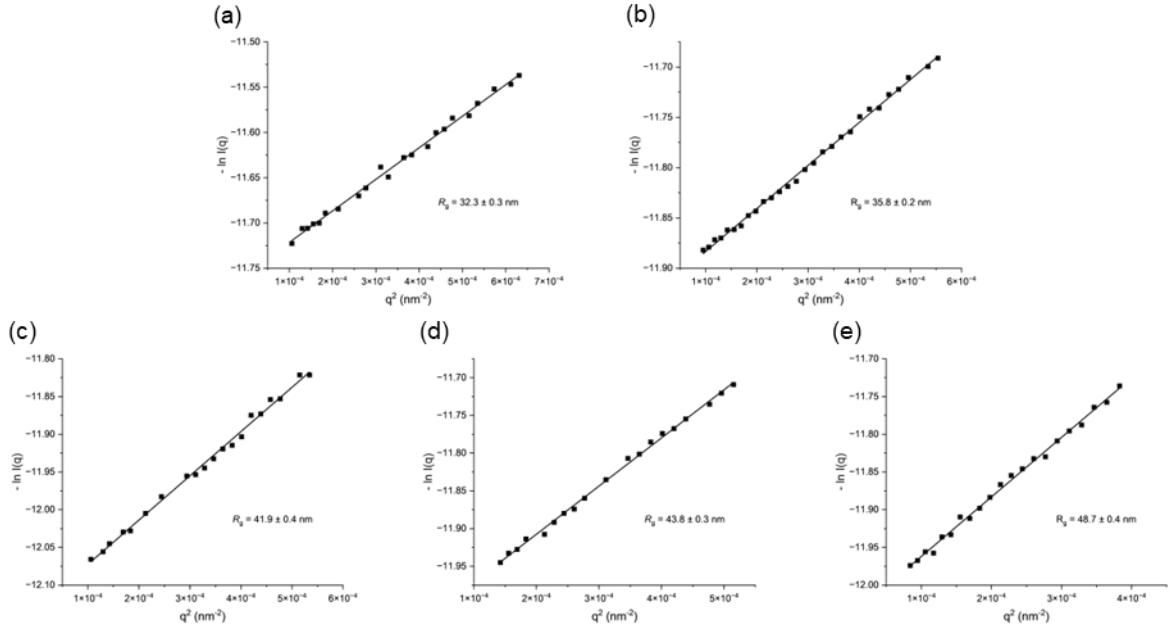

Figure S67. Guinier plots of the scattering intensity for PLSPOSS with M_w of (a) 1306, (b) 1459, (c) 2261, (d) 2430, (e) 2637 kDa. An apparent R_g value from linear regression is reported in each figure.

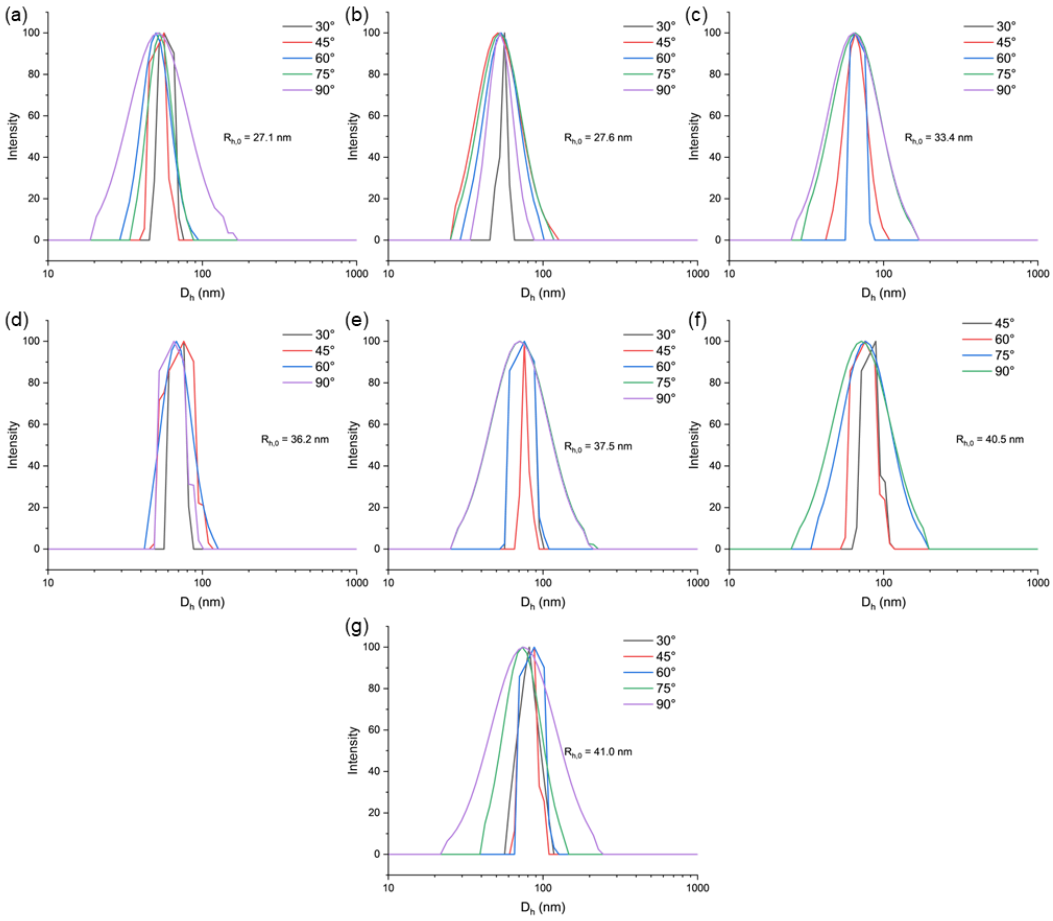

Figure S68. Hydrodynamic diameter distribution at up to five different angles (90°, 75°, 60°, 45° and 30°) of the PSSPOSS with M_w of (a) 1098, (b) 1208, (c) 1836, (d) 2082, (e) 2320, (f) 2743, (g) 2891 kDa. Calculated each $R_{h,0}$ value from extrapolation is reported in each figure.

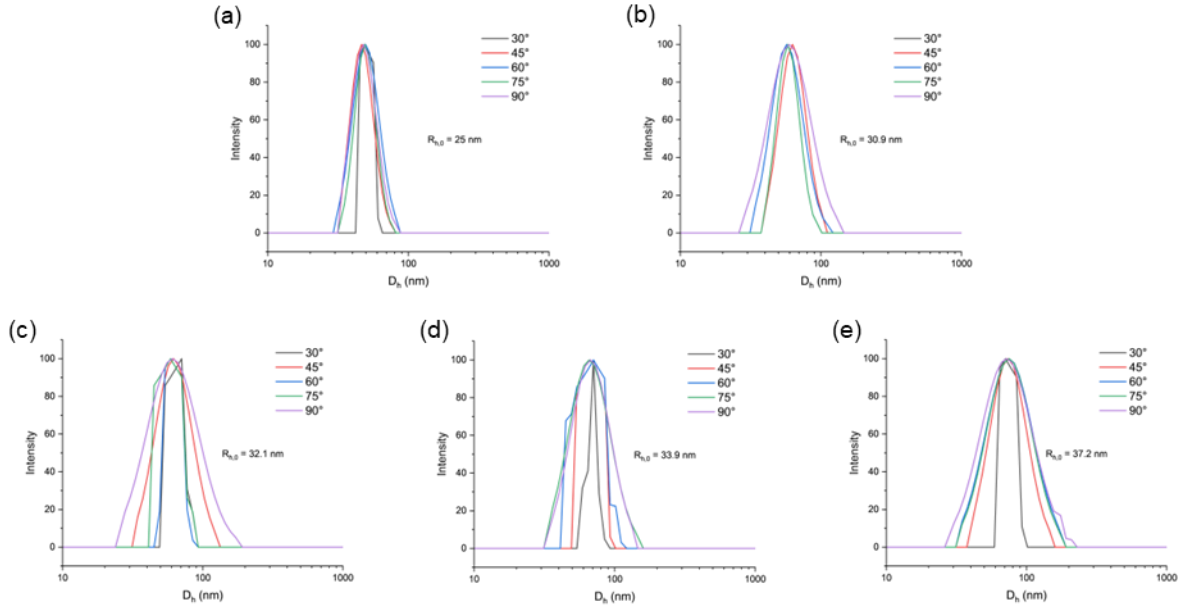

Figure S69. Hydrodynamic diameter distribution at up to five different angles (90°, 75°, 60°, 45° and 30°) of the PMSPOSS with M_w of of (a) 939.8, (b) 1484, (c) 1648, (d) 1893, (e) 2635 kDa. Calculated each $R_{h,0}$ value from extrapolation is reported in each figure.

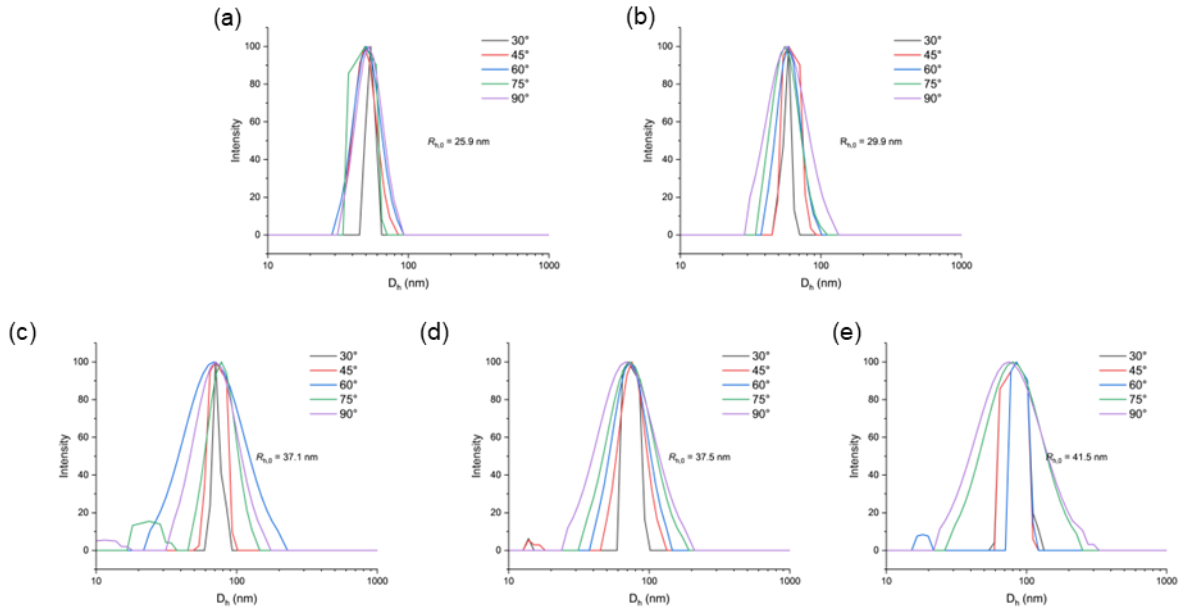

Figure S70. Hydrodynamic diameter distribution at up to five different angles (90°, 75°, 60°, 45° and 30°) of the PLSPOSS with M_w of (a) 1306, (b) 1459, (c) 2261, (d) 2430, (e) 2637 kDa. Calculated each $R_{h,0}$ value from extrapolation is reported in

each figure.

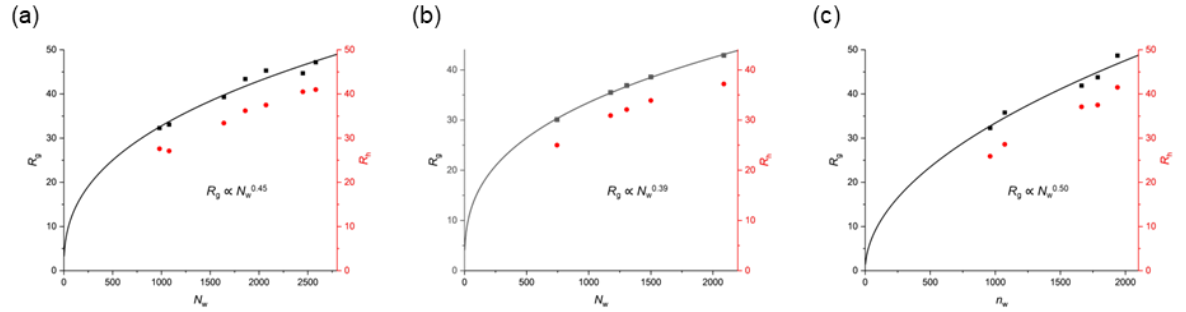

Figure S71. R_g and R_h of (a) PSSPOSS, (b) PMSPOSS, and (c) PLSPOSS against weight average degree of polymerization.

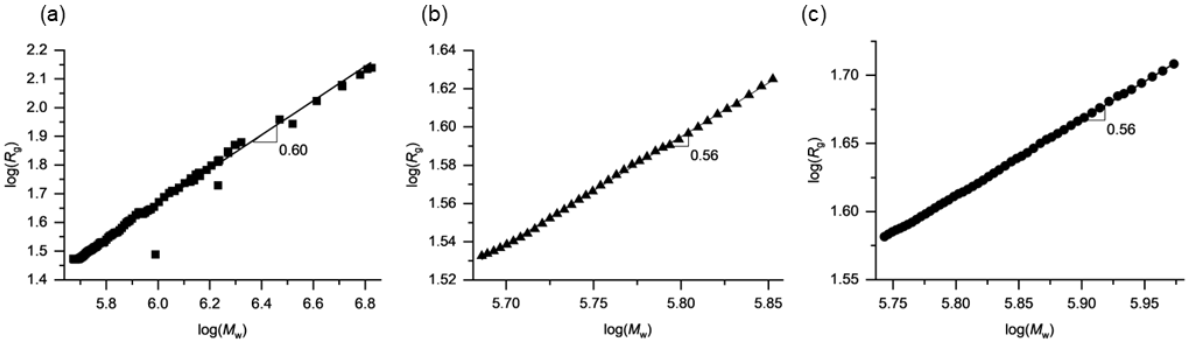

Figure S72. Double log plot of the radius of gyration as a function of weight average molar mass obtained from SEC-MALS. (a) PSS, (b) PMS, (c) PLS

Atomic Force Microscopy

This section describes about the additional details of the AFM analyses of the POSS-containing polymers (PSSPOSS, PMSPOSS and PLSPOSS).

Samples were prepared by spin-coating of polymer solutions with concentration of 10 mg/L in toluene on freshly-cleaved mica substrates. The polymer solutions were prepared using pre-filtered toluene, and further filtered through Aura MT Syringe Filters with PTFE 13 mm filter with 0.22 μm pore size three times after dissolution of polymers. Spin-casting was conducted at 3000 rpm for 10 seconds.

Representative low magnification images of the polymers are shown in Figure S73. The large aggregated samples are typically observed in spots away from the center of the mica substrate where higher concentrations of polymers were observed. Spots without aggregates were used for analyses. The polymers with N_n ~ 1000 were used for preparation of AFM samples.

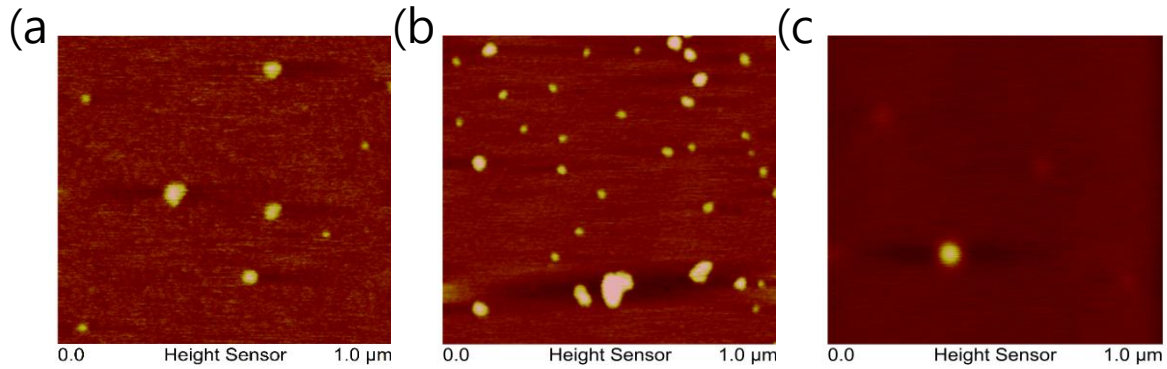

Figure S73. Low-magnification images of (a) PSSPOSS, (b) PMSPOSS, (c) and PLSPOSS.

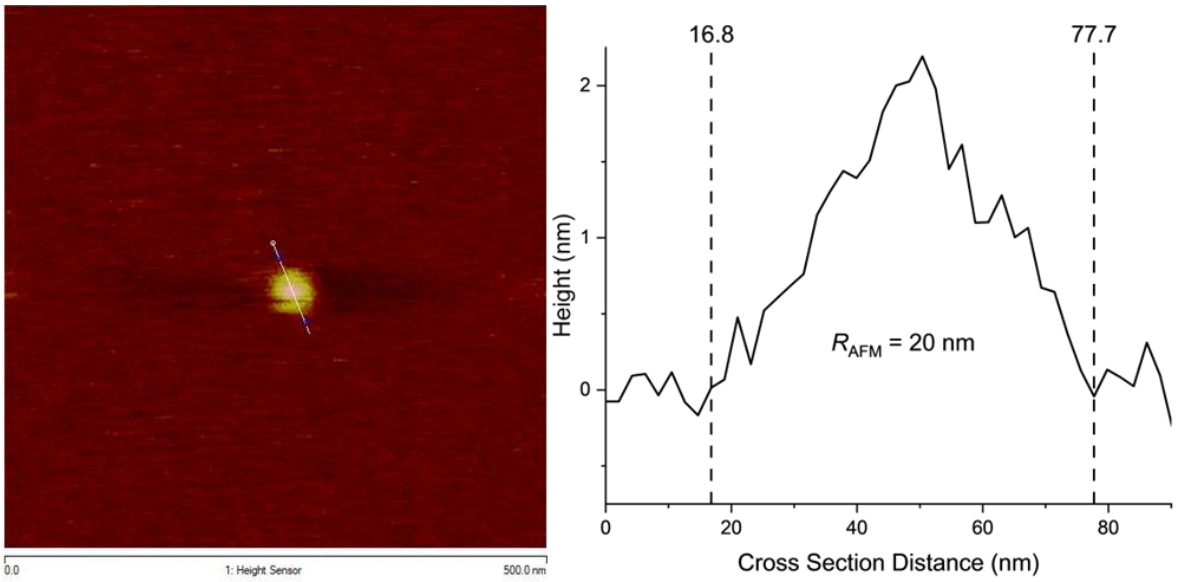

Figure S74. Cross section analysis of the high-magnification image of PSSPOSS. The longest radius was measured to be 30.5 nm.

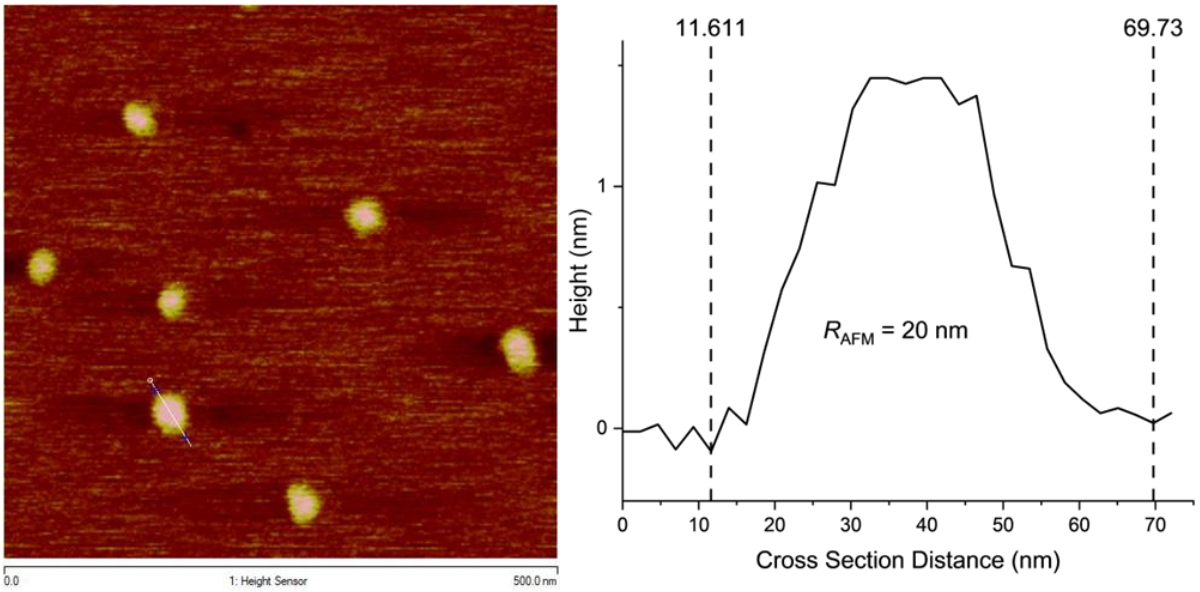

Figure S75. Cross section analysis of the high-magnification image of PMSPOSS. The longest radius of representative polymer with highest intensity was measured to be 29.1 nm.

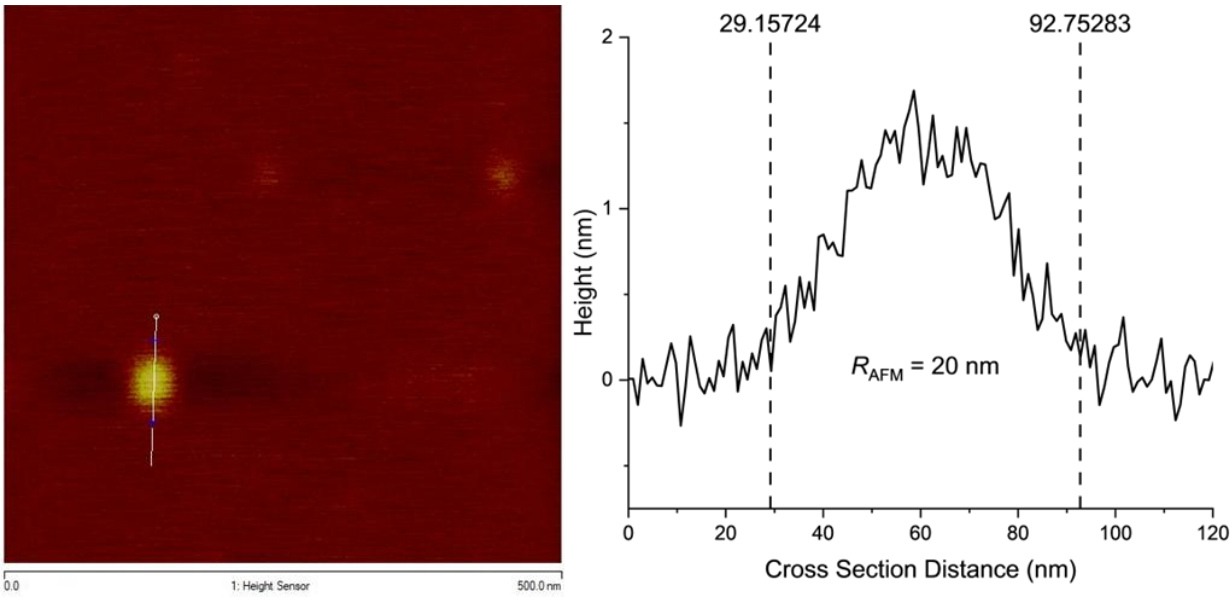

Figure S76. Cross section analysis of the high-magnification image of PLSPOSS. The longest radius of representative polymer with highest intensity was measured to be 31.8 nm.

Ultrasonication

Ultrasonication Kinetics

Ultrasonication experiments were conducted by sonicating 50 mL of 1 mg/mL degassed polymer solutions in THF at 0 °C in N_2 atmosphere. After certain sonication time, aliquots were removed for GPC-MALS (THF) and ^{1}H NMR (500 MHz, $CDCl_3$) analyses to identify molar mass and %RO of each aliquot.

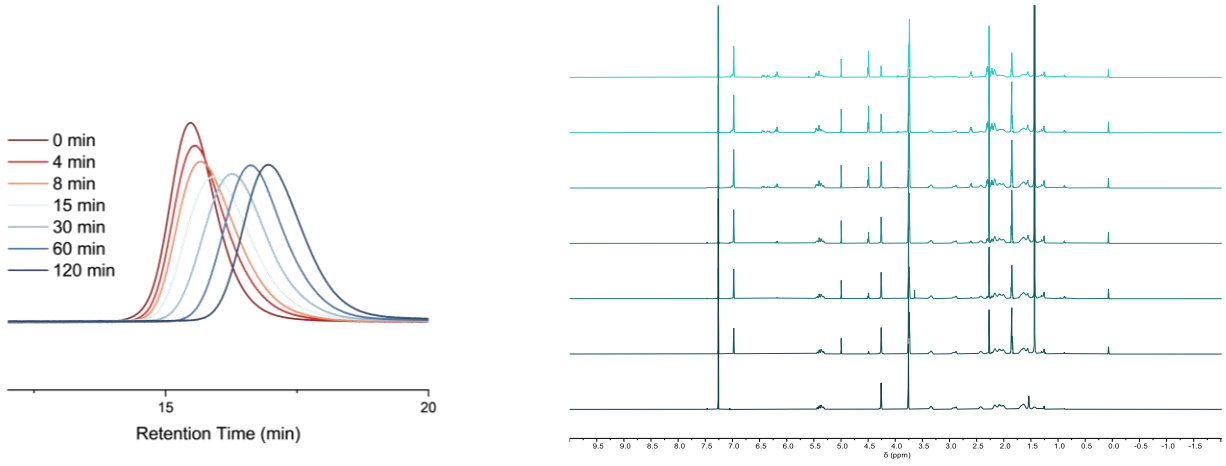

Figure S77. GPC traces of PSS in THF after various sonication times (left) and corresponding ^{1}H NMR (500 MHz, $CDCl_3$) spectra (right) collected after various sonication times: 0, 4, 8, 15, 30, 60, 120 minutes of sonication (plotted from bottom to top, respectively).

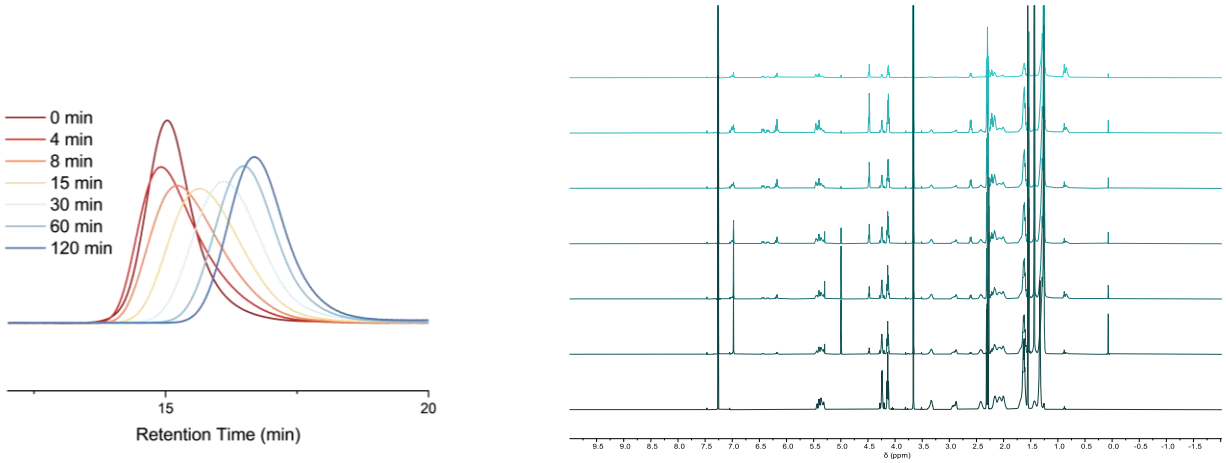

Figure S79. GPC traces of PMS in THF after various sonication times (left) and corresponding ^{1}H NMR (500 MHz, $CDCl_3$) spectra (right) collected after various sonication times: 0, 4, 8, 15, 30, 60, 120 minutes of sonication (plotted from bottom to top, respectively).

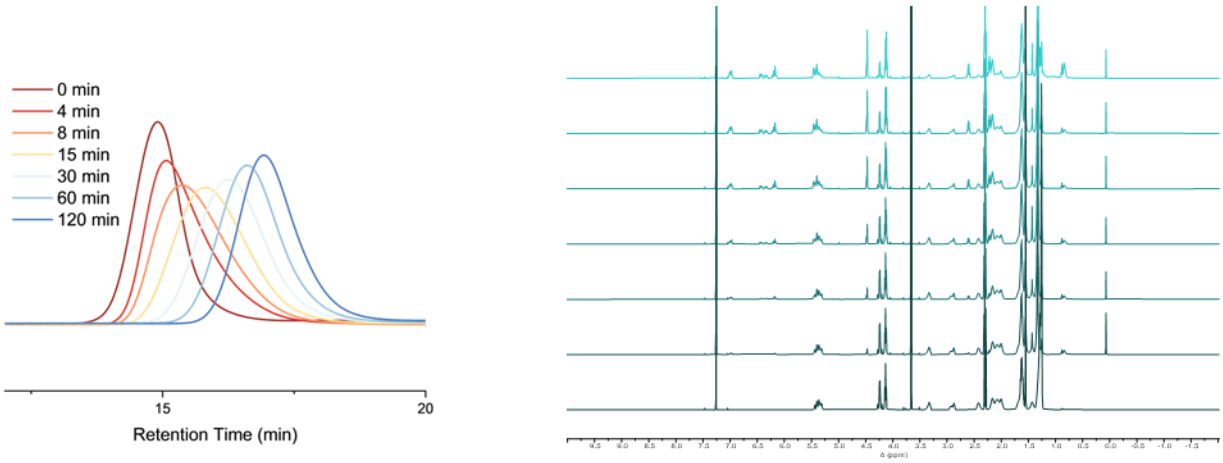

Figure S80. GPC traces of PLS in THF after various sonication times (left) and corresponding ^{1}H NMR (500 MHz, $CDCl_3$) spectra (right) collected after various sonication times: 0, 4, 8, 15, 30, 60, 120 minutes of sonication (plotted from bottom to top, respectively).

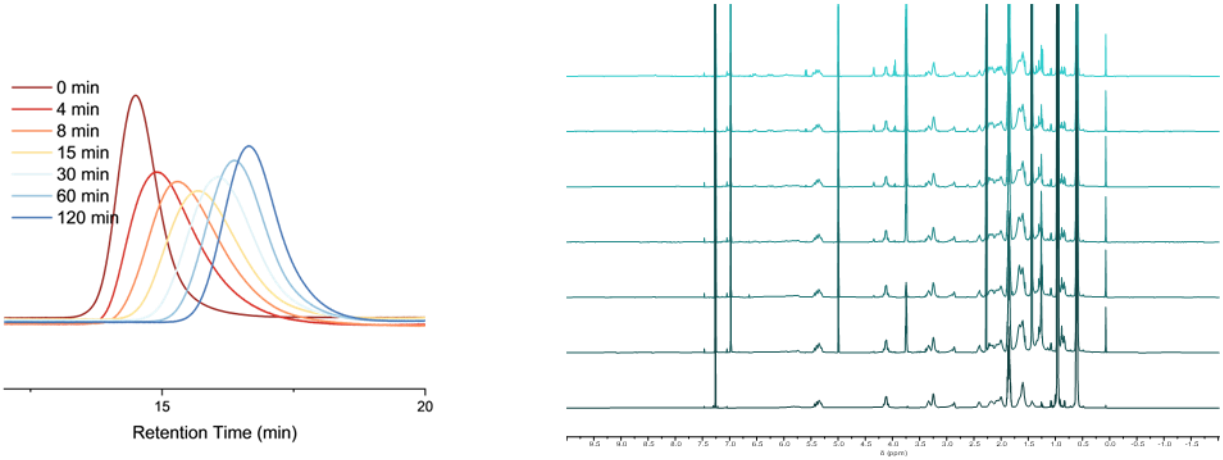

Figure S81. GPC traces of PSSPOSS in THF after various sonication times (left) and corresponding ^{1}H NMR (500 MHz, $CDCl_3$) spectra (right) collected after various sonication times: 0, 4, 8, 15, 30, 60, 120 minutes of sonication (plotted from bottom to top, respectively).

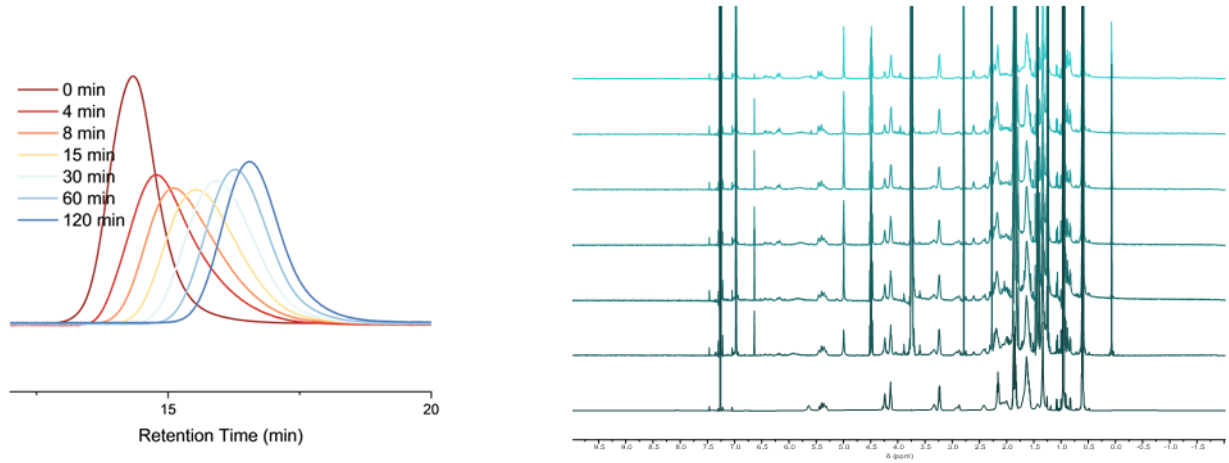

Figure S82. GPC traces of PMSPOSS in THF after various sonication times (left) and corresponding ^{1}H NMR (500 MHz, $CDCl_3$) spectra (right) collected after various sonication times: 0, 4, 8, 15, 30, 60, 120 minutes of sonication (plotted from bottom to top, respectively).

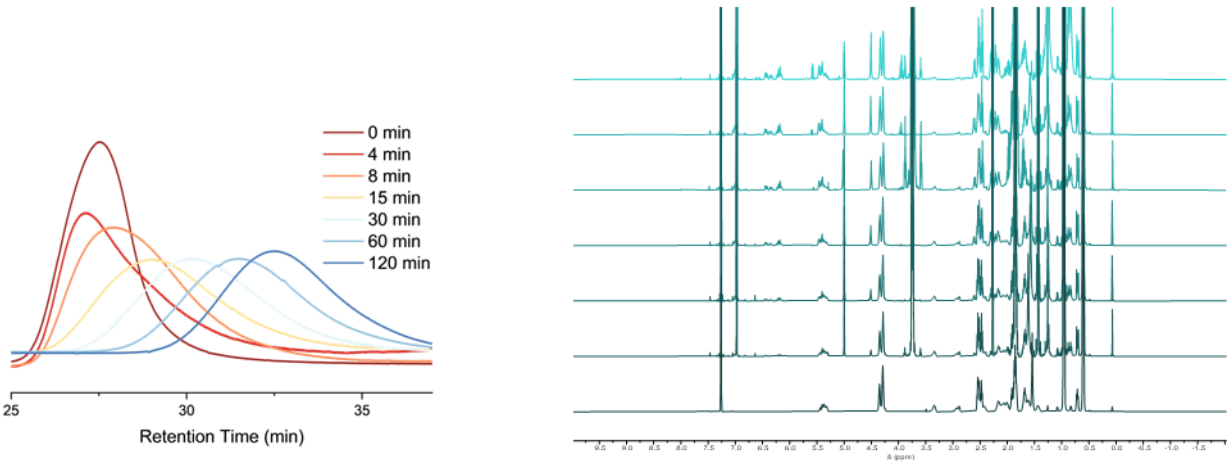

Figure S83. GPC traces of PM'SPOSS in THF after various sonication times (left) and corresponding ^{1}H NMR (500 MHz, $CDCl_3$) spectra (right) collected after various sonication times: 0, 4, 8, 15, 30, 60, 120 minutes of sonication (plotted from bottom to top, respectively).

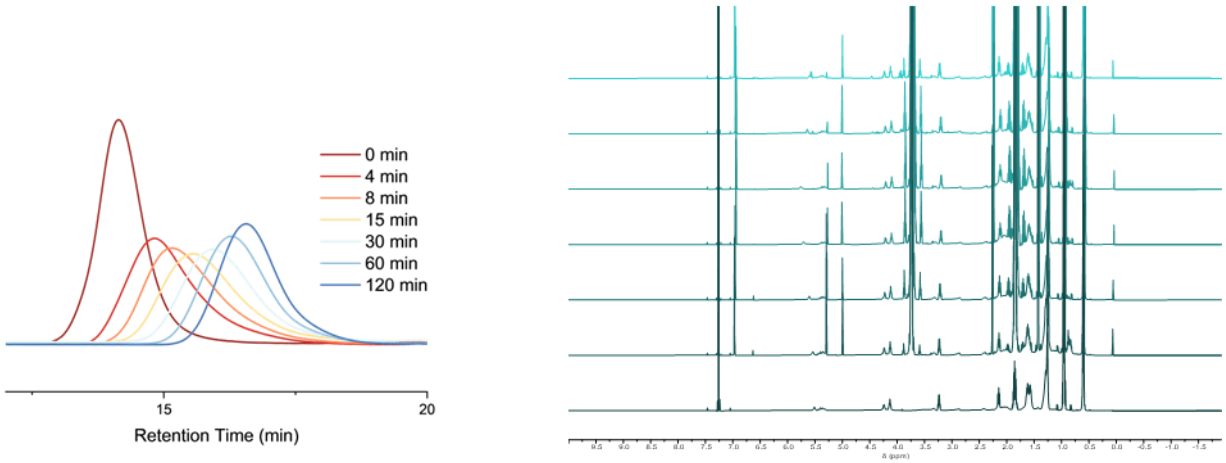

Figure S84. GPC traces of PLSPOSS in THF after various sonication times (left) and corresponding ^{1}H NMR (500 MHz, $CDCl_3$) spectra (right) collected after various sonication times: 0, 4, 8, 15, 30, 60, 120 minutes of sonication (plotted from bottom to top, respectively).

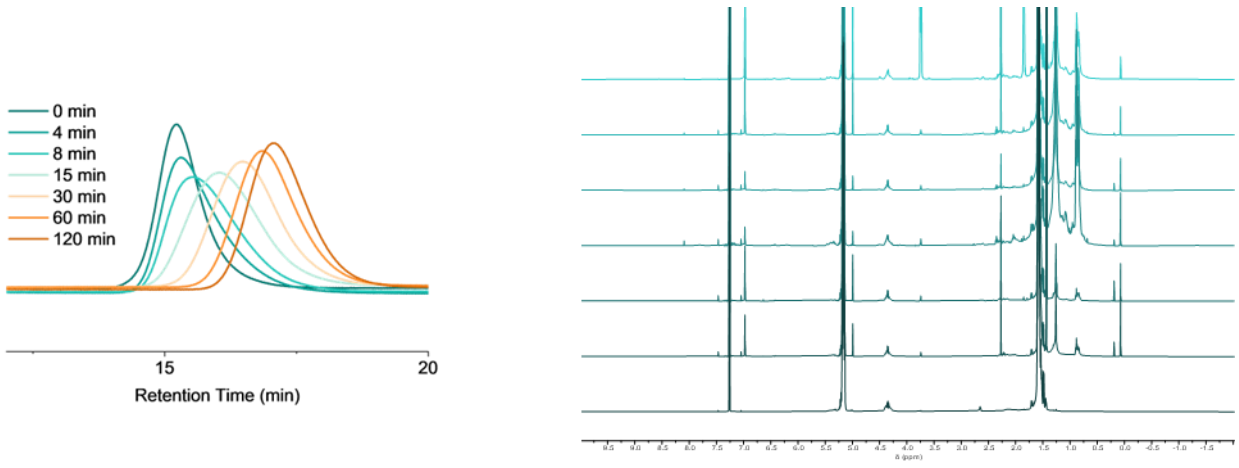

Figure S85. GPC traces of PPLLA in THF after various sonication times (left) and corresponding ^{1}H NMR (500 MHz, $CDCl_3$) spectra (right) collected after various sonication times: 0, 4, 8, 15, 30, 60, 120 minutes of sonication (plotted from bottom to top, respectively).

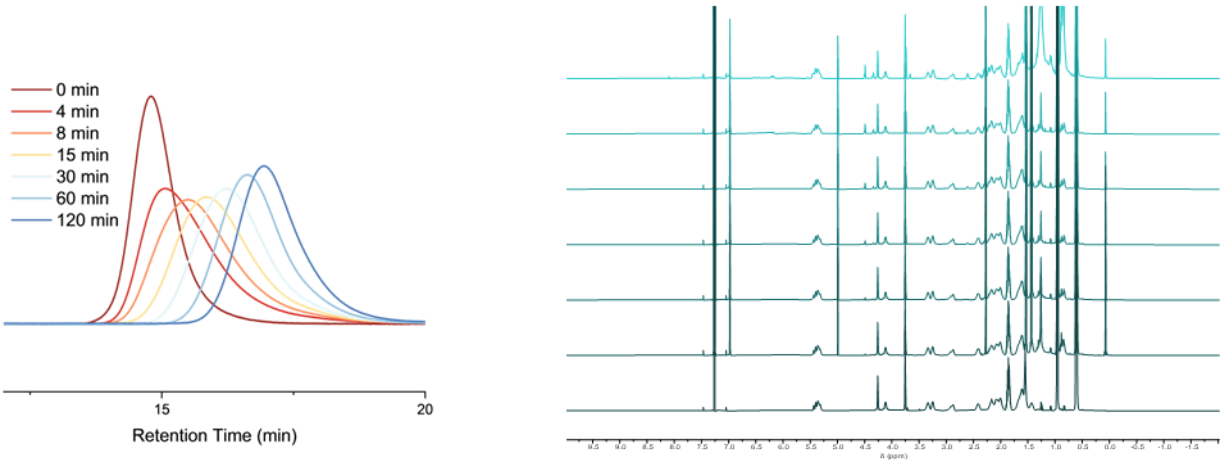

Figure S86. GPC traces of PSSPOSS$_{500}$SS$_{500}$ in THF after various sonication times (left) and corresponding ^{1}H NMR (500 MHz, $CDCl_3$) spectra (right) collected after various sonication times: 0, 4, 8, 15, 30, 60, 120 minutes of sonication (plotted from bottom to top, respectively).

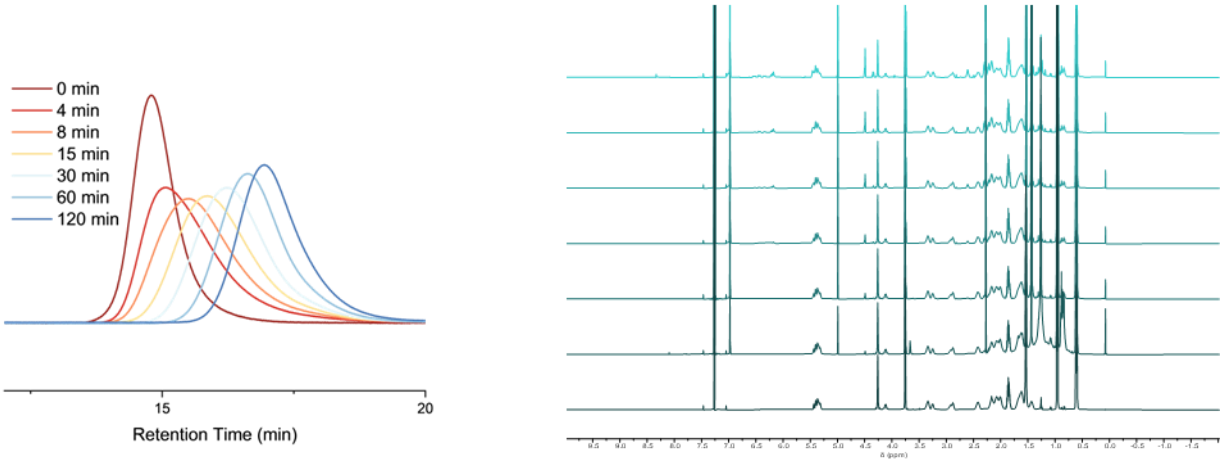

Figure S87. GPC traces of PSSPOSS$_{300}$SS$_{700}$ in THF after various sonication times (left) and corresponding ^{1}H NMR (500 MHz, $CDCl_3$) spectra (right) collected after various sonication times: 0, 4, 8, 15, 30, 60, 120 minutes of sonication (plotted from bottom to top, respectively).

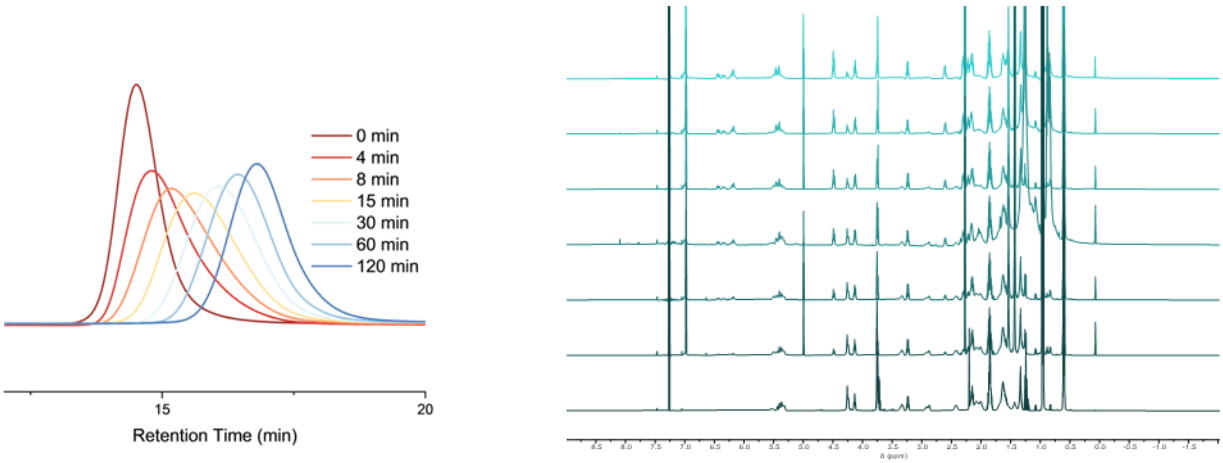

Figure S88. GPC traces of PMSPOSS$_{500}$SS$_{500}$ in THF after various sonication times (left) and corresponding ^{1}H NMR (500 MHz, $CDCl_3$) spectra (right) collected after various sonication times: 0, 4, 8, 15, 30, 60, 120 minutes of sonication (plotted from bottom to top, respectively).

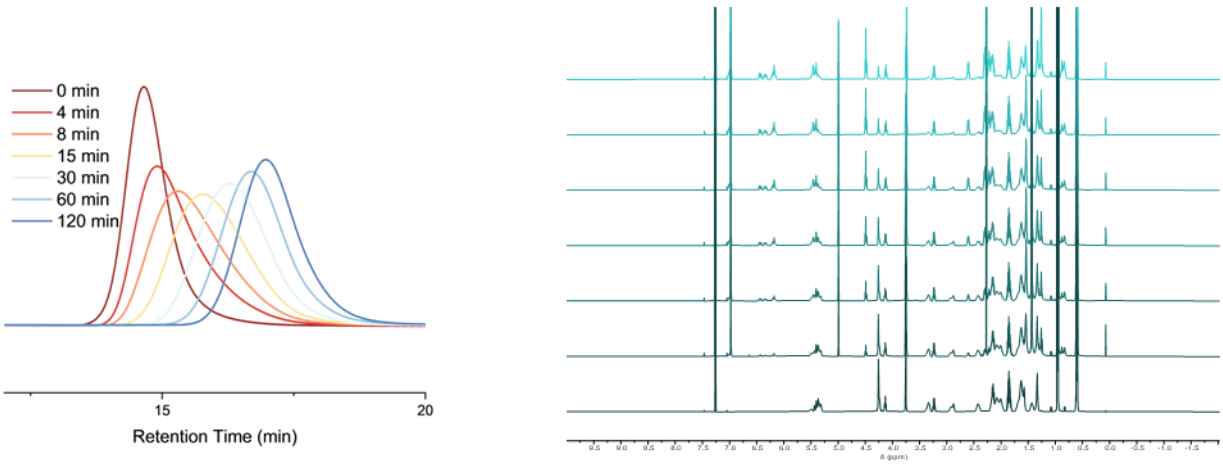

Figure S89. GPC traces of PMSPOSS$_{300}$SS$_{700}$ in THF after various sonication times (left) and corresponding ^{1}H NMR (500 MHz, $CDCl_3$) spectra (right) collected after various sonication times: 0, 4, 8, 15, 30, 60, 120 minutes of sonication (plotted from bottom to top, respectively).

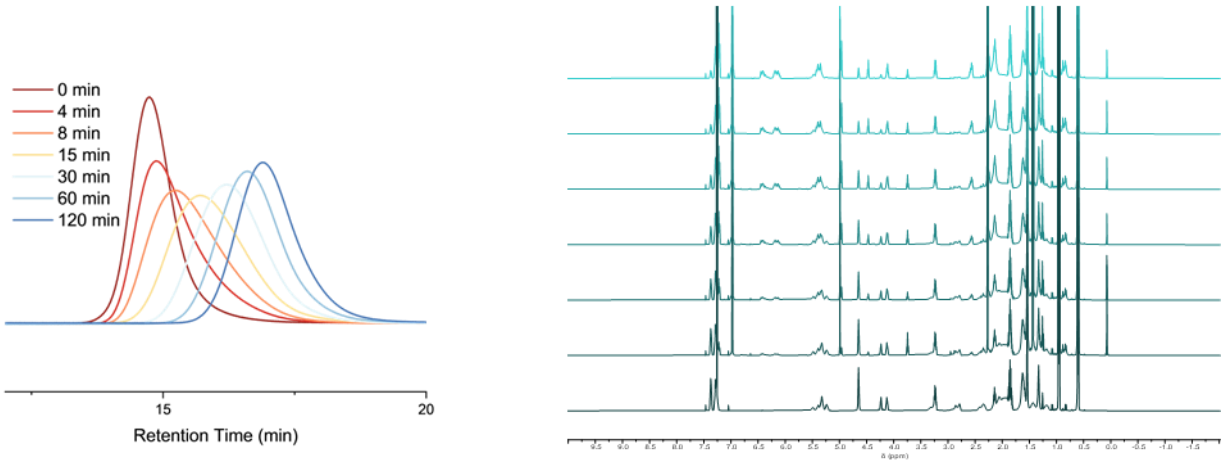

Figure S90. GPC traces of PMSPOSS$_{300}$Bn$_{700}$ in THF after various sonication times (left) and corresponding ^{1}H NMR (500 MHz, $CDCl_3$) spectra (right) collected after various sonication times: 0, 4, 8, 15, 30, 60, 120 minutes of sonication (plotted from bottom to top, respectively).

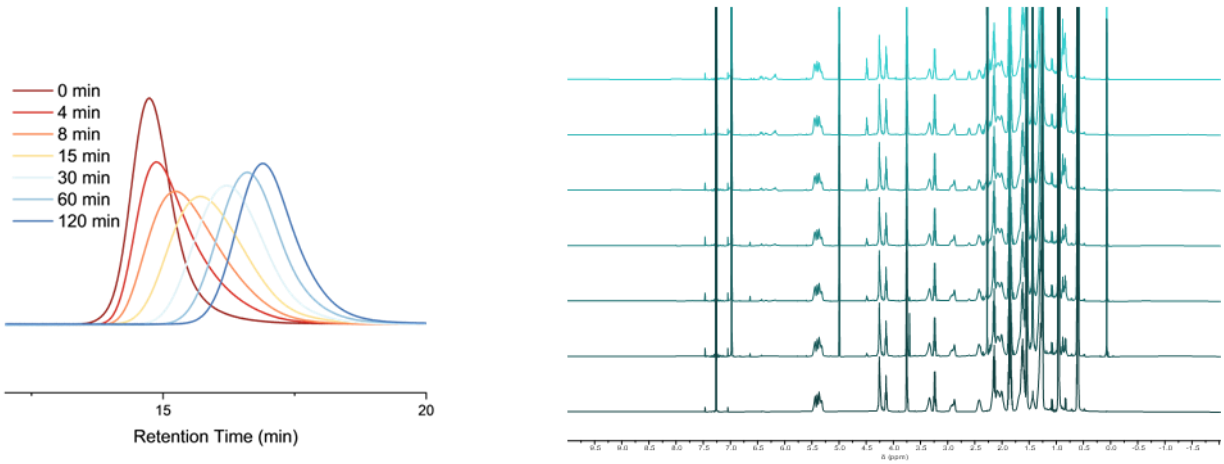

Figure S91. GPC traces of PLSPOSS$_{500}$SS$_{500}$ in THF after various sonication times (left) and corresponding ^{1}H NMR (500 MHz, $CDCl_3$) spectra (right) collected after various sonication times: 0, 4, 8, 15, 30, 60, 120 minutes of sonication (plotted from bottom to top, respectively).

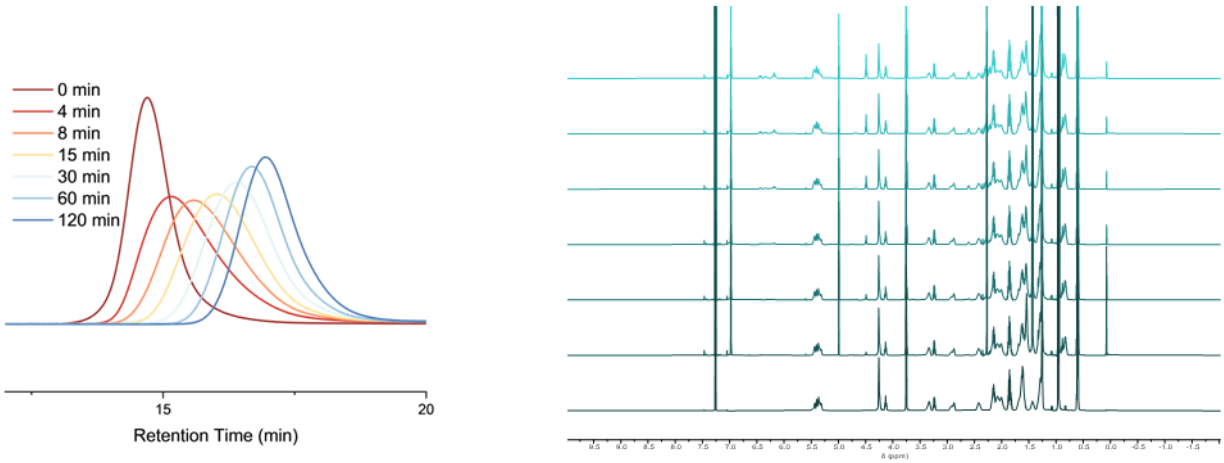

Figure S92. GPC traces of PLSPOSS$_{300}$SS$_{700}$ in THF after various sonication times (left) and corresponding ^{1}H NMR (500 MHz, $CDCl_3$) spectra (right) collected after various sonication times: 0, 4, 8, 15, 30, 60, 120 minutes of sonication (plotted from bottom to top, respectively).

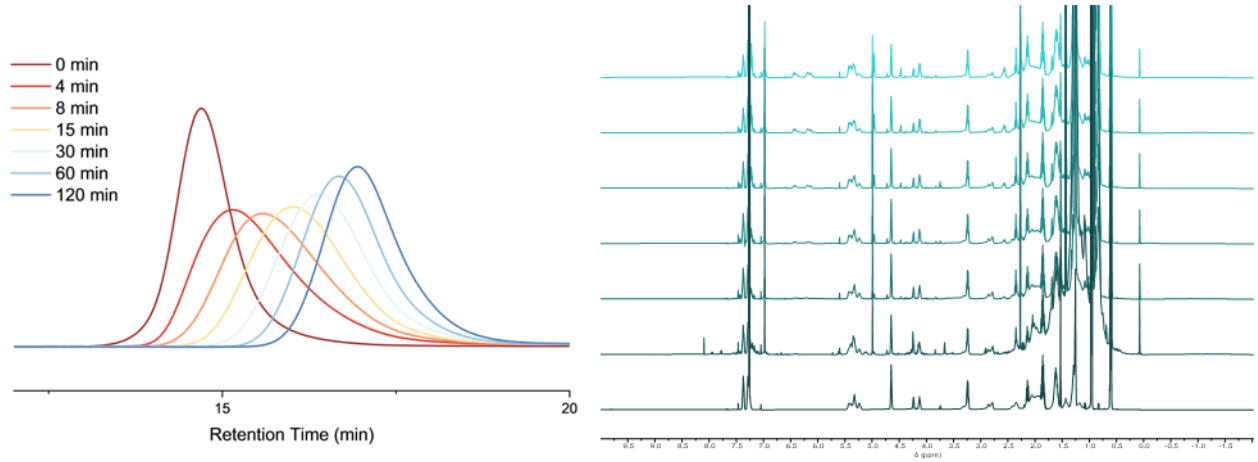

Figure S93. GPC traces of PLSPOSS$_{300}$Bn$_{700}$ in THF after various sonication times (left) and corresponding ^{1}H NMR (500 MHz, $CDCl_3$) spectra (right) collected after various sonication times: 0, 4, 8, 15, 30, 60, 120 minutes of sonication (plotted from bottom to top, respectively).

^{1}H NMR Signal Assignment

^{1}H NMR signals were assigned based on COSY NMR and quantitative ^{1}H NMR of the ultrasonicated PM'SPOSS. The 2 h aliquot of the ultrasonicated PM'SPOSS was purified via prep-SEC before COSY NMR and quantitative ^{1}H NMR analyses.

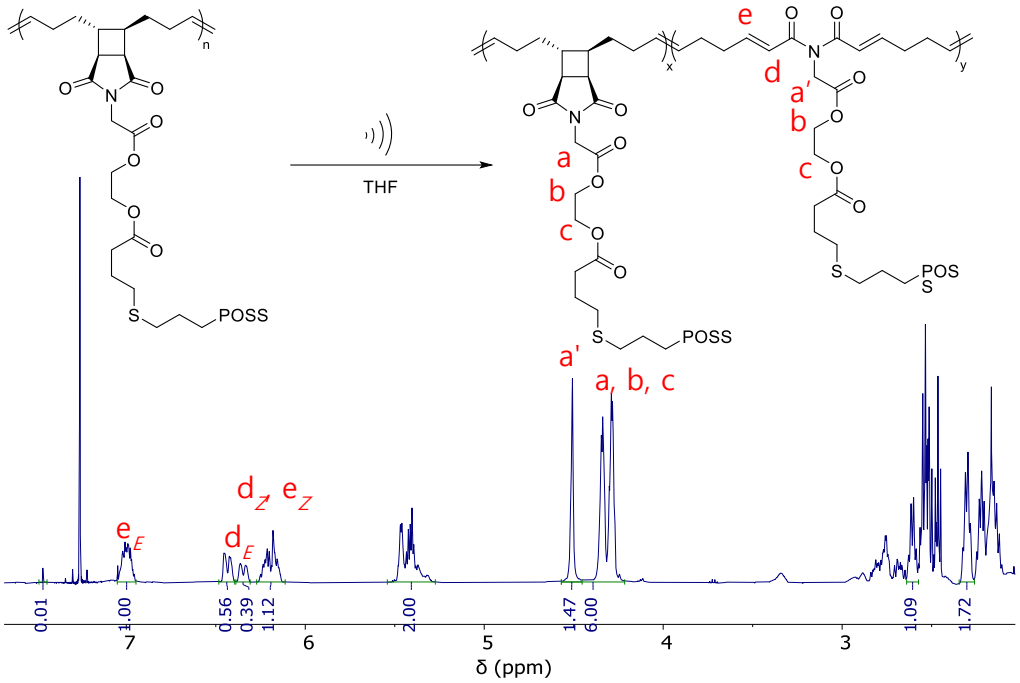

Figure S94. Quantitative ^{1}H NMR (500 MHz, $CDCl_3$) spectrum with assignments of the indicator signals of PM'SPOSS after 2 h ultrasonication and prep-SEC purification.

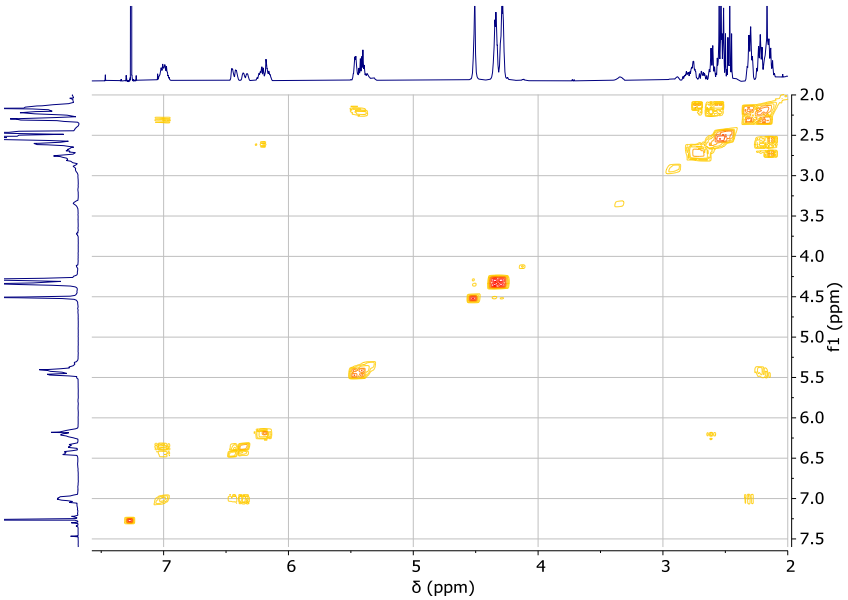

Figure S95. COSY NMR (500 MHz, $CDCl_3$) of PM'SPOSS after 2 h ultrasonication and prep-SEC purification.

General Cyclobutane Mechanophore Activation (%) Calculation

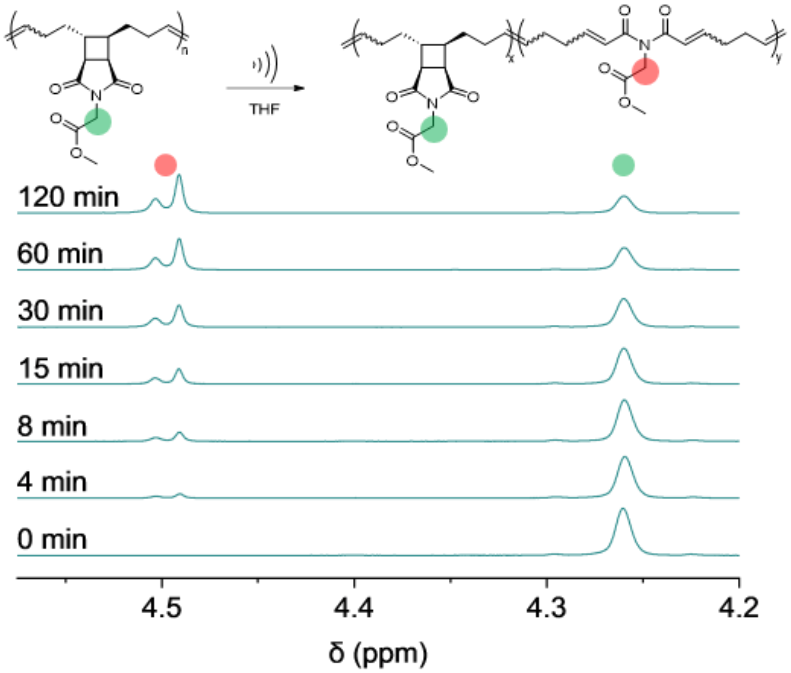

Figure S96. Representative stacked partial ^{1}H NMR (500 MHz, $CDCl_3$) of PSS at each ultrasonication aliquot.

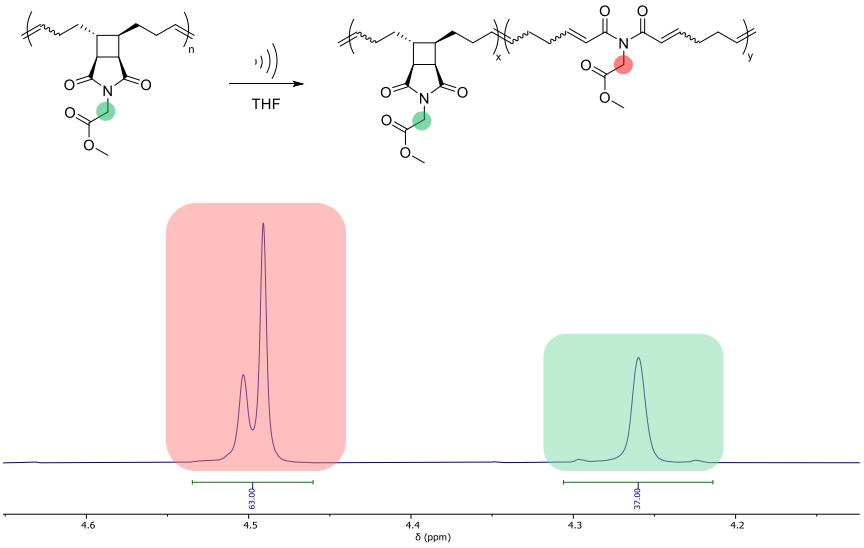

Figure S97. Representative partial ^{1}H NMR (500 MHz, $CDCl_3$) spectrum of PSS after 2 h of ultrasonication.

$$\%RO = \frac{\alpha\ proton\ of\ linear\ imide\ (red)}{\alpha\ proton\ of\ linear\ imide\ (red) + \ \alpha\ proton\ of\ cyclic\ imide\ (green)}$$

For PSS after 2 h of ultrasonication:

$$\%RO = \frac{63.00}{63.00 + \ 37.00} = 63\%$$

Comonomer-Separate Cyclobutane Mechanophore Activation (%) Calculation

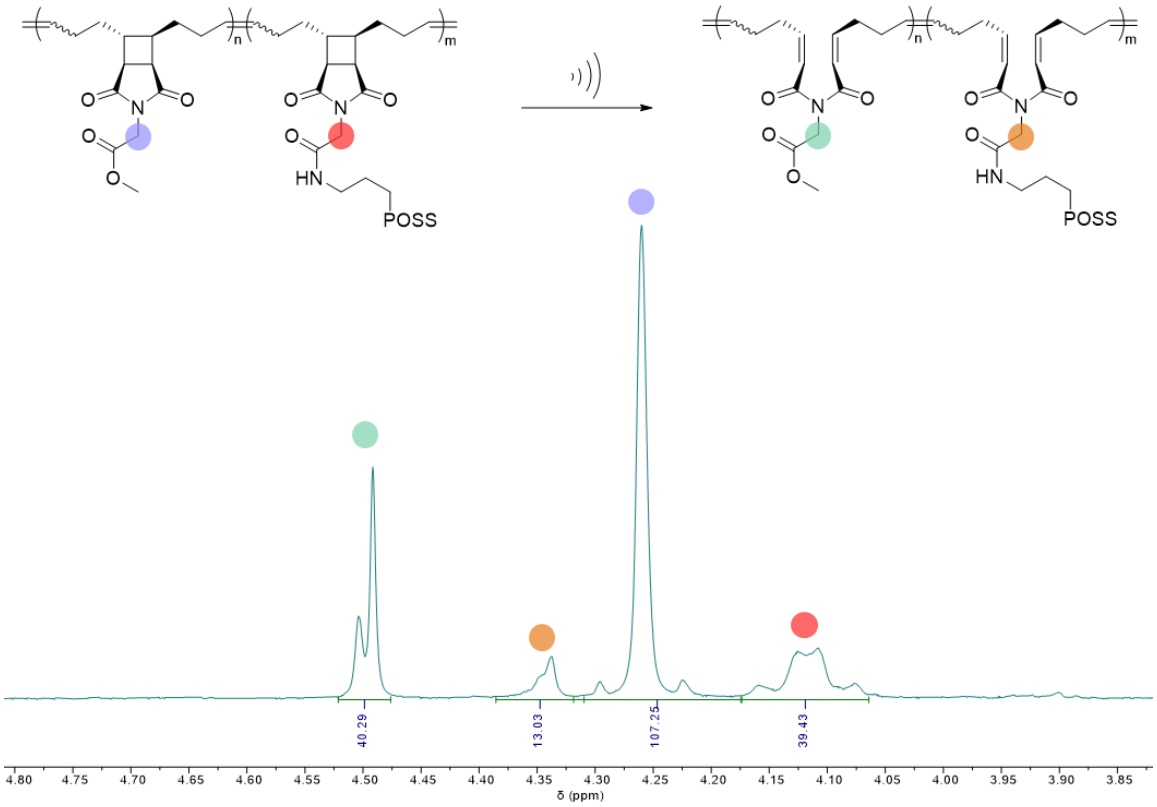

Figure S98. Representative partial ^{1}H NMR (500 MHz, $CDCl_3$) spectrum of $PSSPOSS_{300}SS_{700}$ after 1 h of ultrasonication.

$$\%RO_{SS} = \frac{\alpha\ proton\ of\ linear\ imide\ (green)}{\alpha\ proton\ of\ linear\ imide\ (green) + \ \alpha\ proton\ of\ cyclic\ imide\ (blue)}$$

$$= \frac{40.29}{40.29 + \ 107.25} = \ 27.3\%$$

$$\%RO_{SSPOSS} = \frac{\alpha\ proton\ of\ linear\ imide\ (yellow)}{\alpha\ proton\ of\ linear\ imide\ (yellow) + \ \alpha\ proton\ of\ cyclic\ imide\ (red)}$$

$$= \frac{13.03}{13.03 + \ 39.43} = \ 24.8\%$$

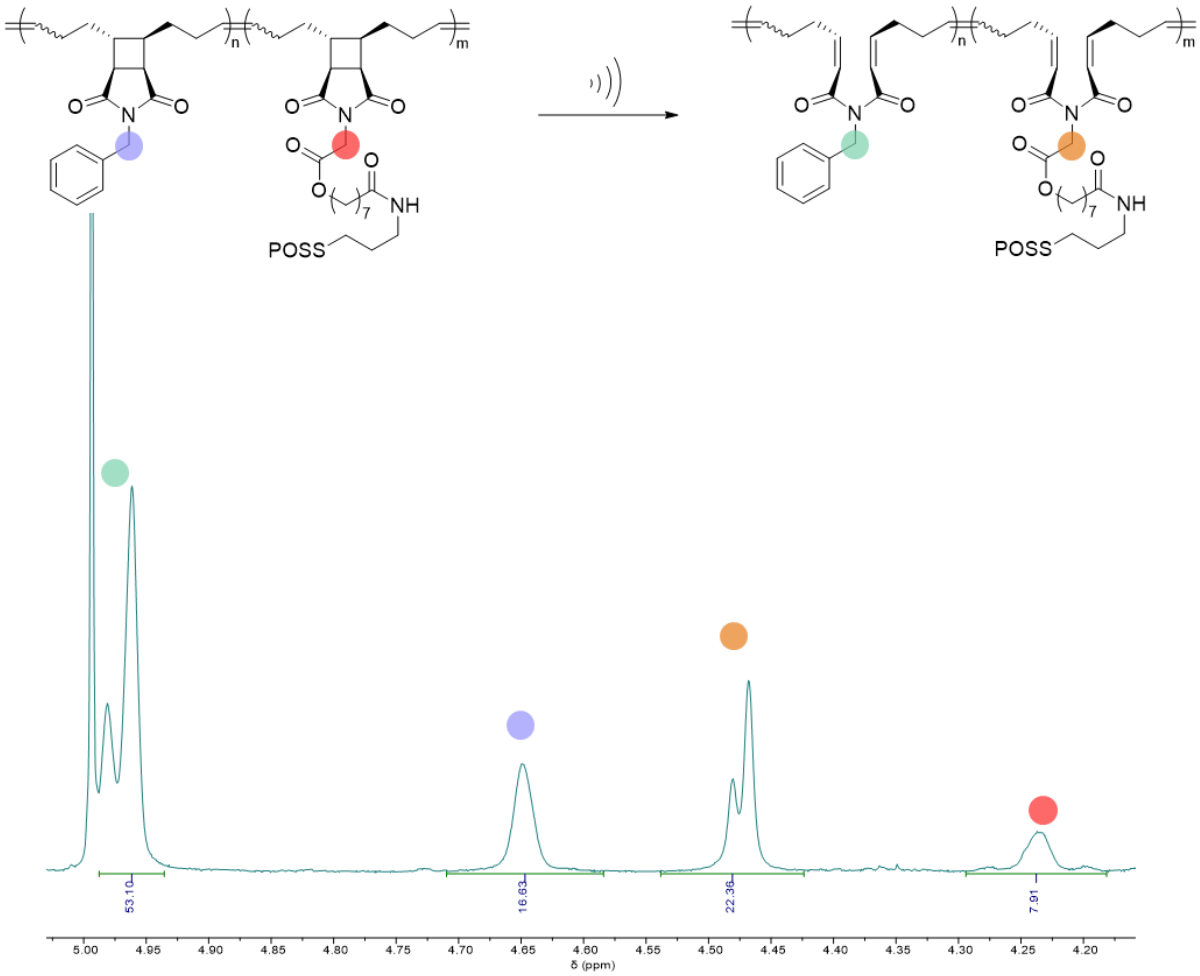

Figure S99. Representative partial ^{1}H NMR (500 MHz, $CDCl_3$) spectrum of $PMSPOSS_{300}Bn_{700}$ after 1 h of ultrasonication.

$$\%RO_{Bn} = \frac{\alpha\ proton\ of\ linear\ imide\ (green)}{\alpha\ proton\ of\ linear\ imide\ (green) + \ \alpha\ proton\ of\ cyclic\ imide\ (blue)}$$

$$= \frac{53.10}{53.10 + \ 16.63} = \ 76.2\%$$

$$\%RO_{MSPOSS} = \frac{\alpha\ proton\ of\ linear\ imide\ (yellow)}{\alpha\ proton\ of\ linear\ imide\ (yellow) + \ \alpha\ proton\ of\ cyclic\ imide\ (red)}$$

$$= \frac{22.36}{22.36 + \ 7.91} = \ 73.9\%$$

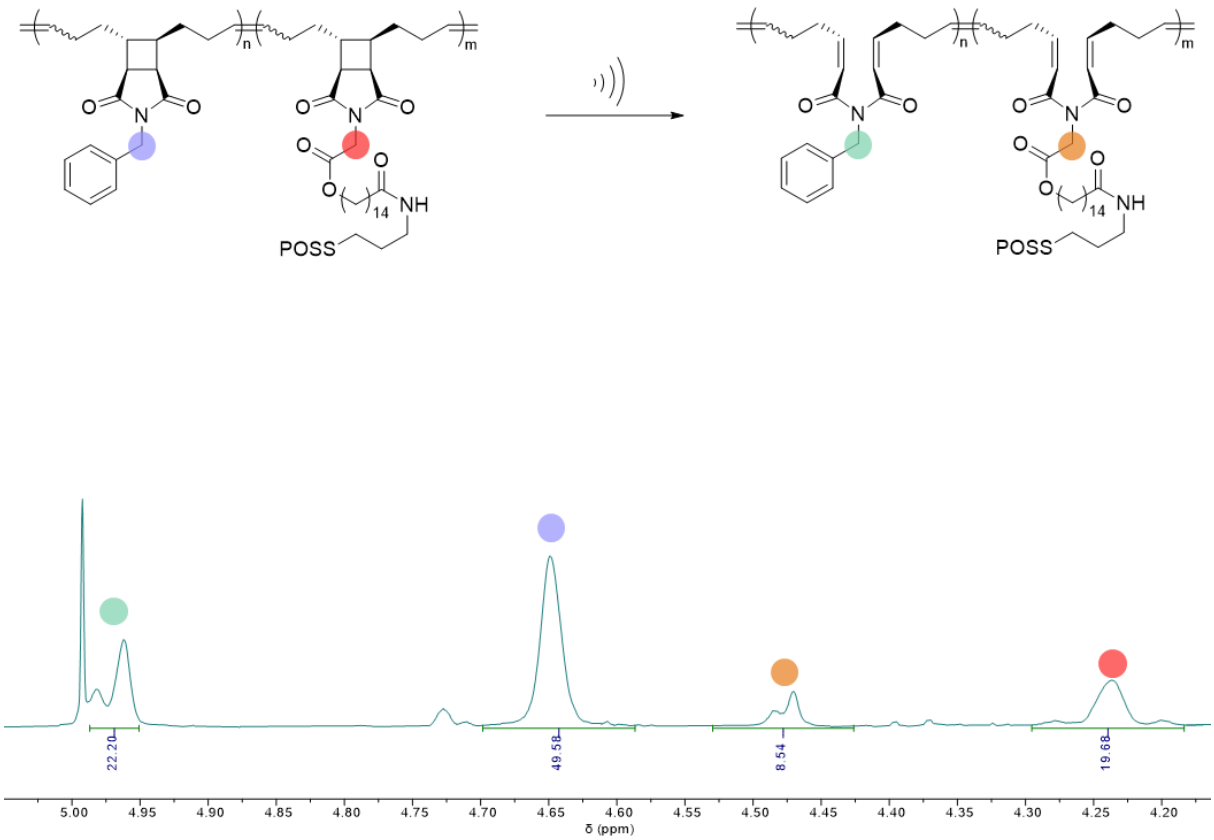

Figure S100. Representative partial ^{1}H NMR (500 MHz, $CDCl_3$) spectrum of $PLSPOSS_{300}Bn_{700}$ after 1 h of ultrasonication.

$$\%RO_{Bn} = \frac{\alpha\ proton\ of\ linear\ imide\ (green)}{\alpha\ proton\ of\ linear\ imide\ (green) + \alpha\ proton\ of\ cyclic\ imide\ (blue)} = \frac{22.20}{22.20 + 49.58} = 30.9\%$$

$$\%RO_{LSPOSS} = \frac{\alpha\ proton\ of\ linear\ imide\ (yellow)}{\alpha\ proton\ of\ linear\ imide\ (yellow) + \alpha\ proton\ of\ cyclic\ imide\ (red)} = \frac{8.54}{8.54 + 19.68} = 30.3\%$$

Scission Cycle Calculation

Scission Cycle (SC) was calculated based on the number average molar mass (M_n) obtained from GPC-MALS according to literature.[5]

$$SC = \frac{\ln(1) - \ln\left(\frac{M_n}{M_{n,0}}\right)}{\ln(2)}$$

Sidechain Composition Effect

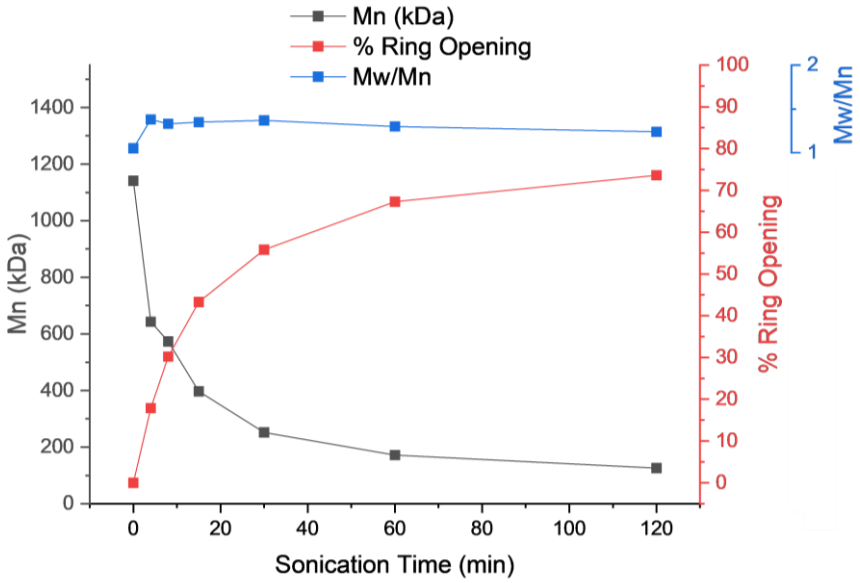

Figure S101. Ultrasonication kinetics results of PM'SPOSS.

Solvent Quality Effect

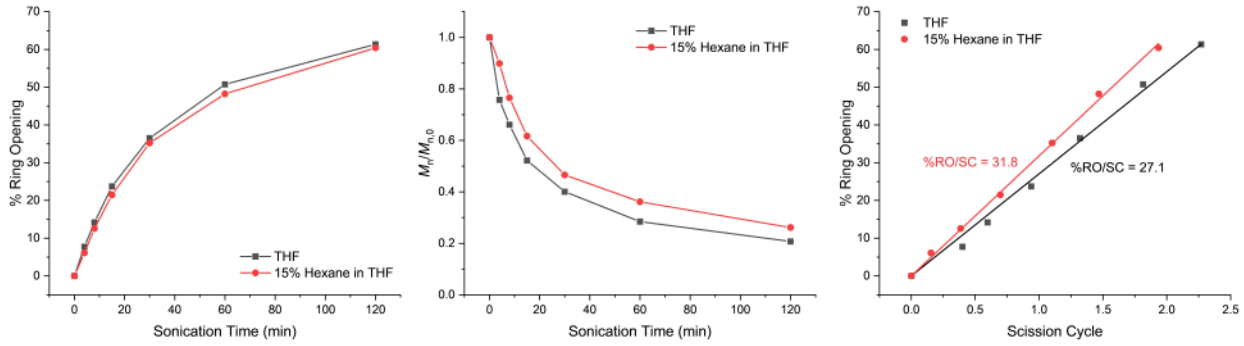

Figure S102. (a) Cyclobutane ring opening fraction and (b) normalized molar mass reduction as a function of sonication time, and (c) %RO as a function of scission cycle for PSS in different solvents.

Mechanochemical Chain Scission Rate Calculation

$$\frac{1}{M_n} = \frac{1}{M_{n,0}} + k_{cs}t \quad ^{6}$$

$$\frac{M_n}{M_{n,0}} = \frac{1}{1 + k_{cs}t}$$

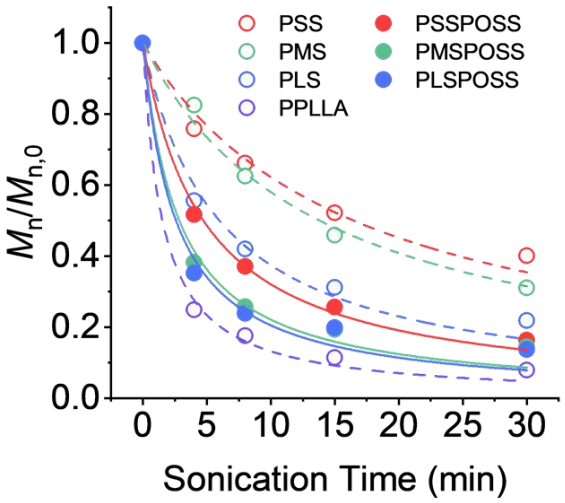

Figure S103. Normalized molar mass as a function of sonication time of polymers with regression line to obtain k_{CS}. First five data points were used for the fitting.

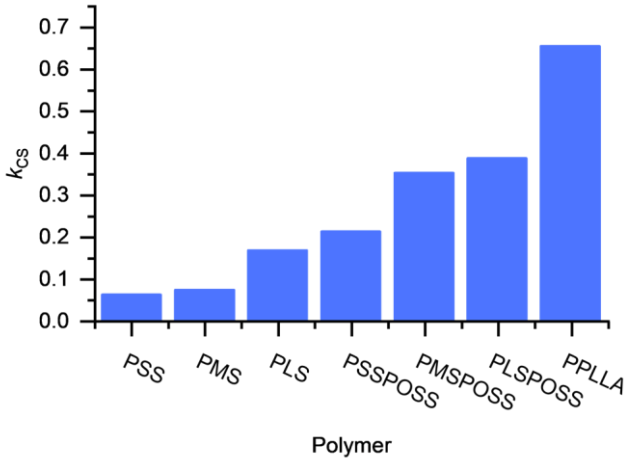

Figure S104. k_{CS} of each polymer subjected to ultrasonication.

Molecular Dynamics Simulation

Conformation Analysis

Molecular dynamics simulations were performed using the LAMMPS package[7,8] to study three single polymer chains (PSSPOSS, PMSPOSS, and PLSPOSS), each composed of 30 monomers. Initial extended conformations of the chains were constructed in Materials Studio package (Materials Studio, by Dassault Systèmes BIOVIA, UK (Accelrys), (License purchased by The University of Akron), and Polymer Consistent Force Field (PCFF)[9] was employed to describe intra/inter molecular interactions. The simulation box, with periodic boundary conditions in all three directions, was set to be 100 Å larger than the fully extended chain length (280 Å) to minimize boundary effects. After energy minimization using the conjugate

gradient algorithm, the system was equilibrated in vacuum at 300 K for 2 ns in the NVT ensemble, employing a Nosé-Hoover thermostat with a timestep of 1.0 fs. The equilibration duration was validated by calculating the normalized autocorrelation function of the chain end-to-end vector, which yielded relaxation times of approximately 0.55 ns for all three cases (0.55, 0.52, and 0.59 ns for PSSPOSS, PMSPOSS, and PLSPOSS, respectively), thus, the chosen equilibrium period of 2 ns was sufficient to obtain statistically independent conformations from the initial conformation. For non-bonded interactions, short-ranged Lennard-Jones and Coulombic potentials calculated using a 15 Å cutoff and long-range electrostatics were handled via the particle-particle particle-mesh (PPPM) method with an accuracy of 1×10^{-4}.

Following equilibration, a 10 ns production run was conducted, with trajectory data sampled every 1.0 ps for analysis. Structural and dynamical properties were evaluated, including the radius of gyration and relative shape anisotropy (κ)[10] for both the entire chain and its backbone.

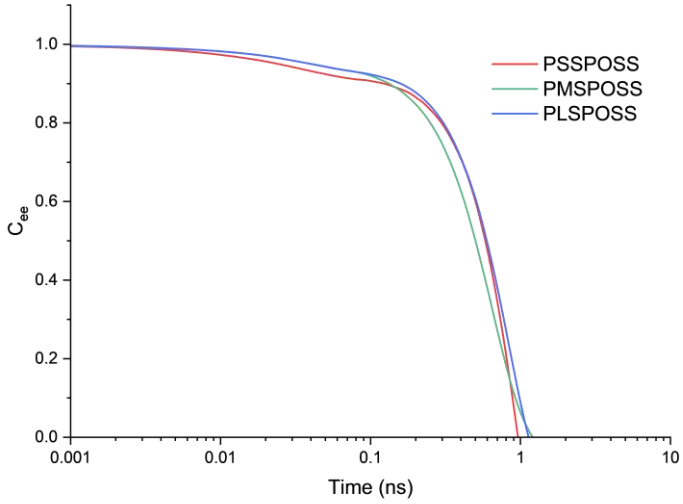

Figure S106. Normalized autocorrelation functions of the chain end-to-end vectors for PSSPOSS, PMSPOSS, and PLSPOSS.

References

1 Sathe, D. *et al.* Olefin metathesis-based chemically recyclable polymers enabled by fused-ring monomers. *Nat. Chem.* **13**, 743-750 (2021). https://doi.org/10.1038/s41557-021-00748-5

2 Thiele, C. *et al.* Tracing Fatty Acid Metabolism by Click Chemistry. *ACS Chemical Biology* **7**, 2004-2011 (2012). https://doi.org/10.1021/cb300414v

3 Guttenberger, N., Sagmeister, P., Glabonjat, R. A., Hirner, S. & Francesconi, K. A. Facile access to arsenic-containing triacylglycerides. *Tetrahedron Lett.* **58**, 362-364 (2017). https://doi.org/https://doi.org/10.1016/j.tetlet.2016.12.040

4 Wang, Z., Yoon, S. & Wang, J. Breaking the Paradox between Grafting-

Through and Depolymerization to Access Recyclable Graft Polymers. *Macromolecules* **55**, 9249-9256 (2022). https://doi.org/10.1021/acs.macromol.2c01609

5 Lenhardt, J. M., Black Ramirez, A. L., Lee, B., Kouznetsova, T. B. & Craig, S. L. Mechanistic Insights into the Sonochemical Activation of Multimechanophore Cyclopropanated Polybutadiene Polymers. *Macromolecules* **48**, 6396-6403 (2015). https://doi.org/10.1021/acs.macromol.5b01677

6 Sato, T. & Nalepa, D. E. Shear degradation of cellulose derivatives. *J. Appl. Polym. Sci.* **22**, 865-867 (1978). https://doi.org/https://doi.org/10.1002/app.1978.070220326

7 Thompson, A. P. *et al.* LAMMPS - a flexible simulation tool for particle-based materials modeling at the atomic, meso, and continuum scales. *Comput. Phys. Commun.* **271**, 108171 (2022). https://doi.org/https://doi.org/10.1016/j.cpc.2021.108171

8 Plimpton, S. Fast Parallel Algorithms for Short-Range Molecular Dynamics. *Journal of Computational Physics* **117**, 1-19 (1995). https://doi.org/https://doi.org/10.1006/jcph.1995.1039

9 Sun, H., Mumby, S. J., Maple, J. R. & Hagler, A. T. An ab initio CFF93 all-atom force field for polycarbonates. *J. Am. Chem. Soc.* **116**, 2978-2987 (1994).

10 Theodorou, D. N. & Suter, U. W. Shape of unperturbed linear polymers: polypropylene. *Macromolecules* **18**, 1206-1214 (1985).